Distribution Agreement

In presenting this thesis or dissertation as a partial fulfillment of the requirements for an advanced degree from Emory University, I hereby grant to Emory University and its agents the non-exclusive license to archive, make accessible, and display my thesis or dissertation in whole or in part in all forms of media, now or hereafter known, including display on the world wide web. I understand that I may select some access restrictions as part of the online submission of this thesis or dissertation. I retain all ownership rights to the copyright of the thesis or dissertation. I also retain the right to use in future works (such as articles or books) all or part of this thesis or dissertation.

Signature:

_____ _____

Lindsey R. Fischer Date

Cu,Zn-Superoxide Dismutase (SOD1) and Oxidative Stress
in the Pathogenesis of Axonal Degeneration

By

Lindsey R. Fischer
Doctor of Philosophy

Graduate Division of Biological and Biomedical Science
Neuroscience

_____
Jonathan D. Glass, M.D.
Advisor

_____
Gary Bassell, Ph.D.
Committee Member

_____
Marie Csete, M.D., Ph.D.
Committee Member

_____
Shawn Hochman, Ph.D.
Committee Member

_____
Gary Miller, Ph.D.
Committee Member

_____
Junmin Peng, Ph.D.
Committee Member

Accepted:

_____
Lisa A. Tedesco, Ph.D.
Dean of the James T. Laney School of Graduate Studies

_____
Date

Cu,Zn-Superoxide Dismutase (SOD1) and Oxidative Stress in the Pathogenesis of Axonal Degeneration

By

Lindsey R. Fischer
B.S., Emory University, 2003

Advisor: Jonathan D. Glass, M.D.

An abstract of
A dissertation submitted to the Faculty of the
James T. Laney School of Graduate Studies of Emory University
in partial fulfillment of the requirements for the degree of
Doctor of Philosophy

Graduate Division of Biological and Biomedical Science
Neuroscience

2009

Abstract

Cu,Zn-Superoxide Dismutase (SOD1) and Oxidative Stress
in the Pathogenesis of Axonal Degeneration

By Lindsey R. Fischer

Axonal degeneration is a common pathologic feature in peripheral neuropathy and neurodegenerative disease. Despite progress in understanding downstream pathways of axon death, the initial trigger(s) for axonal degeneration in neurodegenerative diseases, and motor neuron disease specifically, are unknown. Growing evidence supports the idea that axons are vulnerable to oxidative stress-mediated injury, but models of peripheral neuropathy due to compromised antioxidant defenses are lacking.

Here, we demonstrate that genetic deletion of Cu,Zn-superoxide dismutase (SOD1) causes axonal degeneration both *in vitro* and *in vivo*. *Sod1-/-* dorsal root ganglia showed spontaneous axon degeneration in culture that was mimicked by siRNA knockdown of SOD1 and exposure to superoxide-generating herbicides. *Sod1-/-* primary motor neurons also showed poor axon outgrowth that was attenuated by antioxidant treatment. *In vivo,* denervation and morphologic abnormalities at hind limb neuromuscular junctions were seen by 4 months and progressed out to 18 months of age. Denervation correlated with oxidative stress in peripheral nerve, but not muscle, as determined by measurement of the GSH redox potential. Sensory fibers were spared *in vivo*. These data provide proof of principle that chronic oxidative stress is sufficient to cause a distal motor axonopathy *in vivo*.

We also investigated two strategies to rescue *Sod1-/-* axons. First, *Sod1-/-* mice were crossed with 'slow Wallerian degeneration' (*Wld^S)* mice, an approach that has conferred axonal protection in other models, but did not prevent axonal degeneration due to ablation of SOD1. Next, a targeted approach was used to test the hypothesis that mitochondria are a source of superoxide leading to axonal degeneration in the *Sod1-/-* model. *Sod1-/-* mice were crossed with transgenic mice expressing wild-type human SOD1 exclusively in the mitochondrial intermembrane space (IMS). Robust, long-term rescue of axons was observed. Thus, while SOD1 is normally found throughout the nucleus, cytoplasm, and IMS, restricted expression of SOD1 in the IMS is sufficient for the survival of motor axons. Future studies are needed to determine how IMS-SOD1 influences mitochondrial trafficking and function in axons, and to investigate whether oxidative damage in mitochondria contributes to axonal degeneration in other animal models and in human motor neuropathies.

Cu,Zn-Superoxide Dismutase (SOD1) and Oxidative Stress in the Pathogenesis of Axonal Degeneration

By

Lindsey R. Fischer
B.S., Emory University, 2003

Advisor: Jonathan D. Glass, M.D.

A dissertation submitted to the Faculty of the
James T. Laney School of Graduate Studies of Emory University
in partial fulfillment of the requirements for the degree of
Doctor of Philosophy

Graduate Division of Biological and Biomedical Science
Neuroscience

2009

Acknowledgements:

Many people donated their time, energy, and expertise to make this work possible. First, thank you to Dr. Glass, for your mentorship and your day-to-day example of what it means to be a physician-scientist. You challenged me each step of the way but have also been a constant source of enthusiasm and encouragement. I will always be grateful for the many opportunities that you have given me. Thank you also to my committee members, for your time and advice in helping to shape this project.

To my colleagues in the Glass lab, past and present, thank you for your assistance with experiments, helpful discussions, and friendship. A special word of thanks goes to Yingjie Li for many hours of expert assistance with this project. To all of the students, post-docs, and staff in the Center for Neurodegenerative Disease, it has been a pleasure interacting with and learning from you. Many of you provided advice, equipment, and reagents along the way, particularly Howard Rees, Wilfried Rossoll, Jason Fritz, and Debbie Cooper. I would also like to thank Dean Jones and Bill Liang in the Dept. of Medicine, and Jason Hansen in the Dept. of Pediatrics for assistance with oxidative stress assays. Special thanks go to Marie Csete for providing the SOD1 knockout mice, and to Giovanni Manfredi and Anissa Igoudjil for providing the mitofilin-WTSOD1 mice and for collaboration on the project in chapter VI.

Finally, I would like to thank my family and friends for their encouragement, support, and patience during this long road, especially my parents, Phil and Kathi, my siblings, Avery and Troy, and my dog, Lucy.

This dissertation is dedicated to my grandparents, Wayne and Mary Lee Phillips, in memory of their fight against ALS, as caretaker and patient.

TABLE OF CONTENTS

LIST OF FIGURES

LIST OF TABLES

CHAPTER I. Introduction

Axonal degeneration

Peripheral nervous system (PNS) axons are the anatomic and functional link between motor, sensory, and autonomic neurons and their targets. In humans, axons may extend for distances up to 1 meter from the spinal cord and nearby ganglia to innervate targets in the lower limb, and contain a cytoplasmic volume up to a thousand times greater than the neuronal cell body itself (Höke, 2006). Pathologically, axonal degeneration underlies many forms of peripheral neuropathy and degenerative diseases of the PNS (and CNS), and may in fact represent the most frequent neuronal pathology (Glass, 2002; Griffin, 2007). But despite progress in understanding common downstream pathways of axonal degeneration (Coleman, 2005), the initial triggers for axon degeneration in neurodegenerative disorders, and motor neuron disease specifically, are unknown.

The first half of this chapter discusses axonal degeneration in neurodegenerative disease, with a focus on motor neuron disease in humans and animal models.* The second half covers oxidative stress, focusing on superoxide and superoxide dismutases.

Types of axonal degeneration

The descriptive nomenclature of axonal degeneration provides convenient structural categories for axonal lesions, although the mechanistic distinctions are less well defined. Wallerian degeneration is the simplest model of axonal degeneration

*Portions of chapter I reprinted from *Neurodegenerative Diseases,* Vol. 4, Fischer and Glass, Axonal degeneration in motor neuron disease, p. 431-442, ©2007, with permission from Karger.

(Waller, 1850). After axotomy (nerve transection), the distal nerve stump undergoes a latent phase of continued axonal transport and nerve conduction, followed by a period of rapid fragmentation of the axoplasm and granular disintegration of the cytoskeleton. Schwann cells become activated, and along with invading macrophages, engulf the debris and initiate remodeling in preparation for nerve regeneration. Clinically, Wallerian degeneration is observed following traumatic or ischemic nerve injury.

"Wallerian-like" degeneration, pathologically reminiscent of Wallerian degeneration but not necessarily due to nerve transection, is also seen in a variety of disease states that may involve focal axonal interruption (Glass, 2002). Examples include inflammatory and demyelinating diseases, as well as degenerative diseases that result in formation of large axonal swellings or spheroids or disruption of axonal transport (Coleman, 2005; Griffin et al., 2006).

"Dying-back," or slowly progressive distal to proximal axonal degeneration (Cavanagh, 1964), describes peripheral neuropathy due to a number of causes, including diabetes (Thomas and Tomlinson, 1993), toxic exposures (Spencer and Schaumburg, 1982), HIV infection (Höke and Cornblath, 2004), nutritional deficiencies (Kumar, 2007), normal aging (Baldereschi et al., 2007), and neurodegenerative disease (discussed below). Synonymous terms include "distal axonal degeneration" and "length-dependent axonal degeneration." Spencer and Schaumburg also coined the phrase "central-peripheral distal axonopathy" to describe their observation of synchronous distal axonal degeneration in central and peripheral axons in models of toxic neuropathy (1976).

Of course, axonal degeneration may also occur secondary to neuronal cell death. This scenario is sometimes referred to as a neuronopathy or a "dying-forward" process to

distinguish it from primary axonal lesions. The question of whether axonal degeneration of the "dying-back" type reflects an axonal lesion, or is also a result of a 'sick' cell body that is unable to maintain its axon, is debated (Conforti et al., 2007a). There is evidence that axons are more vulnerable than cell bodies to several insults responsible for distal axonal degeneration (Silva et al., 2006; Akude et al., 2009; Zherebitskaya et al., 2009), and in some cases isolated axonal insults have been demonstrated to cause cell death (Song et al., 2006).

Programmed axon death

Traditionally, axons were considered as passive extensions of the neuronal cell body, and axonal degeneration thought to occur as a result of loss of trophic support. The tendency for degeneration to begin in the distal axon was attributed to this being the 'last field of irrigation,' or the last to receive resources from the cell body. In 1902, Gowers coined the term "abiotrophy" to describe slow neuronal failure characteristic of degenerative diseases, referring to spinal motor neurons as the "vital center" of fibers terminating on skeletal muscle (1902). Cajal wrote of a "dynamic" or "lifegiving" substance radiating from the trophic center and required for axon survival (1928).

However, Cajal also remarked, "We do not wish to deny that the nutrition of the axon is a local process and is to a certain degree autonomous" (1928). Recent studies confirm that mature axons are more autonomous than previously recognized, with the capacity for protein synthesis (Lin and Holt, 2008; Twiss and Fainzilber, 2009), mitochondrial renewal (Amiri and Hollenbeck, 2008), and a regulated axon death program distinct from cell death (Raff et al., 2002). This concept of axonal autonomy has

far-reaching implications for our understanding of the pathogenesis of neurodegenerative diseases.

Growing evidence supports the idea that axonal degeneration may proceed independently of the molecular events controlling programmed cell death. In an *in vitro* model of nerve growth factor (NGF) withdrawal, treatment with the pan-caspase inhibitor zVAD-fmk (Finn et al., 2000), and overexpression of the anti-apoptotic protein Bcl-2 (Garcia et al., 1992) both protected cell bodies, but not axons. In a model of botulinum C toxicity, axonal caspase activation was evident, but zVAD-fmk still failed to rescue axons (Berliocchi et al., 2005). Mice overexpressing Bcl-2, or lacking the pro-apoptotic protein Bax show robust neuronal protection following neonatal axotomy (Dubois-Dauphin et al., 1994; Burne et al., 1996) and in motor neuron disease models (Sagot et al., 1995; Gould et al., 2006). However axons in these models are not protected, even though changes in the levels of Bcl-2 and Bax extend to the axonal compartment. These data support the hypothesis that axonal degeneration proceeds by a mechanism distinct from classic apoptotic pathways. One exception is HIV neuropathy due to gp120 toxicity, where caspase-3 activation in axons does cause axonal degeneration (Melli et al., 2006). Still, experiments in a compartmented culture system show that the modes of axon and cell death due to gp120 are distinctly different.

The concept of "axonal independence" was transformed by the discovery of the slow Wallerian degeneration (Wld^S) mouse, a spontaneous mutant with the remarkable phenotype of prolonged survival of injured axons (Lunn et al., 1989). Following nerve transection, Wld^S axons in the distal nerve stump survive for up to 4 weeks (Glass and Griffin, 1991; Glass et al., 1993), and support action potentials and axonal transport for at

least 2 weeks (Lunn et al., 1989; Smith and Bisby, 1993; Glass and Griffin, 1994). The *Wld*^{S} protective phenotype is intrinsic to the axon (Glass et al., 1993), and the mutant protein is sufficient to provide the phenotype as demonstrated by viral vector delivery of *Wld*^{S} to cultured neurons (Wang et al., 2001b; Conforti et al., 2007b) and the generation of a *Wld*^{S} transgenic mouse (Mack et al., 2001).

The existence of *Wld*^{S} confirms that axonal survival may be regulated independently of cell survival, and provides an important tool for testing differences in axonal and cell body death programs. *Wld*^{S} is protective against toxic (Wang et al., 2001b; Wang et al., 2001a; Wang et al., 2002) and genetic (Ferri et al., 2003; Samsam et al., 2003; Mi et al., 2005) forms of axonal degeneration, but is not protective against the death of neuronal cell bodies (Deckwerth and Johnson, 1994; Adalbert et al., 2006; Beirowski et al., 2008). These data are perhaps the strongest evidence for mechanistic similarities between classic Wallerian degeneration, Wallerian-like degeneration and axonal "dying-back," although *Wld*^{S} does not provide robust protection in some models of distal axonal degeneration including SOD1 mutant mice (Vande Velde et al., 2004; Fischer et al., 2005) and spinal muscular atrophy mice (Rose et al., 2008; Kariya et al., 2009). This could be explained by the observation that the *Wld*^{S} protective phenotype only lasts for a few weeks after injury (Crawford et al., 1995) and is diminished after 3 months of age at the most distal portions of the axon (Gillingwater et al., 2002). Therefore, *Wld*^{S} may be more effective in acute processes or early onset disease and protection may be lost in chronic disease models.

The mechanism of protection by *Wld*^{S} remains a subject of intense investigation, given its widespread therapeutic implications. *Wld*^{S} codes for a unique 42 kD chimeric

protein consisting of the first 70 amino acids of the E4 ubiquitin ligase Ube4b, fused to the full-length *Nmnat1* gene (Conforti et al., 2000). Two studies reported that NMNAT1-mediated increase in NAD+ accounts for the mechanism of Wld^S (Araki et al., 2004; Wang et al., 2005). However, attempts to independently confirm these findings were unsuccessful (Conforti et al., 2007b; Yahata et al., 2009). Recently two groups, one working in *Drosophila* (Avery et al., 2009) and one in mice (Conforti et al., 2009), concluded that the minimum genetic elements required for the *WldS* phenotype are the N-terminal 16-amino acid portion of *Ube4b* (N16) and full length *Nmnat1*. The N16 region is a binding domain for valosin-containing protein (VCP) (Laser et al., 2006), ablation of which abolishes the *WldS* phenotype in *Drosophila* (Avery et al., 2009). The precise details of the interplay between N16 and NMNAT1 in conferring axonal protection remain to be elucidated, but may involve subcellular targeting or regulation of NMNAT1 turnover via the N16/VCP interaction.

Alteration of Wld^S localization has also provided important new information on possible mechanisms of action. Whereas previously the majority of Wld^S was only detected in the nucleus, and not in axons, deletion of the nuclear localization signal in Wld^S causes an increase in axonal Wld^S and a corresponding increase in axonal and synaptic protection (Beirowski et al., 2009). This suggests that the strength of protection is directly correlated with the level of Wld^S in the axon. Proteomic analysis of synaptic protein expression in Wld^S mice showed that half of altered proteins were mitochondrial or regulated mitochondrial stability (Wishart et al., 2007), and studies in mice and *Drosophila* show that overexpression of NMNAT3, the mitochondrial isoform of NMNAT, provides robust axonal protection similar to that seen in Wld^S (Avery et al.,

2009; Yahata et al., 2009). Thus mitochondria may be an important target of the protective action of *Wld*^{S}, and an important site for determining the rate of progression of Wallerian degeneration.

Two other pathways that regulate the rate of axonal degeneration have recently been discovered. The first is translation elongation factor eEF1A2, which is downregulated in the "Wasted" (*Wst*) mouse, a model of dying-back motor neuropathy (Murray et al., 2008a). Tibial nerve axotomy in *Wst* mice revealed a surprising resistance, rather than susceptibility, to Wallerian degeneration. This suggests that the multifunctional protein eEF1A2 is required to prevent dying-back pathology, but also acts to promote Wallerian degeneration, by an unknown mechanism. Another protein recently shown to regulate axonal degeneration is dual lysine kinase (DLK) (Miller et al., 2009). Knockout of DLK strongly inhibited Wallerian degeneration in *Drosophila* and in mouse dorsal root ganglion (DRG) cultures, as did inhibition of c-Jun N-terminal kinase (JNK), a downstream target of DLK that is upregulated after axonal injury (Cavalli et al., 2005). The existence of *Wld*^{S}, together with these emerging data, offers strong support for the theory that axonal degeneration is an intrinsically regulated process.

Axonal degeneration in neurodegenerative disease

Axonal degeneration is the pathologic substrate underlying hereditary and sporadic forms of peripheral neuropathy, defined as primary diseases of PNS axons. However, growing evidence from models of neurodegenerative disease, traditionally associated with death of neurons in the CNS, also demonstrates axon defects that occur prior to cell death and correlate most closely with functional decline.

Morphologic and biochemical evidence from animal models and individuals dying unexpectedly early in the course of Alzheimer's disease shows that synapse loss precedes neuron death and is the most likely cause of cognitive dysfunction (reviewed in Selkoe, 2002; Arendt, 2009). One hypothesis is that soluble Aß oligomers may cause synaptic failure and impair synaptic plasticity. Presymptomatic impairment in axonal transport, associated with axonal swellings and abnormal accumulation of vesicles, organelles, and microtubule-associated proteins has also been demonstrated in affected brain regions (Stokin et al., 2005). Moreover, experimental slowing of anterograde axonal transport exacerbated these changes.

Postmortem analysis of Parkinson's disease patients demonstrates that loss of nigrostriatal axon terminals is more severe than loss of dopaminergic neurons, and axonal degeneration precedes cell death in animal models of MPTP toxicity (reviewed in Dauer and Przedborski, 2003). Introduction of mutant α-synuclein was also recently shown to cause axonal pathology and alterations in proteins associated with axonal transport and synaptic function (Chung et al., 2009). An important role for axonal degeneration in Parkinson's disease is evidenced by the fact that *Wld*^{S} mice are resistant to the toxicity of 6-OHDA (Sajadi et al., 2004) and MPTP (Hasbani and O'Malley, 2006).

Axonal degeneration has long been known to be a feature of amyotrophic lateral sclerosis (ALS), a fatal disease of cortical and spinal motor neurons characterized by progressive weakness and muscle atrophy (Tandan and Bradley, 1985). Electromyographic (EMG) findings of denervation are essential for diagnosis. These include spontaneous fibrillation and fasciculation potentials and loss of motor units. Reinnervation, the motor system's attempt to retain normal function, is also a typical

finding, but inadequate to compensate for ongoing denervation that eventually causes weakness (Hansen and Ballantyne, 1978). Denervation has traditionally been attributed to dysfunction and death of motor neurons, and reinnervation has been assumed to result from sprouting of viable motor axons taking over the territory of the dead motor neuron. These assumptions, however, have not been tested in patients since the progression of pathological changes cannot be followed over time as is possible in animal models (Schaefer et al., 2005).

There are pathologic and clinical data supporting the hypothesis that ALS in humans begins with distal axonal degeneration. Bradley and colleagues used quantitative morphometry to demonstrate a distal to proximal gradient of axonal pathology in phrenic nerves from ALS patients (Bradley et al., 1983). We also had the rare opportunity to examine clinically and then pathologically an ALS patient who died unexpectedly during a minor surgical procedure (Fischer et al., 2004) (Fig. 1). His clinical diagnosis was definite, and he had been symptomatic for at least six months. Autopsy confirmed the severe denervation and reinnervation changes demonstrated by his EMG (Fig. 1A-B), but there were no detectable changes in the corresponding spinal motor neurons (Fig. 1C).

Clinically, investigators employ the technique of motor unit number estimation (MUNE) to quantify degrees of denervation and reinnervation (reviewed in Shefner, 2001). MUNE has been shown to accurately predict the rate of ALS progression and overall survival, suggesting that denervation and loss of motor units may be a primary determinant of these events (Yuen and Olney, 1997; Armon and Brandstater, 1999).

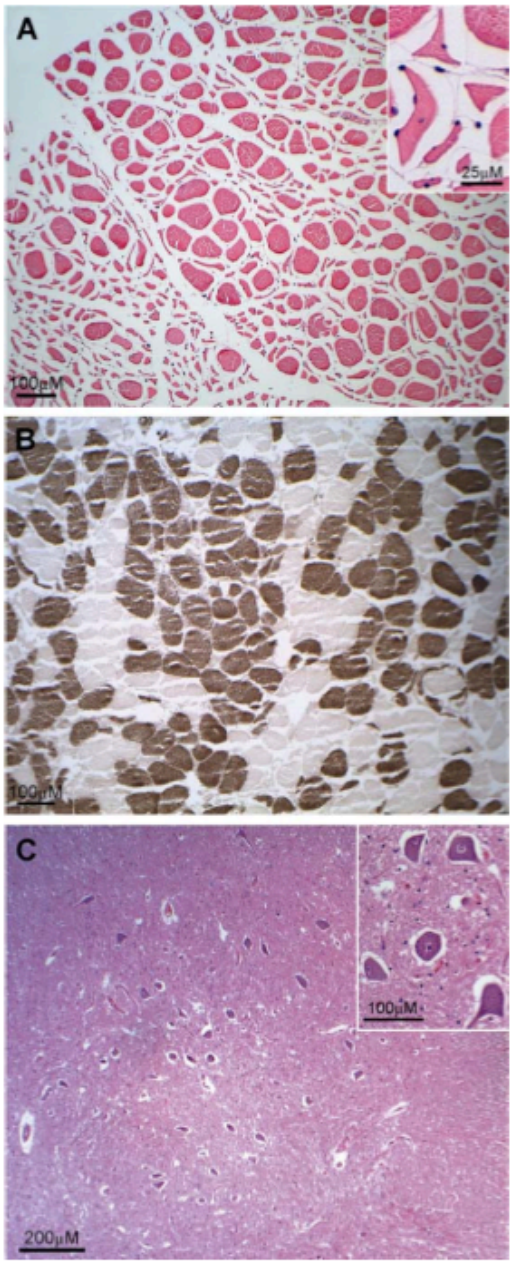

Fig. 1.1 Early neuropathology from a human ALS case. (**A**) H&E-stained section showing grouped atrophy and angulated fibers (insert), indicating acute and chronic denervation/ reinnervation. (**B**) ATPase stain (pH 4.2) showing fiber-type grouping. (**C**) Lumbar spinal cord showing a normal complement of motor neurons.

These findings were replicated in a mouse model (Shefner et al., 2006). The MUNE technique was also used to follow pre-symptomatic individuals carrying disease-causing mutations. In several cases MUNE detected a reduction in motor units months prior to the onset of disease (Aggarwal and Nicholson, 2002). Threshold tracking, which measures axonal excitability, is another electrophysiological technique that demonstrates early abnormalities in ALS patients. An apparent increase in persistent Na^+ current and a decrease in K^+ conductance were observed in two patient populations (Kanai et al., 2006; Vucic and Kiernan, 2006), and these changes were more prominent distally than proximally (Nakata et al., 2006). None of these studies are conclusive regarding the spatiotemporal progression of motor neuron disease in humans, but combined with the data from mouse models (discussed below) they lend support to the idea that ALS may begin as a disease of the distal axon.

The pathologic sequence of motor neuron degeneration in relation to disease course has been investigated in numerous mouse models of motor neuron disease and motor neuropathy (reviewed in Fischer and Glass, 2007). In many of these models, axonal degeneration appears to be the primary deficit, preceding symptom onset and motor neuron death (table 1.1). Even at end-stage, the degree of motor neuron loss in several of these models is surprisingly mild, suggesting that the disease phenotype is more directly related to the degeneration of motor axons. This is logical given that axonal degeneration results in the same functional consequence as motor neuron death, preventing signaling between the motor neuron and its target muscle.

Disease Model	Mutation	Characterization of axon deficits (by first author)
ALS	$SOD1^{G93A}$	Kennel (1996), Frey (2000), Fischer (2004), Pun (2006), Gould (2006), Hegedus (2007)
	$SOD1^{G85R}$	Pun (2006)
pmn	Tubulin-specific chaperone e (*Tbce*)	Holtmann (1999), Frey (2000)
Mnd	Neuronal ceroid lipofuscin (*Cln8*)	Frey (2000)
SMA	$Smn^{-/-}$, $SMN2^{+/+}$	Murray (2008b), McGovern (2008)
	$Smn^{-/-}$, SMNΔ7, $SMN2^{+/+}$	Kariya (2008), Murray (2008b), Kong (2009)
	$Smn^{-/-}$, SMN $A2G^{+/-}$, $SMN2^{+/+}$	Monani (2003), Kariya (2008)
	$Smn^{F7}/Smn^{\Delta 7}$, NSE-Cre^{+}	Cifuentes-Diaz (2002)
HCSMA	(unknown)	Rich (2002)
SBMA	Androgen receptor (CAG repeat expansion)	Katsuno (2006)
Wasted	eEF1A2 translation elongation factor	Newbery (2005), Murray (2008a)
Wobbler	Vacuolar-vesicular protein sorting factor (*Vps54*)	Blondet (2002)
VEGF	VEGF promoter (hypoxia-response element)	Oosthuyse (2001)
gad	Ubiquitin carboxy-terminal hydrolase (*UchI1*)	Miura (1993)
Stathmin knockout mice	Stathmin	Liedtke (2002)
Loa and Cra1	cytoplasmic dynein heavy chain (*Dnchc1*)	Hafezparast (2003)
Dynamitin overexpressers	dynamitin	LaMonte (2002)

Table 1.1 Genetic models of motor neuropathy in which axonal pathology is a primary feature

We performed a quantitative pathologic study to evaluate the spatiotemporal progression of pathology in the Cu,Zn-superoxide dismutase (SOD1) mutant mouse, the most widely-used animal model of familial ALS (Fischer et al., 2004). The high copy number $SOD1^{G93A}$ mutant develops weakness at 80-90 days and dies between 130-140 days. The original pathologic characterization of these mice demonstrated that the onset of symptoms coincided with the death of spinal motor neurons (Chiu et al., 1995). However, subsequent physiologic and pathologic studies detected evidence of denervation of hindlimb muscles much earlier than symptom onset (Kennel et al., 1996; Frey et al., 2000). We compared the time course of denervation at the NMJ, axonal degeneration in the ventral root, and lumbar motor neuron loss in these animals at multiple ages and observed a distal to proximal, or "dying-back" pattern of degeneration (Fig. 2-4). Approximately 30% of hindlimb NMJs were denervated by 47 days (Fig. 2D), long before the onset of clinical symptoms. At the time of symptom onset at 80 days, over 60% of ventral root axons had already degenerated (Fig. 3). Loss of motor neuron cell bodies was not identified until after symptom onset (Fig. 4). Other laboratories have now confirmed these findings in $SOD1^{G93A}$ mice and in other SOD1 mutants (Gould et al., 2006; Pun et al., 2006; Hegedus et al., 2007).

In human ALS and in SOD1 mutant mice, depletion of spinal motor neurons may not directly correlate with clinical symptomatology, but is an inevitable consequence of disease. However, there are data to suggest that motor neuron death is not required for development or progression of symptomatic motor neuron disease. Several studies in SOD1 mutant mice demonstrate that interventions that fully protect motor neuron cell

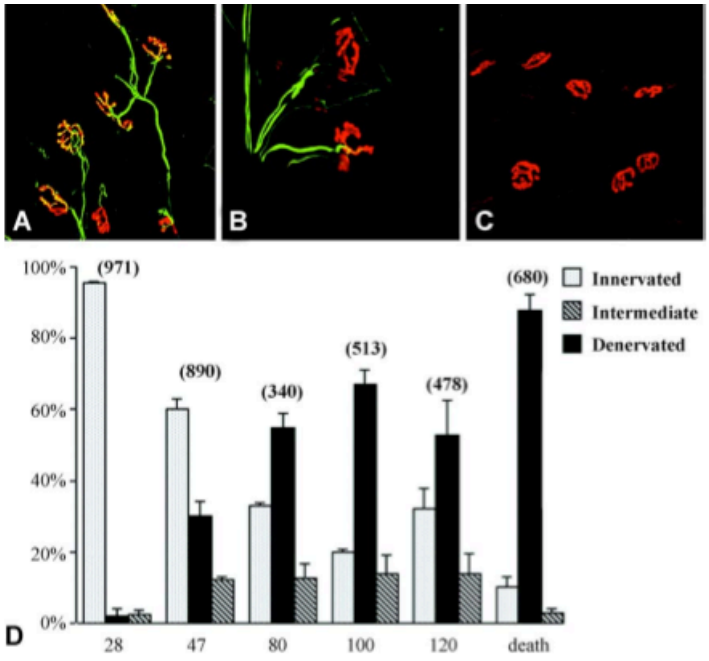

Fig. 1.2 NMJ immunocytochemistry from SOD1^{G93A} gastrocnemius muscle. Motor endplates are identified with a-bungarotoxin (red); axons are identified with neurofilament + SV2 (green). Images depict (**A**) innervated endplates (yellow indicates overlap), (**B**) intermediate endplates, (**C**) denervated endplates, (**D**) quantitative analysis. Data are shown as % of endplates classified as innervated, denervated, or intermediate. Numbers in parenthesis indicate number of endplates quantified per time point.

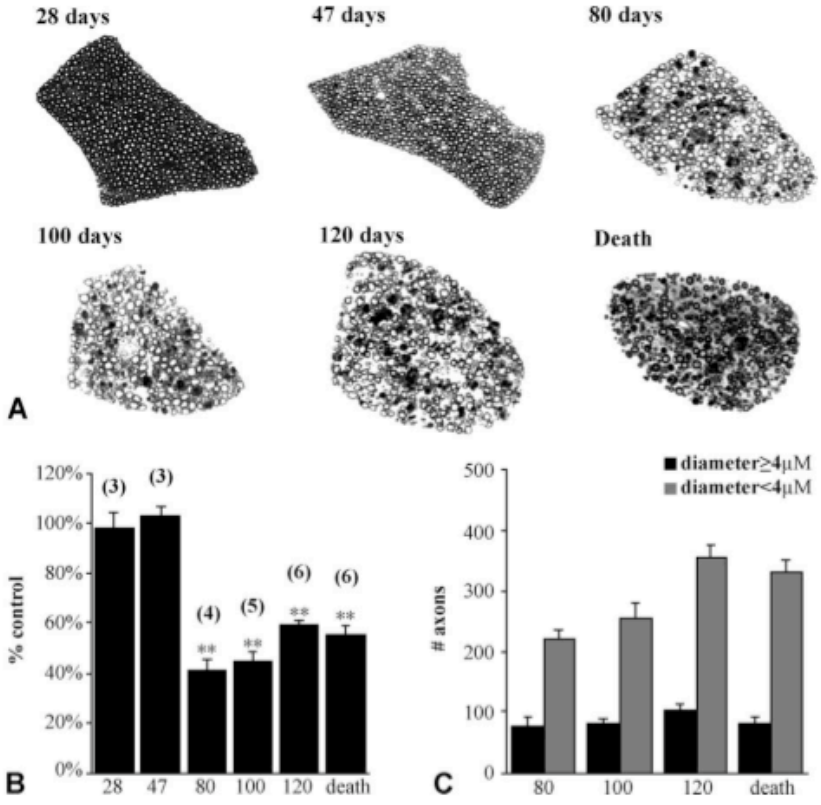

Fig. 1.3 (**A**) Light microscope images of L4 ventral roots from SOD1^{G93A} mice. (**B**) Number of ventral root axons reported as % control. (**C**) Small versus large axons from 80 days to death. Note the relative increase in the proportion of small caliber axons, indicating regeneration. Number of animals examined at each time point in parentheses. Data are means ± SEM (** $p < 0.01$ vs. control).

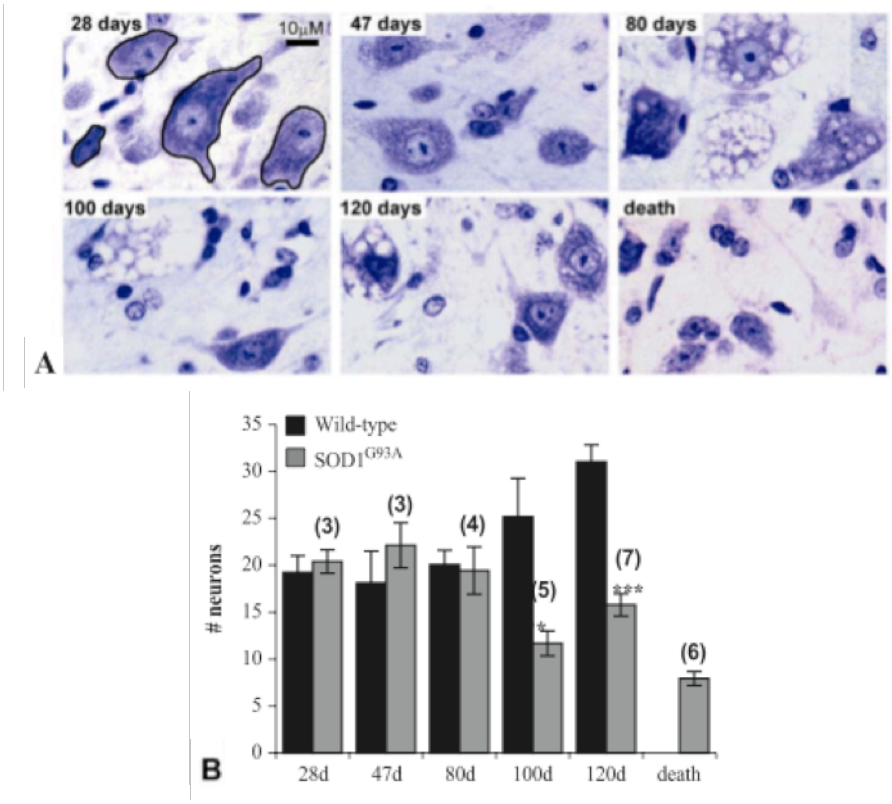

Fig. 1.4 (**A**) Nissl-stained motor neurons in the ventral horn of SOD1^{G93A} lumbar spinal cord. 28-day image depicts outlining of neuron in Image Pro analysis software. (**B**) Number of α-motor neurons per section. Numbers in parentheses indicate number of animals examined. Data are means ± SEM (** $p < 0.01$, *** $p < 0.001$ vs. control).

bodies do not prevent disease progression (Gould et al., 2006; Rouaux et al., 2007; Suzuki et al., 2007). In these studies, animals reached end-stage with a full complement of motor neurons, yet their motor axons still degenerated, suggesting that axonal degeneration alone is sufficient to cause disease. This idea is also supported by data from pmn mice, which show an early and severe phenotype with weakness by 3 weeks of age and death by week 6. Progressive hind limb denervation is evident by 15 days, but motor neuron loss is not detectable at symptom onset and is only 30-40% by end-stage (Sendtner et al., 1992; Holtmann et al., 1999; Frey et al., 2000). Similarly, in SMA mice, nerve terminal abnormalities and/or NMJ denervation are consistent findings (Kariya et al., 2008; Murray et al., 2008b; Kong et al., 2009), but involvement of proximal axons and motor neuron death are only seen in some of the genetic models, and where motor neuron death is seen it occurs late and is very mild (20-30%) (Cifuentes-Diaz et al., 2002; Monani et al., 2003; Kariya et al., 2008). Moreover, functional defects at the NMJ, even in the absence of frank denervation, can also cause motor neuron disease in hereditary canine SMA (Rich et al., 2002) and in $Smn^{-/-}$, SMNΔ7, $SMN2^{+/+}$ mice (Kong et al., 2009).

The idea that functional and/or structural axon defects are sufficient to cause fatal motor neuron disease underscores the idea that axonal degeneration is an important therapeutic target, deserving increased attention in ALS and in other neurodegenerative diseases. If the data from mouse models is consistent with the progression of human disease, many neuronal cell bodies may be morphologically intact at the time of disease onset, and thus may be potentially salvageable with early intervention.

Mechanisms of axonal degeneration

Axonal degeneration due to a diverse array of insults seems to converge on a common final pathway involving: (1) impaired axonal transport, (2) mitochondrial failure, and (3) a rise in axonal Ca^{2+}, leading to calpain activation and subsequent degradation of axon components (reviewed in Coleman, 2005). While the proximal cause(s) of axonal degeneration in motor neuron disease are unknown, substantial evidence supports the idea that degeneration ultimately proceeds through this pathway.

Impairment of fast anterograde axonal transport is well established in human ALS (Bradley et al., 1983; Sasaki and Iwata, 1996) and in SOD1 mutant mice (Zhang et al., 1997; Warita et al., 1999; Williamson and Cleveland, 1999). Slowing of anterograde transport and accumulation of neurofilament in the proximal axon begins at least six months prior to the onset of symptoms in $SOD1^{G37R}$ and $SOD1^{G85R}$ mice, at a time when no pathological changes are seen at the level of the spinal cord (Williamson and Cleveland, 1999). Slowing of retrograde transport has also been reported in motor neurons of SOD1 mutant mice, from as early as embryonic day 13 (Murakami et al., 2001; Kieran, 2005). Recently, mutations in proteins associated with the dynein/dynactin complex were identified in motor neuron disease in mice (Lamonte et al., 2002; Hafezparast et al., 2003) and in humans (Puls et al., 2003). Restoring the rate of retrograde transport in SOD1 mutant mice, via introduction of a dynein mutation, has since been shown to prolong survival (Kieran et al., 2005). Thus slowed transport in both the anterograde and retrograde direction is well established in ALS, and has been linked to disease progression.

There is abundant evidence for abnormalities in mitochondrial morphology, function, and distribution in human ALS and in animal and cell culture models. Ultrastructural abnormalities have been identified in motor neurons, motor axons, and skeletal muscle from ALS patients (Afifi et al., 1966; Atsumi, 1981; Hirano et al., 1984; Sasaki and Iwata, 2007). Severe vacuolar degeneration of mitochondria in spinal motor neurons coincides with disease onset in $SOD1^{G93A}$ mutant mice (Kong and Xu, 1998). Similar damage can be detected in motor axon terminals at the NMJ as early as postnatal day 25 (Gould et al., 2006). Biochemical and histochemical studies have revealed deficiencies in respiratory chain activity, including complexes I and IV, in skeletal muscle and spinal cord from ALS patients (Fujita et al., 1996; Wiedemann et al., 1998; Borthwick et al., 1999; Vielhaber et al., 2000), although one group attributed this to mitochondrial depletion rather than compromised enzymatic function (Wiedemann et al., 2002). ATP synthesis, mitochondrial respiration (measured by oxygen consumption), and electron transport chain function are abnormal in $SOD1^{G93A}$ mice (Jung et al., 2002; Mattiazzi et al., 2002), and these changes may be specific to affected tissues (Kirkinezos et al., 2005). Cell culture models based on expression of mutant human SOD1 also show altered mitochondrial morphology, decreased electron transport chain function (Menzies et al., 2002), loss of mitochondrial membrane potential (Carrì et al., 1997), and decreased ATP production (Beretta et al., 2003). A direct link to mutant SOD1 toxicity is theorized, given that mutant SOD1 accumulates and forms aggregates in the mitochondrial matrix and intermembrane space of mitochondria, and also collects on the outer (cytoplasmic) surface of mitochondria (Higgins et al., 2002; Liu et al., 2004; Pasinelli et al., 2004;

Vijayvergiya et al., 2005; Ferri et al., 2006). The cause of mitochondrial damage in sporadic ALS is unknown.

Recent studies have also provided evidence of mitochondrial abnormalities specifically in axons. De Vos and colleagues reported impaired anterograde transport of mitochondria in primary neurons expressing mutant SOD1 (2007). This resulted in a net increase in retrograde movement, depletion of mitochondria in axons, and accumulation of mitochondria in the cell body. Magrane and colleagues reported a bidirectional impairment of mitochondrial transport in a differentiated motor neuron cell line stably expressing mutant SOD1 (2009). These transport defects were associated with reduced mitochondrial density in neurites and reduced neurite length. Remarkably, mutant SOD1 targeted exclusively to the mitochondrial intermembrane space was sufficient to reproduce these defects. Short, fragmented mitochondria were also reported in this model, suggesting a possible abnormality of mitochondrial fission/fusion in mutant axons (Magrané and Manfredi, 2009). Data from axoplasmic whole mount preparations, derived from $SOD1^{G93A}$ rats, show a distinct propensity for mitochondrial clustering and damage in motor, but not sensory axons (Sotelo-Silveira et al., 2009). These data parallel anecdotal observations from human ALS tissue showing abnormal mitochondrial clustering and mitochondrial accumulation in proximal axons and cell bodies of spinal motor neurons (Sasaki and Iwata, 2007). Thus, not only is mitochondrial morphology and function altered in ALS, but there is also growing evidence for altered mitochondrial dynamics specifically in motor axons.

The final execution pathway in axonal degeneration involves an increase in axonal Ca^{2+} and subsequent activation of calpains (Coleman, 2005). Transient increases

in Ca^{2+} that occur as part of neurotransmitter-mediated signaling are normally harmless to neurons, however impaired recovery from Ca^{2+} flux is a common finding in neurodegenerative disease and aging (reviewed in Mattson, 2007). Increased Ca^{2+} in spinal motor neurons has been demonstrated in human ALS (Kasarskis et al., 1995) and in SOD1 mutant mice (Siklós et al., 1998). Ca^{2+} is also increased in motor nerve terminals from ALS muscle biopsies (Siklós et al., 1996). Increased Ca^{2+} may be closely tied to mitochondrial dysfunction, given the critical role of mitochondria in Ca^{2+} buffering, particularly at synapses where there is a high density of mitochondria (Ly and Verstreken, 2006). Motor neurons cultured from SOD1 mutant mice showed increased intracellular Ca^{2+} but decreased mitochondrial Ca^{2+}, suggesting a decreased loading capacity (Kruman et al., 1999). Mitochondria from $SOD1^{G93A}$ brain and spinal cord, but not liver, also exhibit impaired Ca^{2+}buffering (Damiano et al., 2006). Real-time fluorescent monitoring of mitochondrial Ca^{2+} levels showed abnormal Ca^{2+}-buffering in $SOD1^{G93A}$ NMJs in response to a train of action potentials (Vila et al., 2003). Whereas wild-type NMJs reached a Ca^{2+} plateau, mutant NMJs showed continuous ramping up of mitochondrial Ca^{2+} levels, suggesting an inability to limit stimulation-induced increases in Ca^{2+}.

Ca^{2+}- mediated destruction of axons is carried out via activation of calpains — ubiquitous, calcium-dependent cysteine proteases. Many cellular and animal models of neurological disease, including ischemia, trauma, and exposure to toxic agents, demonstrate calpain-mediated degradation of cytoskeletal and membrane proteins (reviewed in Bartus et al., 1995). Activation of calpains has also been implicated in the pathogenesis of neurodegenerative diseases (Nixon et al., 1994; Adamec et al., 2002),

although not specifically investigated in motor neuron disease to date. Calpain inhibition has shown therapeutic potential for chemotherapy-induced peripheral neuropathy in cell culture (Wang et al., 2000) and in mice (Wang et al., 2004), and also prevented cytoskeletal degradation at the NMJ in a model of acute, immune-mediated nerve terminal injury (O'Hanlon et al., 2003). Whether calpain inhibition can also protect axons in chronic neurodegenerative disease remains to be seen.

Summary

Axonal degeneration is a common pathologic entity and an unexploited therapeutic target in neurodegenerative disease. Data from human patients and animal models of motor neuron disease, including our own studies in the $SOD1^{G93A}$ model of familial ALS, suggest that pathology begins at the NMJ and proceeds in a distal to proximal, or "dying-back" pattern. Protection of cell bodies alone cannot significantly change the course of motor neuron disease, and the extent of motor neuron death does not correlate with disease symptoms or survival. On the other hand, axonal degeneration appears to be sufficient to cause disease, at least in animal models. The cause of axonal degeneration in motor neuron disease remains unknown, but ultimately appears to trigger a common pathway of axon demise involving slowed axonal transport, mitochondrial dysfunction, and increased axonal Ca^{2+} levels. More work is needed to improve our understanding of axonal degeneration in motor neuron disease and to develop strategies for axonal protection.

Oxidative stress

Oxidative stress is traditionally defined as an imbalance between pro-oxidants and antioxidants, leading to oxidative damage. Chronic accumulation of such damage over time is thought to be a major driving force in cell senescence and aging (Harman, 1956), and is the most prominent risk factor for neurodegenerative disease. However, attempts to treat neurodegerative diseases by simply increasing antioxidant levels have been unsuccessful. This and other evidence points to the need for a revised definition of oxidative stress, incorporating the idea of 'disrupted redox signaling and control' (Jones, 2006c). Free radicals may have evolved to serve a host of signaling and regulatory roles within cells (Beckman and Ames, 1998; Jones, 2006a; Giorgio et al., 2007). Perturbations that alter free radical production and/or deplete antioxidants may therefore cause sublethal alterations in cellular physiology, understanding of which may lead to new therapeutic strategies for oxidative stress-mediated injury.

This section reviews the biochemistry of superoxide and superoxide dismutases, and evidence from human disease and animal models that demonstrates a neuroprotective role of SOD1.

Reactive oxygen species

A wide array of reactive oxygen, nitrogen, chlorine, and other species are capable of acting as pro-oxidants (reviewed in Halliwell, 2006). Reactive oxygen species (ROS) are most relevant to this dissertation, so will be discussed here in detail.

ROS are a group of oxygen-containing species that includes free radicals (containing an unpaired electron) such as superoxide ($O_2 \cdot^-$) and hydroxyl radical ($\cdot OH$)

as well as reactive non-radicals such as hydrogen peroxide (H_2O_2) and peroxynitrite ($ONOO^-$). Jensen (1966) was the first to identify mitochondria as a source of ROS. Release of H_2O_2 was subsequently confirmed in isolated mitochondria (Loschen et al., 1971; Boveris and Chance, 1973), and this phenomenon soon attributed to dismutation of $O_2 \cdot^-$ (Loschen et al., 1974). Current dogma holds that $O_2 \cdot^-$ is continuously produced by mitochondrial electron transport, and is the parent species from which other ROS are generated.

Estimates from *in vitro* experiments suggest that 1-4% of oxygen consumed by the mitochondrial respiratory chain is converted to $O_2 \cdot^-$, although the extent to which this reflects the *in vivo* situation is not clear (discussed in Murphy, 2009). The electron transport chain resides in the mitochondrial inner membrane, where complex I (NADH-ubiquinone oxidoreductase) and complex III (ubiquinol-cytochrome c oxidoreductase) are generally regarded as the main sites of $O_2 \cdot^-$ production (summarized in fig. 1.5) (Raha and Robinson, 2000). Investigations into the specific site(s) of $O_2 \cdot^-$ production within complexes I and III, and the direction of $O_2 \cdot^-$ release, are ongoing. Release of $O_2 \cdot^-$ by complex I is thought to occur chiefly into the mitochondrial matrix, and release of $O_2 \cdot^-$ by complex III to occur bidirectionally, into the matrix and into the intermembrane space (Han et al., 2001; Lambert and Brand, 2004; Muller et al., 2004). Other typically minor sources of $O_2 \cdot^-$ include cellular oxidases (e.g. NADPH oxidase, xanthine oxidase, aldehyde oxidase), cytochrome P450s, cyclooxygenases, and activated neutrophils (Fridovich, 1995).

$O_2 \cdot^-$ itself is a relatively inert free radical, and can act either as an oxidizing or reducing agent. Reduction of cytochrome c and nitroblue tetrazolium by $O_2 \cdot^-$, for

example, has been exploited for use in colorimetric assays (McCord and Fridovich, 1969; Beauchamp and Fridovich, 1971). One target of $O_2 \cdot^-$ oxidation is the group of [4Fe-4S] center-containing enzymes, including aconitases and fumarases (Gardner and Fridovich, 1991; Flint et al., 1993). Oxidation of these enzymes by $O_2 \cdot^-$ causes inactivation and release of Fe^{2+}. One theory, for which there is growing experimental evidence (discussed in Jones, 2006a), holds that $O_2 \cdot^-$ is not an 'accidental' byproduct of mitochondrial electron transport, but rather serves an important role in coordinating energy metabolism. $O_2 \cdot^-$ production changes with O_2 and substrate availability for electron transport, and may act in several feedback loops to manage the rate of ATP production, govern ATP transport to the cytoplasm, and regulate Ca^{2+} uptake. $O_2 \cdot^-$ can also activate uncoupling proteins to negatively regulate ATP production (Echtay et al., 2002).

Macromolecular damage attributed to $O_2 \cdot^-$ may in fact be caused by other ROS that are produced from $O_2 \cdot^-$ in a series of enzymatic and non-enzymatic reactions (outlined below and summarized in fig. 1.5). $O_2 \cdot^-$ spontaneously dismutates to H_2O_2 and molecular oxygen (equation [1]) at a rate that is accelerated four-fold by superoxide dismutase enzymes [2]. Note in [1] that $O_2 \cdot^-$ exists in equilibrium with its protonated form, hydroperoxyl radical ($HO_2 \cdot$). $HO_2 \cdot$ makes up only about 0.25% of total $O_2 \cdot^-$ at physiologic pH but is more apt than $O_2 \cdot^-$ to participate in lipid peroxidation and is also capable of crossing lipid bilayers (Halliwell and Gutteridge, 1990).

[1] $$O_2 \cdot^- + H^+ \rightleftarrows HO_2 \cdot$$

$$HO_2 \cdot + O_2 \cdot^- + H^+ \longrightarrow H_2O_2 + O_2$$

[2] $O_2 \cdot^- + SOD\text{-}M^{(n+1)} \longrightarrow O_2 + SOD\text{-}M^{(n)}$ ($M = Cu^+$ or Mn^{2+})

$O_2 \cdot^- + 2H^+ + SOD\text{-}M^{(n)} \longrightarrow SOD\text{-}M^{(n+1)} + H_2O_2$

$2O_2 \cdot^- + 2H^+ \longrightarrow O_2 + H_2O_2$ (Net reaction)

$O_2 \cdot^-$ also reacts with nitric oxide ($NO \cdot$) at a diffusion-limited rate to produce $ONOO^-$, which exists in equilibrium with its protonated form at physiologic pH [4] (Blough and Zafiriou, 1985). $ONOO^-$ and ONOOH are strong oxidants that decompose into other reactive species, including $\cdot OH$ and nitrogen dioxide ($NO_2 \cdot$) [5] (Beckman et al., 1990).

[4] $O_2 \cdot^- + NO \cdot \longrightarrow ONOO^-$

$ONOO^- + H^+ \rightleftarrows ONOOH$

[5] $ONOOH \longrightarrow \cdot OH + NO_2 \cdot \longrightarrow NO_3^- + H^+$

The Fenton reaction [6], another important source of $\cdot OH$, occurs in the presence of H_2O_2 and transition metals (namely Fe^{2+}) (Halliwell and Gutteridge, 1992).

[6] $Fe^{2+} + H_2O_2 \longrightarrow Fe^{3+} + \cdot OH + OH^-$

H_2O_2 produced by these reactions, like $O_2 \cdot^-$, is relatively unreactive and likely to play an important signaling role in cells (reviewed in Giorgio et al., 2007). H_2O_2 causes reversible redox modifications in numerous protein targets, alters gene expression, and depending on the intracellular concentration, alternately mediates cell proliferation or cell death pathways. In contrast, $ONOO^-$, $\cdot OH$, and $NO_2 \cdot$ are more reactive oxidants capable

of damaging proteins, lipids, and DNA (Alvarez and Radi, 2003). Oxidative damage to proteins can cause aggregation, enzymatic inactivation, and trigger degradation by the proteasome. Free radical attack of lipids affects membrane fluidity and permeability, and is often accompanied by damage to integral membrane proteins (Halliwell, 2006). DNA damage, such as ·OH-mediated production of 8-hydroxy-2'deoxyguanosine (8OHdG), is a major cause of mutations (Kasai, 2002). A number of critical targets within axons are known to be susceptible to oxidative damage, although the relevance to disease processes remains to be investigated. Examples include SNARE proteins responsible for vesicle release (Giniatullin et al., 2006), and neurofilament, which is rendered more vulnerable to degradation by calpains (Troncoso et al., 1995; Cookson et al., 1996; Gélinas et al., 2000).

Superoxide dismutases

Control of $O_2 \cdot^-$ levels in eukaryotes is accomplished by a family of abundant and highly conserved superoxide dismutase (SOD) enzymes, discovered by McCord and Fridovich (1969). In mammals, there are three known isoforms of SOD, all of which catalyze the dismutation of $O_2 \cdot^-$ to H_2O_2 and molecular oxygen [2], but differ in localization and structure (Zelko et al., 2002). Cu,Zn-SOD (SOD1) is a homodimer of 16 kD subunits with zinc and catalytic copper in the active site, expressed throughout the nucleus and cytoplasm, as well as in the mitochondrial intermembrane space (Weisiger and Fridovich, 1973; Sturtz et al., 2001; Iñarrea, 2002; Iñarrea et al., 2005). Mn-SOD (SOD2) is a homotetramer of 21 kD subunits with a catalytic manganese ion, found exclusively in the mitochondrial matrix. The most recently discovered, extracellular SOD

(SOD3) is a glycosylated, Cu- and Zn-containing homotetramer secreted by select a select group of cells including alveolar, renal tubular, and vascular smooth muscle cells (Marklund, 1982).

Compartmentalization of SOD enzymes is important given that negatively-charged $O_2 \cdot^-$ cannot freely diffuse across lipid bilayers (Gus'kova et al., 1984). Exceptions to this are $HO_2 \cdot$ as mentioned above, and anion-channel mediated transport of $O_2 \cdot^-$, first identified in erythrocytes (Lynch and Fridovich, 1978) and now attributed in large part to voltage-dependent anion channels in the mitochondrial outer membrane (Han et al., 2003). $O_2 \cdot^-$-derived H_2O_2 can also freely diffuse, although peroxidases that act downstream of SODs to convert H_2O_2 to H_2O are also compartmentalized. Mammalian cells express six isoforms of peroxiredoxins (Prx) that now appear to be the most critical peroxidase for removal of H_2O_2 (Rhee et al., 2005). Prx I, II, and VI are cytosolic, Prx III is mitochondrial, Prx IV is extracellular, and Prx V is found in mitochondria and peroxisomes. Glutathione peroxidase, found in the cytosol and mitochondria, and catalase, found in peroxisomes, also neutralize H_2O_2 (Chance et al., 1979).

Ablation of SODs in model organisms has yielded important information about the functional role of each of these enzymes. Loss of SOD2 causes neonatal lethality in mice associated with CNS and cardiac pathology and extensive mitochondrial damage (Lebovitz, 1996). This demonstrates a vital role for SOD2 in development, although conditional knockout of SOD2 in adult motor neurons showed no spontaneous degeneration (Misawa et al., 2006). SOD3-deficient mice develop normally and show no apparent phenotype at baseline, although are more sensitive to hyperoxia than wild-type

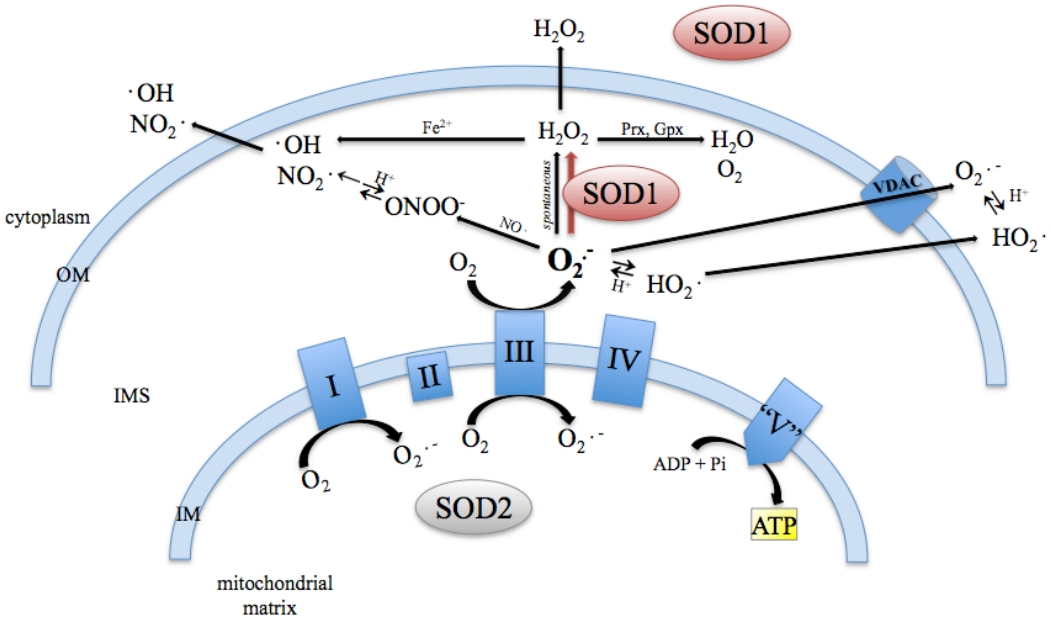

Fig. 1.5 Mitochondrial ROS release and compartmentalization of SOD enzymes.

Fig. 1.5 Mitochondrial ROS release and compartmentalization of SOD enzymes. Complexes I-IV of the mitochondrial electron transport chain are depicted in the mitochondrial inner membrane (IM), along with ATP synthase ("complex V"). Complex I releases $O_2 \cdot^-$ toward the matrix, while complex III releases $O_2 \cdot^-$ in to the matrix and into the intermembrane space (IMS). SOD2 is localized in the mitochondrial matrix where it neutralizes $O_2 \cdot^-$ (not depicted), and SOD1 is localized in the IMS and in the cytoplasm. SOD1 catalyzes the dismutation of $O_2 \cdot^-$ to H_2O_2 and O_2 (red arrow), at a rate 4-fold faster than the spontaneous dismutation of $O_2 \cdot^-$. H_2O_2 can then be neutralized by peroxiredoxins (Prx) or glutathione peroxidase (Gpx). Alternatively, in the presence of Fe^{2+}, H_2O_2 can undergo the Fenton reaction to produce $\cdot OH$. If not converted to H_2O_2, $O_2 \cdot^-$ can react rapidly with $NO \cdot$ to form $ONOO^-$, which decomposes into $\cdot OH$ and $NO_2 \cdot$. Negatively charged $O_2 \cdot^-$ cannot readily cross lipid bilayers, unless in its protonated form, $HO_2 \cdot$, or with access to voltage dependent anion channels (VDAC) in the outer membrane (OM). Other ROS, including H_2O_2, $\cdot OH$, $NO \cdot$, and $NO_2 \cdot$ can freely diffuse. Note that here ROS reactions are depicted in the mitochondrial IMS, but these reactions are not compartment specific. *Please refer to the text for references.*

mice (Carlsson et al., 1995). Loss of SOD1 shortens lifespan by 30% in mice (Elchuri et al., 2005), 80% in *Drosophila* (Phillips et al., 1989), and 25% in *C. elegans*, although *Sod5* also produces cytosolic SOD in these organisms (Yanase et al., 2009). In all three organisms, loss of SOD1 confers hypersensitivity to the $O_2 \cdot^-$-generating herbicide, paraquat (Phillips et al., 1989; Ho et al., 1998; Yanase et al., 2009). SOD1 knockout mice also show female infertility (Ho et al., 1998; Matzuk et al., 1998), a high incidence of hepatocellular carcinoma (Elchuri et al., 2005), and acceleration of age-related pathology, including cochlear hair cell loss (McFadden et al., 2001), noise-induced hearing loss (Ohlemiller et al., 1999), cataract formation (Reddy et al., 2004), retinal degeneration (Hashizume et al., 2008), vascular dysfunction (Didion et al., 2002), and skeletal muscle atrophy (Muller et al., 2006). These data suggest an important role for SOD1 during the aging process.

SOD1 and motor neuron disease

Familial amyotrophic lateral sclerosis (FALS) is currently the only human disease definitively linked to mutations in *SOD1*. The first mutations, most of which are inherited in an autosomal dominant pattern, were reported 15 years ago (Rosen et al., 1993). Since that time the number of *SOD1* mutations identified in FALS patients has grown to 142 (ALS online database, http://alsod.iop.kcl.ac.uk/Als/Index.aspx) (Wroe et al., 2008). Patients with *SOD1* mutations comprise about 20% of FALS, or approximately 2% of all ALS cases. *SOD1* (ALS1) is one of 10 known FALS loci, including two recently identified mutations in *FUS/TLS* (ALS6) and *TARDBP* (ALS10), both of which code for DNA/RNA-binding proteins (reviewed in Valdmanis et al., 2009). The cause of the

majority of ALS, termed sporadic ALS (SALS), remains unknown. Transgenic mice (Gurney et al., 1994; Wong et al., 1995) and rats (Howland et al., 2002) that overexpress mutant human SOD1 develop disease reminiscent of human ALS, and are the most widely used animal models. Since SALS and FALS are indistinguishable from a clinical and neuropathological perspective, it is assumed that findings from FALS models will also inform our understanding of SALS.

The identification of SOD1 mutations in FALS initially seemed to be a "smoking gun" for the idea that oxidative stress causes neurodegeneration (Ischiropoulos and Beckman, 2003), although the pathogenesis of mutant SOD1-mediated ALS, and the role of oxidative stress in disease, are still poorly understood. There is an extensive literature on postmortem tissue from SALS and FALS patients, reporting elevated markers of oxidized protein (Shaw et al., 1995; Beal et al., 1997; Ferrante et al., 1997), products of lipid peroxidation (Pedersen et al., 1998; Shibata et al., 2001), and oxidized DNA (Bogdanov et al., 2000). Similar findings have also been reported in SOD1 mutant mice (Andrus et al., 1998; Hall et al., 1998; Casoni et al., 2005). Markers of oxidative damage in urine and plasma have been proposed as useful biomarkers (Mitsumoto et al., 2008).

Numerous investigators have tested whether SOD1 enzymatic activity is altered in ALS patients (summarized in fig. 1.6). Red blood cell SOD1 activity is consistently reduced in FALS patients (n=8 studies), but not in SALS patients (n=10 studies). The relevance of SOD1 activity in red blood cells to SOD1 activity in motor neurons is questionable, since unlike motor neurons, red blood cells are rapidly turned over. Few studies have measured SOD1 activity levels in brain and spinal cord, and no studies to date have analyzed SOD1 activity in peripheral nerve or muscle. Brain and spinal cord

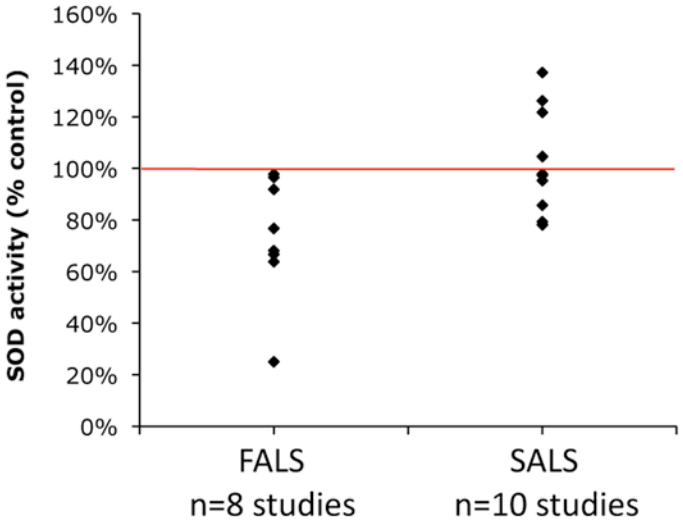

Fig. 1.6 SOD1 activity studies in red blood cells from FALS and SALS patients, expressed as percent of values reported for control patients.

FALS studies: Anderson et al. (1998); Kato et al. (2001); Winterbourn et al, (1995); Przedborski et al. (1996b); Nikolik-Kokik et al. (2006); Naini et al. (2007); Curti et al. (2002); Mase et al. (2001).

SALS studies: Torsdottir et al. (2000); Oteiza et al. (1997); Vinceti et al. (2002); Przedborski et al. (1996b); Nikolic-Kokic et al. (2006); Tuncel et al. (2006); Puymirat et al. (1994); Fiszman et al. (1999); Ihara et al. (1995); Cohen et al. (1996).

show reduced SOD1 activity in patients with SOD1 mutations (Bowling et al., 1993; Jonsson et al., 2004). No difference was seen in two studies of SALS brain tissue (Bowling et al., 1993; Przedborski et al., 1996a). In patients with autosomal dominant mutations, 50% of SOD1 activity is assumed to come from the normal allele, so any decrease in activity in FALS patients is attributed to compromised function of the mutant protein.

The current consensus in the field is that mutant SOD1-mediated motor neuron disease is not due to a loss of enzymatic function, but rather due to a gain of toxic function (reviewed in Rothstein, 2009). This is based on several lines of evidence. Disease duration and age of onset in patients does not seem to correlate with the dismutase activity (Bowling et al., 1995; Cleveland et al., 1995). Moreover, the majority of SOD1 mutations in ALS are point mutations, and are spread throughout the protein, not clustered in key regions such as the active site, metal binding site, or dimerization domain (Cleveland and Rothstein, 2001). Comparison of mutant SOD1 activity in transfected cells shows a range of activity from 0% (G85R) to 100% (G37R) of wild-type SOD1 (Borchelt et al., 1994). A dominant-negative effect of mutant SOD1 on wild-type SOD1 activity has also been ruled out (Borchelt et al., 1995).

The strongest evidence for a toxic gain of function comes from SOD1 mutant mice, in which disease onset and severity are dose-dependent based on the number of copies of the human SOD1 gene (Gurney et al., 1994; Wong et al., 1995). These mice develop disease despite super-normal levels of SOD1 activity (Turner, 2003), and normal expression of endogenous (wild-type) mouse SOD1. The idea that SOD1 knockout mice are normal or lack a neuromuscular phenotype is another commonly used justification for

the toxic gain of function hypothesis (Reaume et al., 1996), but is refuted by published studies (Flood, 1999; Shefner, 1999; Muller, 2006) and by the data in chapter IV.

A number of gains of function by mutant SOD1 have been reported, such as a propensity to misfold and form insoluble aggregates (Johnston et al., 2000; Vijayvergiya et al., 2005). Notably, several novel properties acquired by mutant SOD1 may lead to increased oxidative stress. For example, mutant SOD1 has a greater tendency than wild-type SOD1 to operate in reverse as a peroxidase, utilizing H_2O_2 as a substrate to produce $O_2 \cdot^-$ (Wiedau-Pazos et al., 1996). This reaction ultimately causes inactivation of SOD1 (Hodgson and Fridovich, 1975). Another common feature of mutant SOD1 proteins is a decreased affinity for zinc, possibly due to relaxation of the active site (Lyons et al., 1996). Zn-deficient SOD1 is less efficient at neutralizing $O_2 \cdot^-$ and more likely to interact with $ONOO^-$ to cause tyrosine nitration (Crow et al., 1997), which is increased in SOD1 mutant mice (Ferrante et al., 1997). Moreover, Zn-deficient SOD1 causes apoptosis of motor neurons by a $NO \cdot$ - dependent mechanism (Estévez et al., 1999). Thus, one hypothesis is that dose-dependent toxicity of mutant SOD1 may be related to a dose-dependent increase in aberrant oxidative chemistry. Particularly interesting are recent studies showing that experimental oxidation of wild-type SOD1 protein can cause it to behave more like mutant SOD1(Ezzi et al., 2007; Kabashi et al., 2007).

Neuromuscular phenotype of SOD1 KO mice

The SOD1 KO mouse shows a phenotype of accelerated senescence, susceptibility to environmental oxidants, and age-related pathology. Studies in these mice also point to an important neuroprotective role for SOD1. Spontaneous degeneration of

cochlear hair cells (McFadden et al., 1999) and retinal neurons (Hashizume et al., 2008) is observed *in vivo,* and CNS neurons in these animals are more susceptible to excitotoxic (Schwartz et al., 1998), ischemic (Kondo et al., 1997), and traumatic injury (Reaume et al., 1996). *In vitro*, antisense knockdown of SOD1 causes apoptosis of PC12 cells (Troy and Shelanski, 1994), and protracted death of spinal motor neurons in organotypic slice cultures (Rothstein et al., 1994). Still, neither spinal motor neuron loss, nor degeneration of ventral or dorsal root axons is seen *in vivo*, even out to 17 and 19 months of age, respectively (Reaume et al., 1996; Flood et al., 1999; Shefner et al., 1999). These data, combined with lack of a motor phenotype in young animals (Reaume et al., 1996), led to the general consensus in the ALS field that SOD1 KO mice lack neuromuscular deficits.

However, cross sections of SOD1 KO hind limb muscles at 6 and 12 months demonstrate muscle fiber atrophy and fiber-type grouping (Flood et al., 1999), and EMG recordings show spontaneous activity and progressive loss of motor units (Shefner et al., 1999), classic findings consistent with the presence of a motor axonopathy. By 15 months of age, SOD1 KO mice perform poorly on rotarod, and by 20 months of age, 50% loss of muscle mass is seen (Muller et al., 2006). Thus, when followed out to an advanced age, SOD1 KO mice do, in fact, develop a neuromuscular phenotype. Since no motor neuron loss is seen in these animals, an obvious question is whether oxidative stress-mediated defects in motor axons and/or muscle may account for the phenotype. The observations of neurogenic atrophy and spontaneous activity in these animals strongly suggest the presence of motor axonopathy; however, morphologic analysis of NMJ innervation has not been previously carried out in SOD1 KO mice, nor has oxidative stress been measured in their peripheral nerves.

SOD1 KO skeletal muscle has been more extensively studied, based on the hypothesis that oxidative stress in muscle may be the underlying cause of age-related sarcopenia in these animals. Muller and colleagues measured markers of oxidative damage to protein, lipids, and DNA in muscle at 5 and 20 months of age (2006). F_2-isoprostanes, a marker of lipid peroxidation, were significantly increased at both time points, and protein carbonyls were increased by 40% relative to controls at 5 months, although no difference was seen at 20 months. These same investigators also reported increased ROS release from isolated skeletal muscle mitochondria (Muller et al., 2007). When SOD1 KO mice, SOD1 mutant (FALS) mice, and aging wild-type mice were compared, a close correlation was observed between the severity of skeletal muscle atrophy and mitochondrial ROS release. However, when sciatic nerve axotomy was performed to test the influence of denervation, a dramatic and persistent (30-fold) increase in ROS release by skeletal muscle mitochondria was observed. This does not take away from the idea that ROS in muscle causes atrophy, but suggests that innervation may be a critical factor controlling muscle ROS release.

The observation of increased mitochondrial ROS release due to loss of SOD1 may be surprising, given the traditional concept of SOD1 as the 'cytoplasmic' SOD, and SOD2 as the 'mitochondrial' SOD. However, SOD1 is widely acknowledged to be expressed and active in the mitochondrial intermembrane space (IMS) (Weisiger and Fridovich, 1973; Sturtz et al., 2001; Iñarrea, 2002; Iñarrea et al., 2005), and emerging evidence from SOD1 KO models suggests that IMS SOD1 may be functionally important. SOD1 knockdown in SH-SY5Y cells causes preferential protein carbonylation within mitochondria and not in the cytosol, associated with loss of mitochondrial

membrane potential and decreased ATP production (Aquilano et al., 2006). Progressive inactivation of cytosolic and mitochondrial aconitase is detected in *Sod1-/-* liver tissue (Elchuri et al., 2005). Increased ROS generation in isolated mitochondria was also recently reported in *Sod1-/- C. elegans* (Yanase et al., 2009), similar to the data from SOD1 KO mice (Muller et al., 2007). Still, the hypothesis that mitochondrial defects due to loss of SOD1 in the IMS play a role in age-associated pathology remains to be tested.

Summary

Mitochondrial electron transport is a continuous source of $O_2 \cdot^-$ and $O_2 \cdot^-$-derived ROS, which may play an important role in normal physiology and in disease. Evidence from motor neuron disease patients and animal models suggests that oxidative stress, and SOD1 specifically, may play a central role in disease pathogenesis, although the underlying mechanism is poorly understood. Data from SOD1 KO mice suggest an important role for SOD1 in maintaining neuronal viability under stress and during the aging process. Progressive muscle atrophy and EMG changes reported in this model are consistent with the presence of a motor axonopathy. Therefore the SOD1 KO may be an important experimental model in which to study oxidative stress-mediated changes in axons and to investigate the normal role of SOD1 in axon survival.

Research overview

The focus of this dissertation is oxidative-stress mediated distal axonal degeneration. Oxidative stress is commonly implicated in the pathogenesis of human neurodegenerative disease and peripheral neuropathy, but poorly understood in part due to lack of good animal models. SOD1 knockout mice display a phenotype consistent with a possible motor axonopathy, although morphologic changes in axons of these mice have not been previously characterized. We carried out a series of studies to characterize axonal degeneration and oxidative stress in the SOD1 KO model *in vitro* and *in vivo,* and investigated two approaches for axonal protection. We provide proof of principle for the idea that chronic oxidative stress is sufficient to cause distal axonal degeneration *in vivo*, and demonstrate a non-canonical role for SOD1 in mitochondria.

I. Characterization of axon dependence on SOD1 *in vitro* and *in vivo*, and confirmation of oxidative stress as the mechanism of axon injury.

Previous studies from the SOD1 KO mouse demonstrated a neuroprotective role for SOD1 in certain neuronal subtypes and in models of CNS injury. However, the requirement for SOD1 in PNS axons is essentially unexplored. We first tested whether SOD1 is necessary for axon survival *in vitro* using dorsal root ganglion (DRG) cultures, and report spontaneous degeneration of *Sod1-/-* axons that was attenuated by antioxidant treatment. We also show data consistent with the idea that axons are more vulnerable to loss of SOD1 than neuronal cell bodies. These findings were recapitulated by treatment of DRGs with paraquat and diquat, redox-cycling herbicides that generate superoxide

within cells. This study reinforces the hypothesis that oxidative stress due to loss of SOD1 causes axonal degeneration.

Next, we characterized the spatiotemporal progression of axonal degeneration *in vivo*. We systematically analyzed the morphology of distal motor and sensory axons from 1 to 18 months of age, and monitored for changes proximally in peripheral nerve, nerve roots, and spinal cord. We demonstrate that pathology specifically affects distal motor axons, sparing sensory axons and proximal regions. Oxidative stress in peripheral nerve, but not muscle, coincided with the onset of denervation, and primary motor neuron culture showed poor axon outgrowth and limited survival that was rescued by antioxidant treatment. This study demonstrates that oxidative stress due to loss of SOD1 causes a progressive motor axonopathy *in vivo,* and implicates oxidative stress as a potential mechanism of axon degeneration in motor neuron disease and other motor neuropathies.

II. Investigation of strategies to rescue SOD1 KO axons, based on (A) a general axon protective approach, or (B) a targeted approach.

Approaches for treating oxidative stress-mediated disease based on antioxidant therapy alone have been largely unsuccessful. We tested whether the gene for 'slow Wallerian degeneration' (Wld^S) may provide an alternative means of axon protection in the *Sod1-/-* model. We saw no effect of Wld^S on motor axonopathy in the *Sod1-/-* model, an also found no protective effect in DRG cultures due to loss of SOD1 or treatment with paraquat. Thus, Wld^S is ineffective against oxidative stress-mediated axonal degeneration.

Ideas for altered expression or localization of *Wld*^{S} are discussed that may improve the outcome.

Next we tested a targeted approach, in an attempt to neutralize the source of superoxide we hypothesized may be causing axonal degeneration. *Sod1-/-* mice were crossed with mice expressing wild-type human SOD1 only in the mitochondrial IMS. We observed robust protection of axons *in vitro* and *in vivo* that did not diminish over time. This suggests that, in contrast to the common perception of SOD1 as the "cytoplasmic SOD", an important and perhaps vital role of SOD1 for motor axon survival is carried out in mitochondria.

CHAPTER II. Materials and Methods

Animals

All animal procedures were approved by the Emory University Institutional Animal Care and Use Committee and carried out according to current AVMA recommendations. Mice were housed in microisolator cages on a 12 hr light-dark cycle and given free access to food and water. Genotyping was by standard PCR analysis on tail-snip DNA, with the exception of *thy1-YFP16* mice. YFP status was determined by fluorescent examination of ear punch biopsies taken at weaning. Male and female mice showed comparable findings on all analyses, so data were combined.

Genotypes and breeding strategies

Sod1-/- mice, generated by Huang and colleagues (1997), were obtained from Marie Csete (Emory University) (Muller et al., 2006). *Sod1-/-* males were crossed with *thy1-YFP16* females (Feng et al., 2000) to obtain *Sod1+/-, thy1-YFP16* breeders, expressing yellow fluorescent protein (YFP) in all motor axons. Both transgenic lines were on a C57BL/6 background. For ease of description, *thy1-YFP16* will be omitted from the genotype and expression should be assumed unless otherwise noted.

Wld^S mice, maintained in-house, were crossed with *Sod1-/-* mice in a two-step breeding process to generate animals of the genotype *Sod1-/-,* Wld^S. First, *Sod1-/-* males were bred with homozygous Wld^S females to generate F1 heterozygotes of the genotype: *Sod1+/-,* Wld^S. F1 heterozygotes were then crossed to generate mice of the target genotype: *Sod1-/-,* Wld^S, and littermate controls. Copy number of Wld^S (homozygous or heterozygous) was not determined, and all Wld^S-positive mice were included.

Transgenic mice overexpressing wild-type human SOD1 targeted to the mitochondrial intermembrane space (IMS, abbrev. *IMS-SOD1*) were generated and characterized in the lab of Giovanni Manfredi on a hybrid background (Cornell University). Following transfer to Emory, a two-step mating process was carried out to generate mice expressing only *IMS-SOD1*. *Sod1-/-* males were crossed with *IMS-SOD1* females to generate F1 heterozygotes: *IMS-SOD1, Sod1+/-*. F1 heterozygotes were then crossed to generate mice of the target genotype *IMS-SOD1, Sod1-/-* and littermate controls.

Behavioral analysis

Grip strength was assayed by a wire hang test as described (Sango et al., 1996). Mice were given three trials of 300 seconds to remain suspended from a 10 cm x 10 cm wire grid. The maximum latency to fall (in seconds) over two consecutive days of testing was recorded for each animal.

Wallerian degeneration study

Sciatic nerve axotomy was performed in four month-old *Sod1+/+*, *Sod1+/+, Wld*^{S}, *Sod1-/-,* and *Sod1-/-, Wld*^{S} mice (n=3 per genotype). Mice were anesthetized with 4% chloral hydrate, the right sciatic nerve exposed, and several mm of nerve excised at mid-thigh level. The left sciatic nerve was left intact to serve as a control. Three days later, animals were sacrificed for pathologic analysis.

Neuropathology

Animals were deeply anesthetized with 4% chloral hydrate and perfused with saline and/or 4% paraformaldehyde (PFA). Muscle tissues were removed immediately, and other tissues were post-fixed *in situ* for 24 hours prior to dissection.

NMJ morphology

NMJs in hindlimb muscles were assessed as previously described (Fischer et al., 2004). Medial gastrocnemius (MGC), tibialis anterior (TA) and soleus muscles were dissected, pinned in mild stretch, and fixed by immersion for 30 min in 4% PFA/PBS (pH 7.4). After rinsing in PBS, muscles were cryoprotected in 30% sucrose/PBS (47-72 hrs at 4°C) and flash-frozen in supercooled isopentane. Muscles were sectioned longitudinally at 35 μm and mounted on Superfrost Plus slides (Fisher) for staining. Acetylcholine receptors at the motor endplate were labeled with Alexa Fluor 555-conjugated α-bungarotoxin (Invitrogen), diluted 1:5000 in PBS (30 min., RT). Motor axon terminals were identified by YFP fluorescence in *thy1-YFP16*-positive animals. In a few animals that were *thy1-YFP16*-negative, motor axons were immunostained with rabbit anti-PGP9.5 (1:500, UltraClone Ltd., Isle of Wight, UK), followed by FITC goat anti-rabbit secondary (1:150, Jackson Immuno). No difference in innervation was seen between the two methods (not shown), so the data were pooled.

Every fourth section through each muscle was examined for quantification. Innervated, intermediate, and denervated endplates were defined by complete, partial, or absent overlap between nerve terminal and endplate, respectively. Ultraterminal sprouts were defined as processes originating from the endplate region that could be clearly

distinguished from the incoming axon (Aigner et al., 1995; Tam and Gordon, 2003), and were reported as a percent of total endplates assessed. By this method, the average number of endplates assessed per muscle was 898 ± 203 (TA), 1210 ± 249 (MGC), and 262 ± 52 (soleus).

Epidermal nerve fibers

The density of nerve fibers in the second plantar footpad was determined by the method of Hsieh and colleagues (Hsieh et al., 2000). 30 µm frozen sections were cut perpendicular to the skin surface along the entire footpad. Every fourth section was immunostained for the neuronal marker PGP9.5 (1:600), followed by FITC goat anti-rabbit secondary (1:100). Intra-epidermal nerve fibers (excluding branches) were counted by an investigator who was blinded to genotype. Results were expressed as the number fibers per millimeter of epidermis, as determined using ImageJ software (http://rsb.info.nih.gov/ij/).

Spinal cord immunohistochemistry

The entire lumbar spinal cord was dissected following 24 hrs post-fixation (4% PFA, 4°C). The tissue was dehydrated and embedded paraffin wax. 8-10 µm serial sections were cut, deparaffinized in xylene, and stained with cresyl violet to evaluate motor neuron histology. Additional sections were immunostained according to standard procedures with the following antibodies: GFAP for astrocytes (1:1000, DAKO), Iba1 for microglia (1:1000, Wako), SMI-31 for phosphorylated neurofilament (NF-H/NF-M, 1:500, Sternberger Monoclonals), ubiquitin (1:400, DAKO), and TDP-43 (1:1000,

Proteintech). Sections were developed using the Vectastain ABC kit (Vector Labs, Burlingame, CA), and reacted with diaminobenzidine (DAB).

Peripheral nerve histology

Nerves and nerve roots were dissected out and immersion-fixed in 5% buffered glutaraldehyde (pH 7.4) at 4°C for 24-48 hrs. Tissue was then stored in 0.1 M phosphate buffer at 4°C until processing. Tissue was treated with 1% osmium tetroxide for 90 min, dehydrated through graded alcohols, and embedded in Epon plastic (EM Sciences, Cincinnati, OH). Cross-sections (720 nm) were stained with toluidine blue, rinsed, and coverslipped.

Imaging

Confocal microscopy (for NMJs and epidermal nerve fibers) was performed on a Zeiss LSM 510 NLO META system, coupled to a Zeiss Axiovert 100M inverted microscope. Z-stack projections were obtained with LSM Image Examiner software (Zeiss). Light microscopy (for histology and immunostaining) was performed on a Nikon Optiphot-2 microscope equipped with an Olympus DP25 digital camera. Brightness and contrast of images were adjusted using Photoshop CS (Adobe).

Tissue analysis

SOD1 expression and activity.

Lumbar spinal cord, sciatic nerve, and TA from saline-perfused 12 month-old mice were homogenized in lysis buffer containing 1.5% NP-40, 1 mM EGTA, 2 mM Na_3VO_4, 6 mM NaF, and complete protease inhibitor cocktail (Roche). SOD1 protein was detected by standard immunoblotting using sheep anti-SOD1 (1:5000, Calbiochem). The loading control for spinal cord and sciatic nerve was mouse anti-β-actin (1:5000, Sigma), and the loading control for tibialis anterior was mouse anti-EF1α (1:25,000, Upstate). SOD1 enzymatic activity was assayed as previously described (Beauchamp and Fridovich, 1971). Proteins were separated by native PAGE. Gels were immersed in 2.45 mM nitroblue tetrazolium (Sigma) in 36 mM potassium phosphate buffer, pH 7.8 for 20 minutes in the dark at room temperature, followed by 15 minutes in the same buffer containing 28 μM riboflavin (Sigma) and 28 mM TEMED (Bio-Rad). Gels were placed on a light box for approximately 15 minutes or until maximum contrast was reached, and digitally photographed using an AlphaImager HP (Alpha Innotech).

GSH Redox Potential

Concentrations of glutathione (GSH) and glutathione disulfide (GSSG) in tibial nerve and MGC were determined by HPLC as described (Jones, 2002; Jones et al., 2004). Fresh tissues were rapidly dissected and homogenized in 5% (w/v) perchloric acid containing 0.2 M boric acid and 10 μM γ-EE (internal standard). Thiols were derivitized with iodoacetic acid and dansyl chloride to form *S*-carboxymethyl, *N*-dansyl derivatives for HPLC analysis with fluorescence detection. Quantitation was obtained by integration

relative to the internal standard and normalized to protein concentration as measured by the DC Protein Assay (Bio-Rad). The redox potential E_h (in mV) was calculated using the Nernst equation: $E_h = E_0 + (2.303RT/nF)*\log([GSSG]/[GSH]^2)$.

Primary neuronal cultures:

Dorsal root ganglia (DRGs)

DRG explants were derived from postnatal day 4 (P4) mice and plated four per dish in 35mm tissue culture-treated dishes. Dishes were coated with a thin layer of rat tail collagen type 1 (BD Bioscience, No. 354236), dried overnight at room temperature and rehydrated with DMEM and 1% FBS for at least 1 hour prior to use. Growth medium was changed weekly and consisted of DMEM (with 4.5g/L glucose and L-glutamine) supplemented with N2 (Invitrogen) and 100 ng/mL 7S NGF (Alomone Labs, Jerusalem, Israel). Non-neuronal cells were not depleted due to toxicity of anti-mitotic agents in preliminary studies (not shown). For culture at 6% O_2 (5% CO_2), cells were placed in modular incubators (Billups-Rothenberg, DelMar CA, USA) after equilibration in a gas-controlled environment. Incubators were re-equilibrated to 6% O_2 every 24 hours.

Serial digital images were taken at regular intervals on an Olympus CK40 inverted light microscope equipped with a Cohu 2222-1040 digital camera. Due to the large size of DRG explants, overlapping frames were captured and reassembled in Photoshop CS (Adobe) using the automated photomerge feature. The length of the longest axon and total area of the DRG and the surrounding axon halo were measured using ImageJ software (http://rsb.info.nih.gov/ij/). To normalize for the variation in starting size between different DRGs, measurements were expressed as percent of day 2

(the first day of measurement), or as percent of baseline (day 0 of treatment). DRGs grown in 6% O_2 were not removed for serial imaging, so data are reported as absolute measurements acquired on day 6 (final day in culture).

Viability of DRG axons versus cell bodies was evaluated using the MTT assay, as previously described (MacInnis and Campenot, 2005; Song et al., 2006). A 5 mg/ml stock solution of 3-(4,5-dimethylthiazol-2-yl)-2,5-diphenyltetrazolium bromide (Sigma M5655) was prepared in DMEM, and added directly to culture dishes at a 1:10 dilution. Cells were returned to the incubator for 2 hours, and then fixed with 4% PFA/PBS for 15 min. Viability was assessed qualitatively by light microscopy, to evaluate NADPH and NADH-dependent conversion of the yellow tetrazolium dye to dark purple MTT formazan crystals (Berridge and Tan, 1993).

SOD1 siRNA sequence 396 (Yokota et al., 2004) was synthesized and cloned into a lentiviral vector for delivery to DRG neurons as previously described (Conforti et al., 2007b). Prior to use in DRG neurons, efficacy of knockdown was tested in mitomycin-inactivated mouse embryonic fibroblasts. One week following lentivirus delivery, SOD1 expression was determined by Western blotting for SOD1 (sheep anti-SOD1, Calbiochem) using standard protocols. Band density was measured using Odyssey software (LI-COR), and normalized to ß-actin. Lentivirus was added to wild-type DRGs at day 7 ("day 0" for axon measurements), at a final titer of 1×10^7 particles/mL culture medium. DRGs were fixed on day 24 and immunostained with a rabbit polyclonal antibody for PGP9.5 (1:700, UltraClone Ltd., Isle of Wight, UK). Distal axons were viewed on an Olympus IK51 fluorescent microscope and 100 axons per DRG were

scored as either continuous or discontinuous (fragmented) by an investigator blinded to treatment group. Images were captured with an Olympus Qcolor3 digital camera.

Paraquat (PQ; 1,1′-Dimethyl-4,4′-bipyridinium dichloride) and diquat (DQ; 1,1'-Ethylene-2,2'-bipyridyldiylium dibromide) were obtained from Sigma. Stock solutions were prepared in ddH_2O and stored at 4°C. To evaluate toxicity in DRG cultures, a single dose of PQ (25, 50, or 100 μM) or DQ (50 μM) was added to wild-type DRGs on day 14 in culture ("day 0" for axon measurements). DRGs were imaged at regular intervals following PQ/DQ exposure and axon length and DRG area were measured. To determine the effect of endogenous SOD1 expression, *Sod1*+/+ DRGs were compared to DRGs from *Sod1*+/- littermates.

Spinal motor neurons

Motor neurons were enriched from E12.5 mouse embryos by density centrifugation through 10% (v/v) Optiprep (Axis Shield) as previously described (Zhang et al., 2006). By this method, 84.7 ± 4.8% of cells at 24 hours were immunoreactive for Hb9 (1:1000, Abcam). Hb9 is a transcription factor selectively expressed by post-mitotic neurons (Wichterle et al., 2002), and by a population of spinal interneurons (Kwan et al., 2009) that should be excluded by the density centrifugation (Henderson et al., 1995; Arce et al., 1999).

Neurons were plated on Matrigel-coated coverslips (1:25, BD Bioscience) in Neurobasal medium (Invitrogen) with 2% B27 supplement minus antioxidants (Invitrogen), 2% horse serum, 0.5 mM Glutamax (Invitrogen), BDNF, CNTF, GDNF, and NT-3 (10 ng/mL, Peprotech). For antioxidant experiments, 1.25, 2.5, or 5 mM N-

acetylcysteine (NAC) was added at the time of plating. Individual spinal cords were kept separate during cell isolation and plating, and genotype determined afterward by PCR.

Axon length was determined by systematic random sampling of cells along a pre-marked grid at 24 hours. Motor neurons were identified morphologically under phase contrast and photographed at 20x magnification. Axons were manually traced and measured using Image J software. In cells with multiple processes, the axon was considered to be the longest process. The average number of neurons analyzed in each of four trials was 130 ± 41 (*Sod1+/+)*, 158 ± 34 (*Sod1+/-)*, and 163 ± 19 (*Sod1-/-)*, or 500-600 neurons per group (n=4 was used for the purpose of statistical analysis).

Mitochondrial density in axons was evaluated using Mitotracker Red CM-H_2XRos (Invitrogen). Dye was added to cells at a final concentration of 250 nM for 30 minuntes in serum-free medium. Cells were returned to growth medium for 10 min. and fixed in pre-warmed 4% PFA/PBS (15 min., room temperature). Coverslips were inverted onto slides using anti-fade mounting medium (Vectashield + DAPI, Vector Labs), and neurons examined by standard fluorescence microscopy. In some experiments, Mitotracker staining was followed by immunostaining with a mouse monoclonal antibody specific for human SOD1 (Sigma, 1:500). 25 neurons per coverslip were selected and photographed at 40x magnification by unbiased coverslip scanning. Mitochondrial density was evaluated morphologically using Image J software. Length of individual mitochondria were determined, combined, and divided by the length of the axon. At least three replicates per genotype were obtained over the course of multiple motor neuron preparations.

Statistical analysis

Results from animal experiments are expressed as mean ± standard deviation unless otherwise noted. Cell culture studies are expressed as mean ± SEM for at least three independent replicates per genotype or treatment condition. Comparisons between groups were made by Student's t-test or ANOVA, with Tukey post-hoc analysis (α = 0.05) using Prism software (GraphPad).

CHAPTER III. Loss of Cu,Zn-superoxide dismutase (SOD1) and superoxide-generating herbicides cause axonal degeneration in mouse DRG cultures

Introduction

Axonal degeneration underlies numerous inherited and sporadic forms of peripheral neuropathy, and is increasingly recognized as a key pathologic feature and therapeutic target in neurodegenerative disease (Coleman and Perry, 2002; Raff et al., 2002). Growing evidence from models of motor neuron disease (Fischer and Glass, 2007), Parkinson's disease (Chung et al., 2009), Alzheimer's disease (Stokin et al., 2005), and Huntington's disease (Li et al., 2001) demonstrates axonal defects that occur prior to neuronal death and correlate closely with functional decline. But despite progress in understanding common downstream pathways of axonal demise (Coleman, 2005), the initial triggers for axon degeneration in disease remain largely unknown.

Aging is the most prominent risk factor for degenerative diseases of the nervous system, even in patients with disease-causing mutations. Normal aging may, in fact, represent the most common cause of peripheral neuropathy, affecting an estimated 7 percent of individuals 65 to 84 (Baldereschi et al., 2007). Spontaneous, age-related peripheral neuropathy is also a well-described phenomenon in laboratory mice (Ceballos et al., 1999) and rats (Sharma et al., 1980). One obvious factor that may increase susceptibility to neuropathy with aging is oxidative stress.

There is experimental evidence to support the idea that oxidative stress causes axonal degeneration. Hyperglycemia-induced free radical production is a widely used model of diabetic neuropathy (reviewed in Figueroa-Romero et al., 2008). Several *in*

vitro models of oxidative stress-mediated axonal degeneration have also been developed using exogenous agents such as rotenone (Press and Milbrandt, 2008), H_2O_2 (Lourenssen et al., 2009), and 4-hydroxynonenal (Akude et al., 2009). Although localized knockdown of manganese-superoxide dismutase (SOD2) has been shown to cause optic neuropathy (Qi et al., 2003), models of peripheral neuropathy due to loss of antioxidant defenses are lacking. This may be related to the lethal consequences of loss of some antioxidant enzymes (Lebovitz, 1996; Dalton et al., 2000), and the comparatively mild effects of others, presumably due to redundancy or compensation (Carlsson et al., 1995; Ho et al., 1997).

SOD1 is an abundant and highly conserved enzyme found in the cytoplasm, nucleus, and mitochondrial intermembrane space that converts superoxide ($O_2\cdot^-$) to H_2O_2 and O_2 (McCord and Fridovich, 1969). Loss of SOD1 in mice is not lethal, but causes a 30% reduction in lifespan (Elchuri et al., 2005) and accelerated age-related pathology, including cataract formation (Reddy et al., 2004), cochlear hair cell loss (McFadden et al., 1999), retinal degeneration (Hashizume et al., 2008), and skeletal muscle atrophy (Muller et al., 2006). Anti-sense knockdown of SOD1 has been shown to cause death of PC12 cells (Troy and Shelanski, 1994) and motor neurons in spinal cord slice culture (Rothstein et al., 1994), although axons were not evaluated in these studies. Here, we tested whether SOD1 may be required for survival of axons *in vitro,* using the DRG culture model that we have used previously in studies of chemotherapy-induced neuropathy (Wang et al., 2000; Wang et al., 2002).

We report spontaneous axonal degeneration in *Sod1-/-* DRGs, and in wild-type DRGs following siRNA knockdown of SOD1. We also found that exposure to paraquat

(PQ) and diquat (DQ), redox-cycling herbicides that increase intracellular $O_2\cdot^-$ (Sandy et al., 1986), caused robust, dose-dependent axon degeneration. Toxicity in this paradigm was exacerbated by SOD1 deficiency. Finally, we provide evidence using vital staining to suggest that DRG axons are more vulnerable to injury than neuronal cell bodies in these models. We conclude that DRG axons *in vitro* are highly susceptible to oxidative stress-mediated degeneration due to loss of SOD1 or increased $O_2\cdot^-$ production. These data reinforce the idea that oxidative stress may contribute to the pathogenesis of axonal degeneration in peripheral neuropathy.

Results

SOD1 is required for DRG survival in vitro

To test the effect of loss of SOD1 on DRG survival, DRG explants were cultured from P4 *Sod1-/-* mice and their *Sod1+/-* and *Sod1+/+* littermates (fig. 1). *Sod1-/-* DRGs initially extended short axons that were intact on day 2 (fig. 1a), but then fragmented and degenerated over a period of several days. In contrast, *Sod1+/-* and *Sod1+/+* axons grew rapidly over the first week in culture, as quantified by measurement of the longest axon and the total DRG area (fig. 1b-c). By day 6, *Sod1+/+* and +/- DRG area increased to 231 ± 11% and 243 ± 13% of day 2, respectively, while *Sod1-/-* DRG area dropped to 49 ± 5% ($p<0.001$).

Viability of axons and neuronal cell bodies was evaluated qualitatively using the MTT assay. On days 2, 4, and 6, MTT dye was added to the culture medium, and MTT reduction product indicating metabolic activity was visualized by bright field microscopy (fig. 2). In *Sod1+/+* and *Sod1+/-* DRGs, MTT staining was readily visualized in the ganglion and throughout the axons. *Sod1-/-* DRGs had a similar appearance on day 2. By

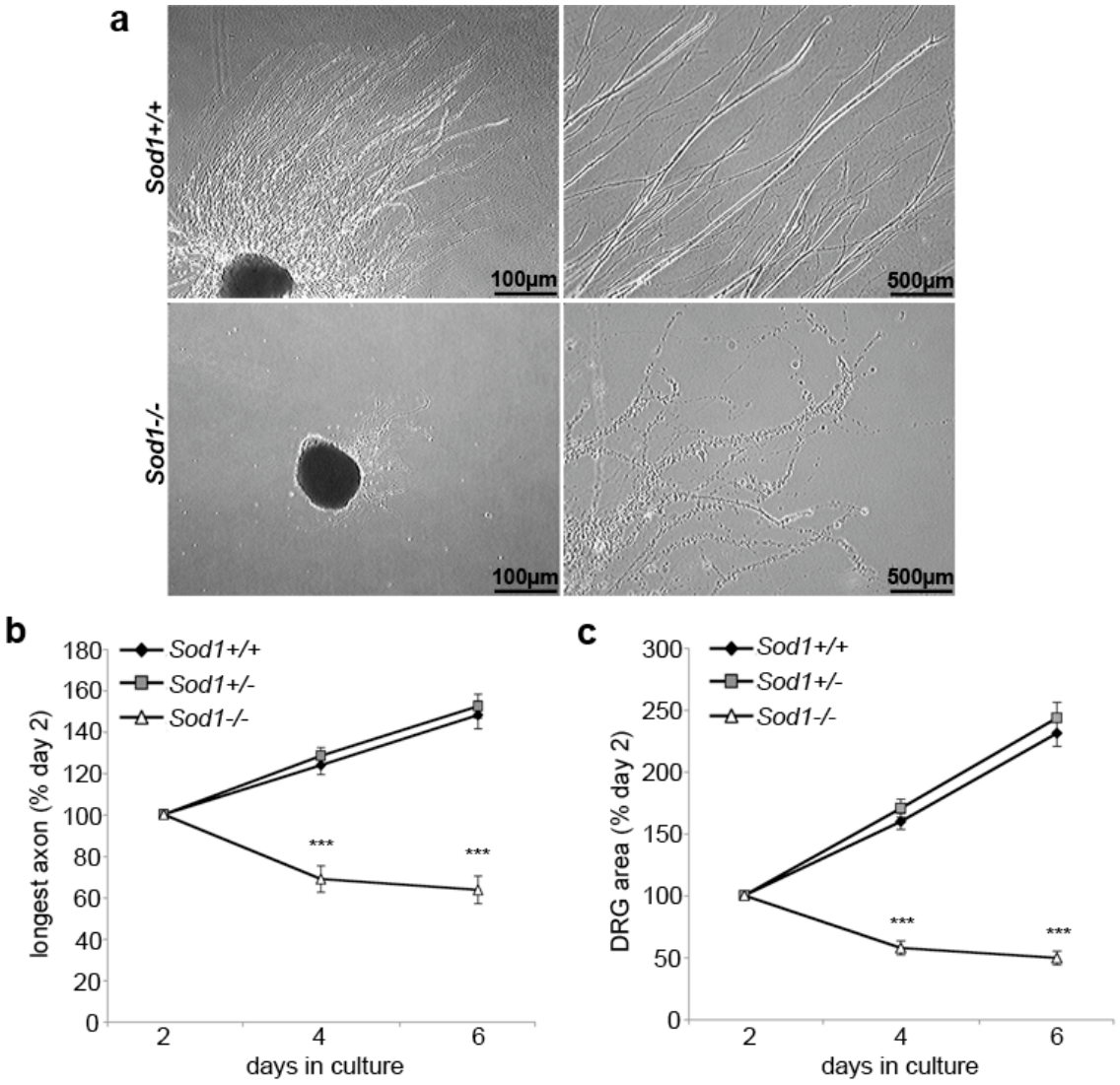

Fig. 3.1 SOD1 is required for DRG axon outgrowth and survival. DRGs were cultured from P4 *Sod1-/-* mice and their *Sod1+/-* and *Sod1+/+* littermates, and serial images taken every 2 days for morphologic analysis. **(a)** Representative DRGs from *Sod1+/+* and *Sod1-/-* mice, on day 6 in culture. *Sod1-/-* DRGs extended short axons that fragmented and degenerated beginning at 48 hours. **(b)** Length of the longest axon, expressed as percent of day 2 (***p<0.001 vs. *Sod1+/+* and +/-, two-way ANOVA). **(c)** DRG area, expressed as percent of day 2 (***p<0.001 vs. *Sod1+/+* and +/-, two-way ANOVA). In **(b)-(c),** n=4-9 animals per group (4-8 DRGs per animal).

day 4, numerous *Sod1-/-* axons were devoid of MTT staining (fig. 2, arrowheads), in contrast to the cell bodies and some axons that were still stained (fig. 2, arrows). By day 6, the majority of *Sod1-/-* axons were MTT-negative, while many ganglia were still MTT-positive (for an example of an MTT-negative ganglion, see fig. 3f). Taken together, these data demonstrate that SOD1 is required for DRG survival *in vitro* and suggest that axonal degeneration due to loss of SOD1 may precede degeneration of neuronal cell bodies.

Axonal degeneration is oxidative stress-mediated

To verify a role for oxidative stress in degeneration of *Sod1-/-* axons, we tested several antioxidant strategies, beginning with N-acetylcysteine (NAC). NAC is hydrolyzed to cysteine inside cells, where it acts as a precursor for GSH synthesis, a free radical-scavenger, and has GSH-independent effects on the thiol redox state (Jones et al., 1995; Schafer and Buettner, 2001). When a single dose of 1 or 5 mM NAC was added to culture media at the time of plating, increased axon outgrowth was observed (fig. 3a-c). Protection persisted over time in the 5 mM group, while axonal degeneration still occurred in the 1 mM group from days 2-6. On day 6, area of *Sod1-/-* DRGs treated with 5 mM NAC was 117 ± 10% of day 2 ($p<0.01$), compared to 60 ± 7% in 1 mM NAC-treated DRGs and 56 ± 6% in untreated DRGs.

Next, we treated *Sod1-/-* DRGs with ß-mercaptoethanol (BME), which facilitates cysteine uptake for GSH synthesis (Ishii et al., 1981). When 50 or 100 µM BME was added at the time of plating, a 58% ($p<0.05$) and 108% ($p<0.01$) increase in DRG area was observed, respectively (fig. 3d).

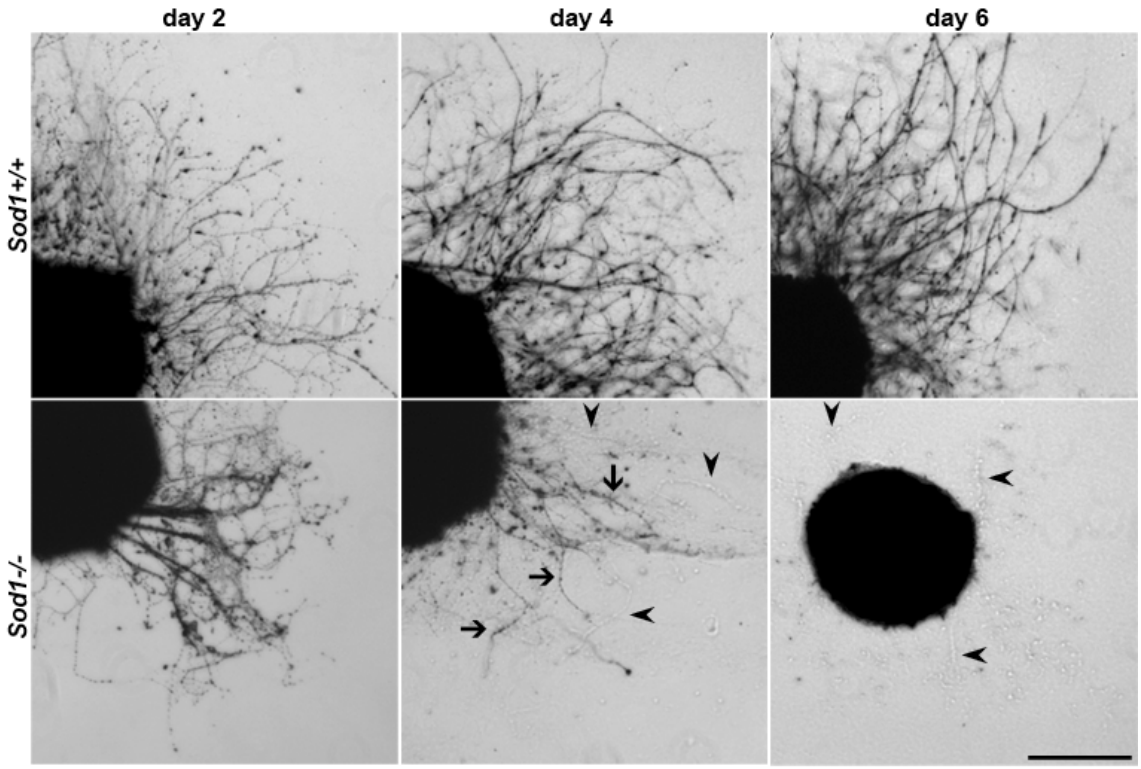

Fig. 3.2 Axonal degeneration due to loss of SOD1 precedes cell body degeneration. Viability of *Sod1+/+* and *Sod1-/-* DRGs was evaluated every two days via the MTT assay. On day 2, ganglia and axons in both groups were metabolically active (marked by the dark MTT reduction product). By day 4, some distal axons in *Sod1-/-* DRGs were devoid of MTT staining (➤), in contrast to axons that were still viable (➔). By day 6, all *Sod1-/-* axons were MTT-negative (➤), but many ganglia were still MTT-positive. Representative bright field images are shown. *Scale bar = 250 µm*

Finally, *Sod1-/-* DRGs were cultured at low (6%) oxygen, which more closely approximates physiologic oxygen levels (Studer et al., 2000), and reduces oxidative stress in cultured cells (Hansen et al., 2007). On day 6, morphology and viability were compared to DRGs cultured in standard conditions (20% O_2). *Sod1-/-* DRGs cultured at 6% O_2 showed an approximately two-fold increase in DRG area compared to those cultured at 20% O_2 ($0.94 \pm .13$ mm^2 vs. 0.52 ± 0.8 mm^2, $p<0.05$) (fig. 3e). Viability of axons and cell bodies was preserved in 6% O_2, as determined by the MTT assay (fig. 3f). These data support the conclusion that axonal degeneration in the *Sod1-/-* model is due to oxidative stress.

Degeneration of mature DRG axons is triggered by siRNA knockdown of SOD1

Degeneration in DRGs from *Sod1-/-* mice is severe and begins as early as 48 hours in culture. To determine whether loss of SOD1 also causes degeneration of mature axons, we infected wild-type DRGs with lentiviral SOD1 siRNA on day 7 in culture (fig. 4). Preliminary experiments in mitotically inactivated fibroblasts showed approximately 40% knockdown of SOD1 by this approach (fig. 4b). siRNA-treated *Sod1+/+* DRGs were followed out to day 24, stained with the neuronal marker PGP9.5, and morphology compared to untreated *Sod1+/+* and *Sod1+/-* DRGs. A marked difference in the integrity of distal axons was observed (fig. 4c). In siRNA-treated DRGs, 59% of distal axons in were fragmented, compared to 39% in *Sod1+/-* DRGs ($p<0.05$), and 10% in *Sod1+/+* DRGs ($p<0.001$). A trend towards reduced DRG area was also observed (fig. 4d). Thus, while SOD1 knockdown in DRG cultures was likely incomplete (based on efficacy in fibroblasts), even partial knockdown caused degeneration of distal axons exceeding that

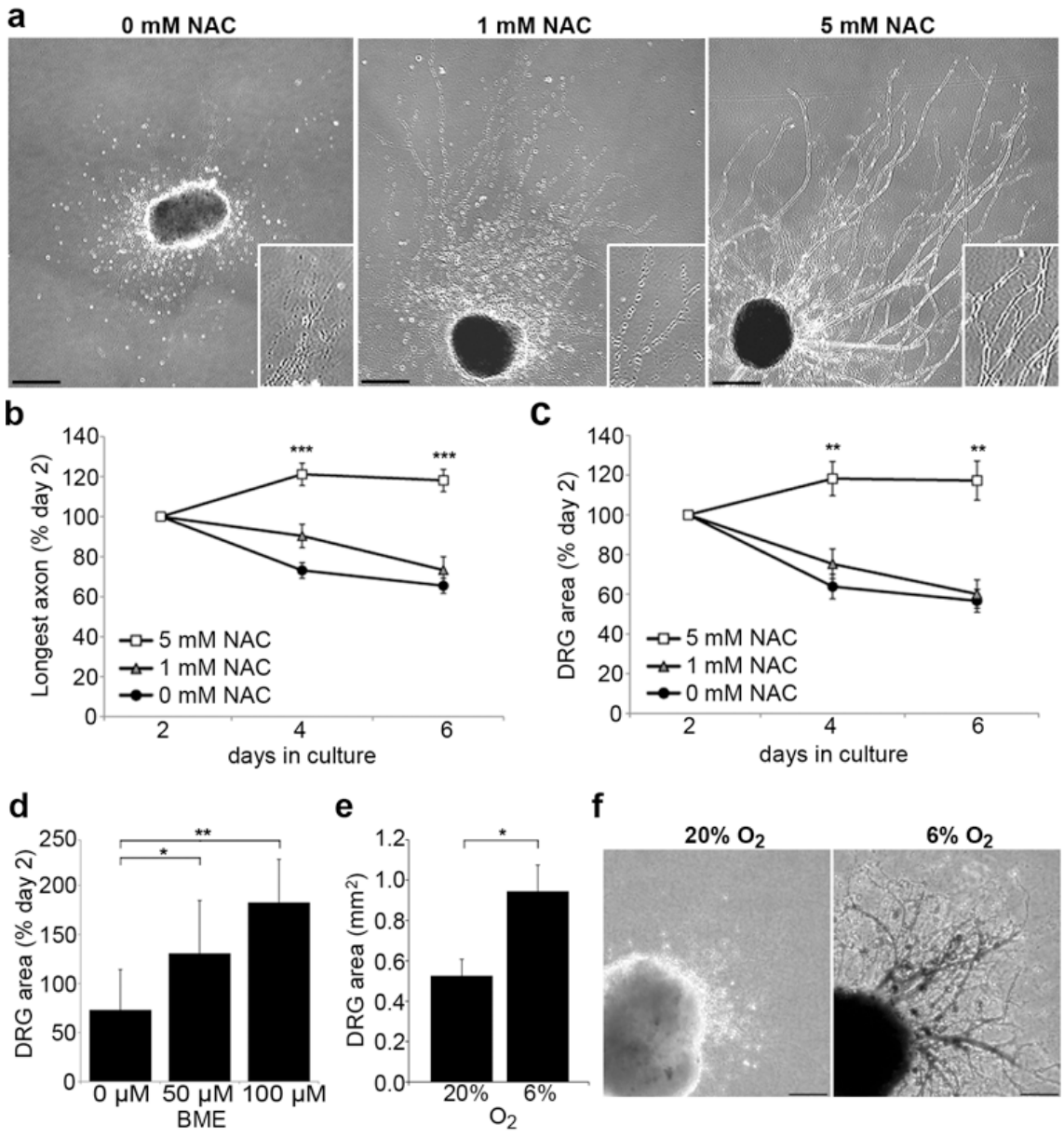

Fig. 3.3 Antioxidant protection in *Sod1-/-* DRGs.

Fig. 3.3 Antioxidant protection in *Sod1-/-* DRGs. **(a)** *Sod1-/-* DRGs after 6 days of 0, 1, or 5 mM NAC treatment. Improved axon outgrowth was seen in 1 and 5 mM NAC-treated DRGs, but only maintained in the 5 mM group. *Scale bar = 250 μm*. **(b)** Length of the longest axon and **(c)** Area of NAC-treated DRGs, expressed as % day 2 (**p<0.01, ***p<0.001 vs. untreated, two-way ANOVA). In **(b)-(c)**, n=8-11 animals/group (4 DRGs/animal). **(d)** *Sod1-/-* DRG area after 6 days of treatment with 0, 50, or 100 μM BME (*p<0.05, **p<0.001, one-way ANOVA). **(e)** *Sod1-/-* DRG area after 6 days in 20% or 6% O_2 (*p<0.05, Student's t-test). **(f)** MTT-stained *Sod1-/-* DRGs from the same mouse, cultured for 6 days in 20% or 6% oxygen. Note the complete loss of viability of axons and ganglia at 20% O_2, which was prevented by culturing at 6% O_2. *Scale bar = 50 μm*

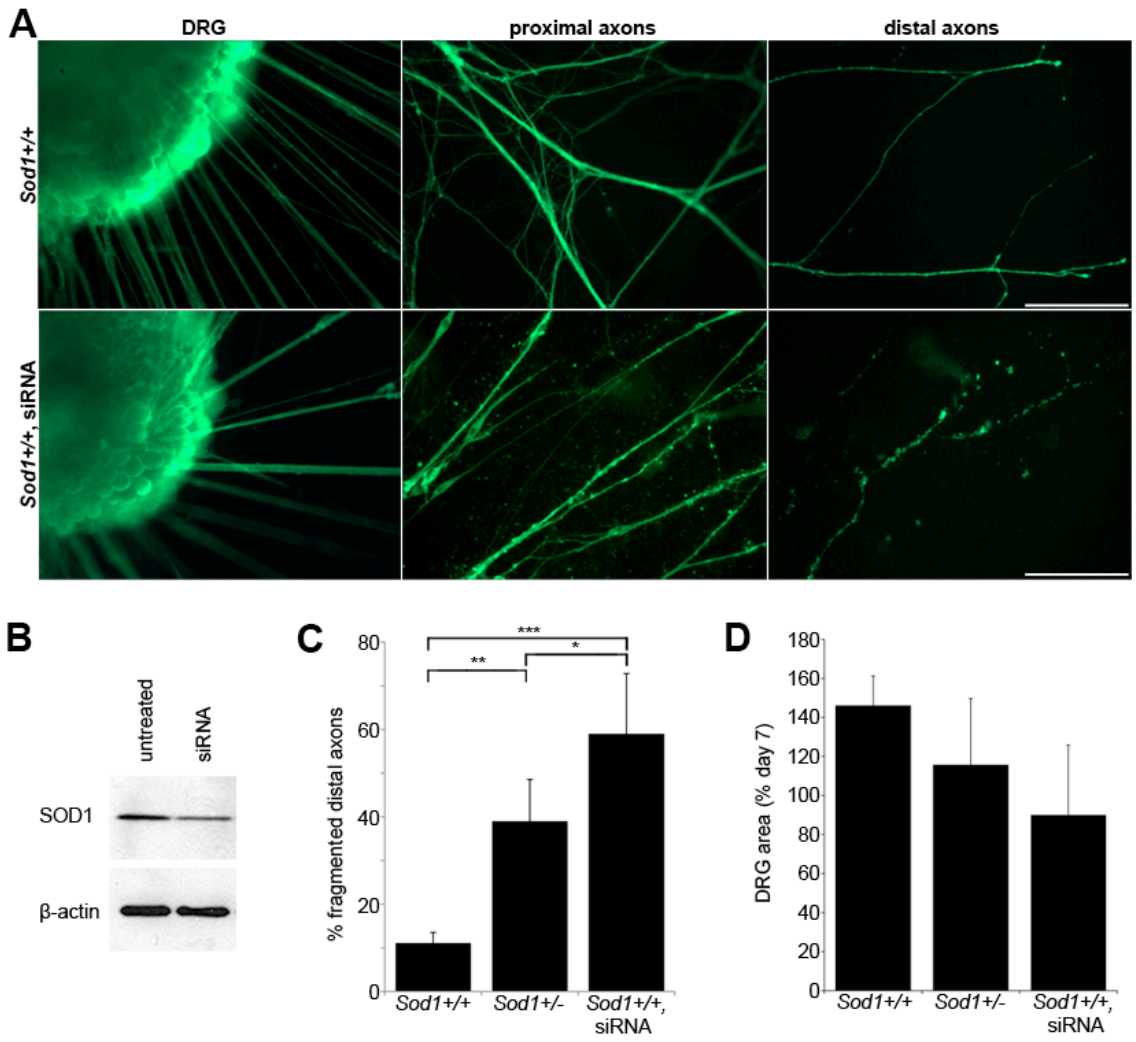

Fig. 3.4 Degeneration of mature DRG axons is triggered by siRNA knockdown of SOD1.

Fig. 3.4 Degeneration of mature DRG axons is triggered by siRNA knockdown of SOD1. Lentivirus was used to deliver SOD1 siRNA to wild-type DRGs on day 7 in culture. On day 24, DRGs were fixed and immunostained with PGP9.5 for morphologic examination. **(a)** Representative PGP9.5-labeled control and siRNA-treated DRGs. Cell bodies and proximal axons of siRNA-treated DRGs are still intact, but distal axons are fragmented. **(b)** Representative western blot of siRNA-treated mouse fibroblasts, to verify knockdown of SOD1. **(c)** Percent of fragmented (discontinuous) distal axons in siRNA-treated DRGs (day 24) compared to *Sod1*+/+ and *Sod1*+/- DRGs. The percent of fragmented axons in siRNA-treated DRGs was significantly higher than that seen in untreated *Sod1*+/+ (***$p<0.001$), and *Sod1*+/- DRGs (*$p<0.05$, one-way ANOVA). 100 distal axons were evaluated per DRG, per group. **(d)** DRG area on day 24. *Scale bar = 100 μm*

seen in *Sod1*+/- DRGs when maintained in culture long-term.

seen in *Sod1*+/- DRGs when maintained in culture long-term.

PQ and DQ cause axonal degeneration

The redox-cycling herbicides PQ and DQ cause intracellular superoxide production by a well-described mechanism (Bus et al., 1974; Sandy et al., 1986). To determine whether increased superoxide production, as opposed to loss of SOD1, is toxic to DRGs, we exposed wild-type DRGs to PQ on day 14 in culture. Dose-dependent axon degeneration was observed (fig. 5a-b). By day 8, the area of PQ-treated DRGs fell to 88 ± 3% ($p<0.05$), 51 ± 8% ($p<0.001$), and 16 ± 5% of day 0 ($p<0.001$) in 25 μM-, 50 μM-, and 100 μM-treated groups, respectively. Toxicity of 50 μM DQ was similar in severity to 50 μM PQ in wild-type DRGs (fig. 5a,c). When we compared susceptibility of *Sod1*+/+ and *Sod1*+/- DRGs to DQ, we found that *Sod1*+/- DRGs were significantly more susceptible (fig. 5c). By day 6 of DQ exposure, *Sod1*+/+ DRG area was 60 ± 8% of day 0, while *Sod1*+/- DRG area was only 9 ± 3% of day 0 ($p<0.001$). This suggests that SOD1 plays an important role in protection against DQ toxicity.

MTT staining in PQ and DQ-treated DRGs again showed a distinction between vulnerability of axons versus cell bodies (fig. 6). After one week of 50 μM PQ or DQ exposure, marked loss of axonal staining was seen, but DRG cell bodies were still MTT-positive. Thus, increased superoxide production also causes toxicity to DRGs *in vitro,* and qualitative evidence from MTT staining suggests that axons may be more susceptible than cell bodies.

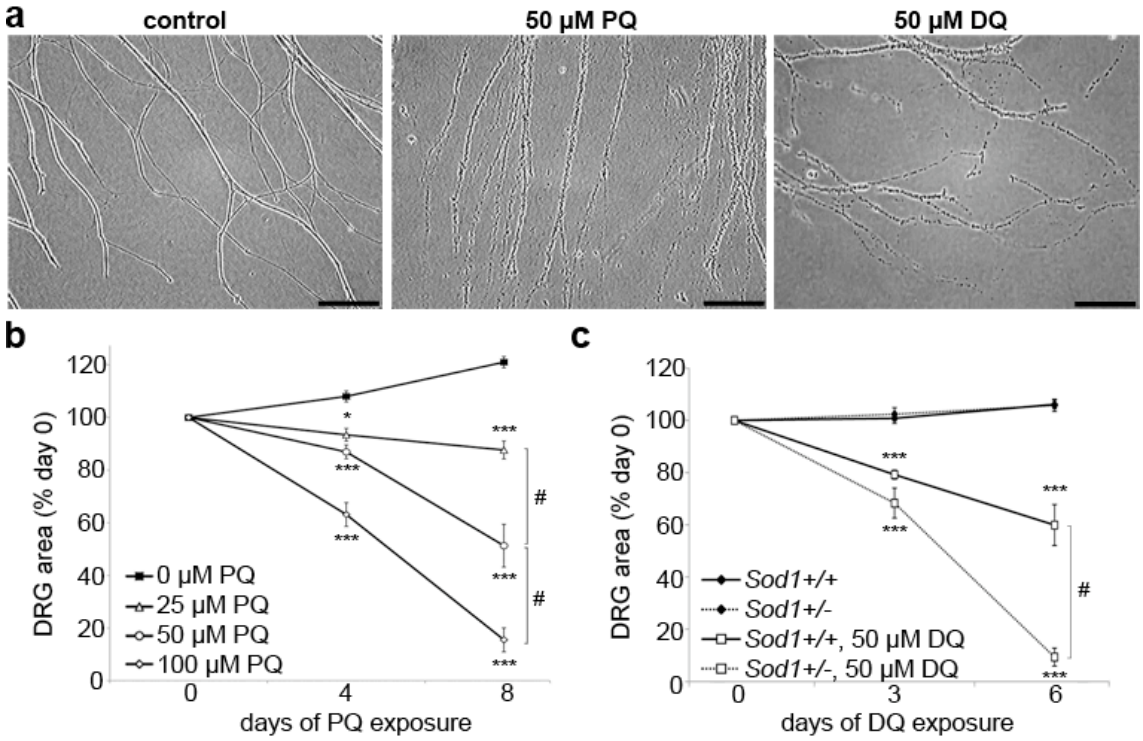

Fig. 3.5 Superoxide-generating herbicides paraquat (PQ) and diquat (DQ) are toxic to DRGs *in vitro*. DRGs were cultured for 2 weeks, at which time PQ or DQ was added to the culture media. **(a)** Representative images of degenerating axons after 8 days of PQ exposure or 6 days of DQ exposure. **(b)** DRG area in PQ-exposed wild-type DRGs. Dose dependent toxicity was seen. n=4 mice per group (4 DRGs per animal). **(c)** DRG area in DQ-exposed *Sod1*+/+ and *Sod1*+/- DRGs. DQ toxicity was significantly more severe in *Sod1*+/- DRGs. n=3 mice per group (4 DRGs per animal). **p*<0.05, ****p*<0.001 vs. untreated, #*p*<0.001 between the indicated groups (two-way ANOVA). *Scale bar = 100 µm*

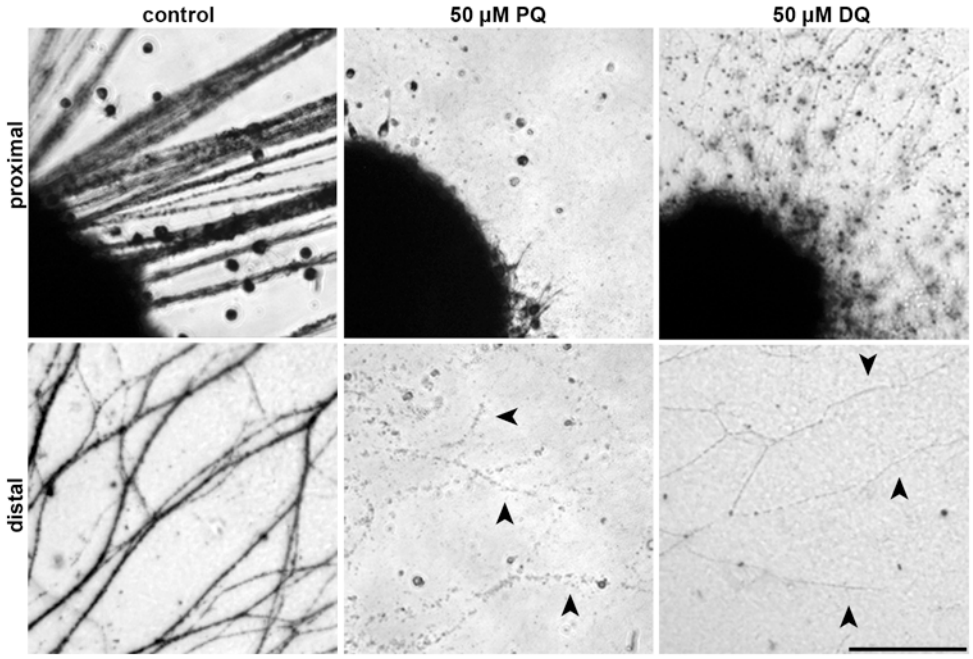

Fig. 3.6 DRG axons are more sensitive to PQ and DQ toxicity than their parent cell bodies. Viability of wild-type DRGs exposed to 50 µM PQ or 50 µM DQ for one week was evaluated by the MTT assay. MTT staining was retained in the ganglia, which were similar in intensity to control (untreated) DRGs. In contrast, PQ- and DQ-exposed axons from these same DRGs were devoid of MTT staining (➤). *Scale bar = 200 µm*

Discussion

Growing evidence supports a role for oxidative stress in causing neurodegeneration in aging and disease. In this study, we tested the effect of loss of the antioxidant enzyme SOD1 on the survival of mouse DRGs *in vitro*. We show that SOD1 is required for DRG axon survival, and that axon outgrowth in *Sod1-/-* DRGs can be improved by antioxidant treatment. This is unlikely to be a developmental effect, since siRNA knockdown of SOD1 also triggered degeneration of mature DRG axons. In related experiments, we found that exposure to PQ and DQ caused degeneration of wild-type DRGs, and that toxicity depended on SOD1 expression. These novel *in vitro* models reinforce the idea that oxidative stress may participate in the pathogenesis of peripheral neuropathy, and will be useful for future mechanistic and therapeutic studies of oxidative stress-mediated axon degeneration.

Superoxide-mediated neurotoxicity

$O_2 \cdot^-$ is continuously produced in cells as a byproduct of mitochondrial electron transport. If not efficiently neutralized by SODs, $O_2 \cdot^-$ can undergo reactions to produce highly toxic free radicals such as peroxynitrite and hydroxyl radical. Neurodegeneration in *Sod1-/-* mice has been reported in retinal neurons (Hashizume et al., 2008), and cochlear hair cells (McFadden et al., 1999), and evidence from muscle pathology and EMG recordings in these mice is consistent with a possible motor neuropathy (Flood et al., 1999; Shefner et al., 1999). *Sod1-/-* neurons also show increased cell death in ischemic (Kondo et al., 1997), excitotoxic (Schwartz et al., 1998), and traumatic injury models (Reaume et al., 1996). These data suggest an important role for SOD1 in

maintaining neuronal viability under stress and during the aging process.

$O_2{\cdot}^-$-mediated toxicity may be particularly relevant to the pathogenesis of diabetic neuropathy, which most commonly presents as a symmetrical, distal sensory and autonomic neuropathy (Thomas and Tomlinson, 1993). Hyperglycemia-induced mitochondrial $O_2{\cdot}^-$production is thought to initiate multiple downstream pathways of tissue damage in diabetes (Nishikawa et al., 2000). Consistent with this hypothesis, *Sod2*+/- DRG neurons exhibit increased $O_2{\cdot}^-$production and decreased neurite outgrowth in hyperglycemic conditions, and *Sod2*+/- mice are more susceptible to development of diabetic neuropathy (Vincent et al., 2007). The effect of SOD1 expression on susceptibility to diabetic neuropathy has not been reported, but SOD1 deficiency does exacerbate diabetic nephropathy (DeRubertis et al., 2007) and cataract formation (Olofsson et al., 2009). Genetic variations in SOD1 and SOD2 are linked to the risk of diabetic complications in humans (Al-Kateb et al., 2008; Flekac et al., 2008), and a reduction in plasma SOD activity was reported in diabetic patients (Flekac et al., 2008).

Oxidative stress, and SOD1 specifically, are also implicated in the pathogenesis of amyotrophic lateral sclerosis (ALS). Over 100 mutations in SOD1 have now been linked to the inherited form of this fatal motor neuron disease (ALS online database, http://alsod.iop.kcl.ac.uk/Als/Index.aspx) (Wroe et al., 2008). We and others have shown distal axon degeneration to be an early pathologic event in mutant SOD1 models of ALS (Frey et al., 2000; Fischer et al., 2004; Pun et al., 2006). The current consensus is that mutant SOD1 causes disease by a toxic gain of function, not a loss of antioxidant function (reviewed in Rothstein, 2009). Still, oxidative damage to proteins (Ferrante et al., 1997), lipids (Pedersen et al., 1998), and DNA (Bogdanov et al., 2000) is increased in

human ALS and in SOD1 mutant mice (Andrus et al., 1998; Hall et al., 1998), and antioxidants have provided robust extensions of life span in SOD1 mutant mice (Crow et al., 2005; Harraz et al., 2008). Some proposed gains of toxic function by mutant SOD1 enzymes are likely to increase oxidative stress, including aberrant redox chemistry (Wiedau-Pazos et al., 1996), alterations in metal binding (Estévez et al., 1999), and formation of insoluble SOD1 aggregates in mitochondria (Vijayvergiya et al., 2005). Mechanistic comparisons between oxidative injury in the SOD1 mutant and SOD1 KO model with regard to axonal degeneration may be fruitful to pursue.

Axonal degeneration due to PQ/DQ

The neurotoxicity of PQ is well-established in neuron-like cell lines (Fordel et al., 2006) and in primary dopaminergic (Bonneh-Barkay et al., 2005), cortical (Kim et al., 2004), and motor neuron cultures (Kriscenski-Perry et al., 2002). The doses of PQ and DQ used here were selected based on previous primary neuron studies, whereas much higher doses are typically required to cause toxicity in cell lines. We observed dose-dependent toxicity of PQ in mouse DRGs. Moreover, we saw a close correspondence between the effect of DQ and PQ, which have similar chemical structures and mechanisms of toxicity (Bonneh-Barkay et al., 2005). As opposed to previous studies, which focused primarily on cell death as an endpoint, we found that DRGs exposed to PQ or DQ showed severe axon fragmentation and loss of axonal MTT staining, at a time when the cell bodies were still MTT-positive. Axonal toxicity of DQ was exacerbated by SOD1 deficiency, consistent with previous reports that suggest SOD1 plays a key role in protection against PQ toxicity (Huang et al., 1997). PQ toxicity has also been shown to be

attenuated by GSH supplementation (Kriscenski-Perry et al., 2002), similar to *Sod1-/-* DRGs. PQ/DQ exposure may therefore be a useful adjunct to SOD1 deficiency, for experiments that require the ability to manipulate spatial and temporal aspects of oxidative injury to axons.

Axonal degeneration vs. cell death

In the current study we used axon length as a primary measure of toxicity, and provide preliminary data to suggest increased susceptibility of axons vs. neuronal cell bodies to loss of SOD1 or increased $O_2{\cdot}^-$ production. However, the axonal degeneration we observed could also have been due to cell death not detected by our methods, or due to sublethal injury to the cell bodies, causing failure to maintain distal axons. As in previous studies of axonal degeneration (MacInnis and Campenot, 2005; Song et al., 2006), we used the MTT assay as a way to measure viability without disrupting the spatial organization of the cultures. This assay depends on metabolic activity present throughout the cell, as opposed to cell death assays that rely on nuclear/nucleic acid staining and are unsuitable for comparison of cell bodies and axons. The current data are by no means conclusive, but our observation of apparent axonal > neuronal toxicity in both the *Sod1-/-* and PQ/DQ models suggests that further evaluation of relative susceptibility to oxidative stress is warranted.

The issue of axonal vs. neuronal susceptibility may be important for understanding why, in diabetic (and other) neuropathies, length-dependent, distal to proximal axonal degeneration occurs in the absence of significant cell death (Said et al., 1992; Watkins et al., 1995). Recent studies support the idea that axons may be

preferentially susceptible to oxidative stress. DRG neurons isolated from diabetic rats and subjected to hyperglycemia showed increased oxidative stress in axons, but not cell bodies, and an associated reduction in axon length (Zherebitskaya et al., 2009). Similarly, the concentration of 4-hydroxynonenal, a product of lipid peroxidation, required for 50% reduction of axon outgrowth in cultured DRG neurons had no effect on cell viability . In an *in vivo* model of diabetic neuropathy, markers of oxidative damage in DRG neurons were significantly increased, yet few apoptotic neurons were detected (Zochodne et al., 2001; Akude et al., 2009). It is unclear why axons may be more susceptible to oxidative stress-mediated injury than their parent cell bodies, although sciatic nerves of normal rats were reported to have ten-fold less total GSH content than brain (Romero et al., 1991). This suggests that peripheral nerve may be highly susceptible to oxidative stress at baseline due to a low GSH reserve.

In summary, we demonstrated that the antioxidant enzyme SOD1 is required for survival of DRG axons *in vitro*, and also showed susceptibility of DRG axons to increased superoxide production by the redox-cycling herbicides PQ and DQ. These *in vitro* models provide a novel means of investigating oxidative stress-mediated injury in mammalian axons, to improve our understanding of axonal redox control and dysfunction as it relates to human aging and disease.

CHAPTER IV: Genetic deletion of SOD1 causes a distal motor axonopathy

Introduction

Axonal degeneration is perhaps the most common pathological feature in neurodegenerative diseases (Coleman and Perry, 2002; Raff et al., 2002). Decades of research demonstrate that numerous structural, metabolic, and genetic lesions may lead to axonal degeneration, however the ultimate triggers that cause the dissolution of axons in neurodegenerative disorders are unknown.

Axonal degeneration was traditionally regarded as a passive process resulting from loss of trophic support from the cell body (Cajal, 1928). Recent evidence demonstrates that axonal survival and degeneration can occur independent of the influence of the cell body, and may involve mechanisms distinct from cell death. The *Wld*^{S} mouse is an example of an experiment of nature where a spontaneous mutation prolongs axonal survival after axotomy ("slow Wallerian degeneration") (Lunn et al., 1989). Importantly, *Wld*^{S} also protects against axonal degeneration and neurological deficits in models of neurodegenerative disease (Ferri et al., 2003; Samsam et al., 2003; Sajadi et al., 2004). This supports the hypothesis that protection of axons is a rational therapeutic approach, and underscores the need for better understanding of mechanisms of axonal degeneration. Similarly, there is evidence from models of motor neuron disease (Sagot et al., 1995; Gould et al., 2006; Suzuki et al., 2007), and Parkinson's disease (Eberhardt et al., 2000), that protection of cell bodies may not provide concomitant protection for axons, and thus does not necessarily preserve function or slow disease progression.

In this study we investigated the role of oxidative stress as a mechanism of axonal degeneration in the *Sod1-/-* mouse. Interest in this model from the neuroscience community was initially based on the hypothesis that loss of enzymatic activity causes motor neuron disease (ALS) due to SOD1 mutations. An early report concluded that *Sod1-/-* mice had no motor phenotype or motor neuron loss (Reaume et al., 1996). Subsequent studies, however, demonstrated abnormalities in muscle (Flood et al., 1999), and on EMG (Shefner et al., 1999), consistent with a motor axonopathy. *Sod1-/-* mice followed to 20 months performed poorly on rotarod and showed 50% loss of hind-limb muscle mass (Muller et al., 2006). However, analysis of motor neurons and ventral root axons showed no decrease in number (Flood et al., 1999; Shefner et al., 1999). To date, denervation at the NMJ has not been investigated, nor has oxidative stress in peripheral nerve been evaluated as a cause of axonal degeneration in this model.

Here we confirm by systematic examination of NMJ morphology the presence of a motor axonopathy in *Sod1-/-* mice. We demonstrate oxidation of the GSH pool in peripheral nerve coinciding with the onset of denervation, and show that treatment with NAC provides dose-dependent rescue of *Sod1-/-* motor axons *in vitro*. Denervation predominantly affects fast-twitch muscle, and is accompanied by extensive sprouting and axonal swellings, features seen in other animal models of motor neuron disease. Sensory fibers are unaffected. We conclude that loss of SOD1 causes a progressive motor axonopathy, a finding that implicates oxidative stress as a potential mechanism of axon degeneration in motor neuron disease and other peripheral neuropathies.

Results

To facilitate analysis of NMJ pathology, we crossed *Sod1-/-* mice (Muller et al., 2006) with *thy1-YFP16* mice (Feng et al., 2000) to generate *Sod1+/-, thy1-YFP16* breeders expressing YFP in all motor axons. *Sod1-/-, thy1-YFP16* offspring (hereafter referred to as *Sod1-/-*) showed pronounced hind-limb weakness with age, evidenced by significant loss of grip strength by 12 months (Fig 1A-B). Whereas most *Sod1+/+ and Sod1+/-* mice could remain suspended from a wire grid for at least 300 seconds, the mean latency to fall for *Sod1-/-* animals was 134 seconds ($p<0.001$). *Sod1-/-* mice had obvious difficulty gripping the wire with their hind limbs (Fig. 1A, inset), and hind limb grip was typically lost first, followed by forelimb grip. Western blot and SOD1 zymography were used to verify the absence of SOD1 protein and enzymatic activity in spinal cord, sciatic nerve, and tibialis anterior muscle from *Sod1-/-* mice (Fig 1C).

Progressive denervation in Sod1-/- mice

Quantitative morphologic analysis of NMJs was carried out from 1-18 months in TA and soleus muscles (Fig. 2). TA is composed predominantly of fast-twitch (type II) fibers, while soleus has a higher proportion of slow-twitch (type I) fibers (Wigston and English, 1992; Hegedus et al., 2007). *Sod1-/-* mice showed progressive denervation in both muscles, but denervation in TA began earlier and was more severe (Fig. 2B). At one month, *Sod1-/-* TA was fully innervated, but by four months only 69.5% of endplates were fully innervated, falling to 53.1% at 12 months and 33.9% at 18 months ($p<0.001$ vs. *Sod1+/+*). In a subset of mice, MGC (similar to TA in fiber type composition) was also analyzed and identical results were seen (not shown). In soleus, significant

denervation did not occur until 12 months of age (Fig. 2C). At 18 months, 78.6% of endplates in *Sod1-/-* soleus were still innervated ($p<0.05$ vs. *Sod1+/+*). Thus, fast twitch muscle appears more susceptible to denervation than slow twitch muscle in the *Sod1-/-* model.

Interestingly, *Sod1+/-* mice were identical to *Sod1+/+* mice until 18 months. Innervation of *Sod1+/-* TA dropped to 79.9% at 18 months, compared to 92.2% in *Sod1+/+* mice. This difference was not statistically significant, but suggests that even haploinsufficiency of SOD1 may increase susceptibility to denervation with aging.

Morphologic abnormalities at the NMJ

Striking morphologic abnormalities were seen in distal motor axons of *Sod1-/-* mice, including widespread axonal and ultraterminal sprouting and large terminal axon swellings (Fig. 3). At 1 month of age, 5.4% of NMJs in *Sod1-/-* TA already had ultraterminal sprouts, compared to <1% in *Sod1+/-* and +/+ TA ($p<0.001$) (Fig. 3C). This was surprising given that we saw no obvious denervation or reinnervation in TA until 4 months. The same trend occurred in soleus, where 6.3% of endplates had ultraterminal sprouts by 4 months, prior to the onset of denervation at 12 months ($p<0.01$ vs. *Sod1+/+*) (Fig. 3D). The extent of sprouting was more severe in TA than in soleus at every time point, peaking at 16.4% in *Sod1-/-* TA at 12 months, and 8.9% in *Sod1-/-* soleus at 18 months.

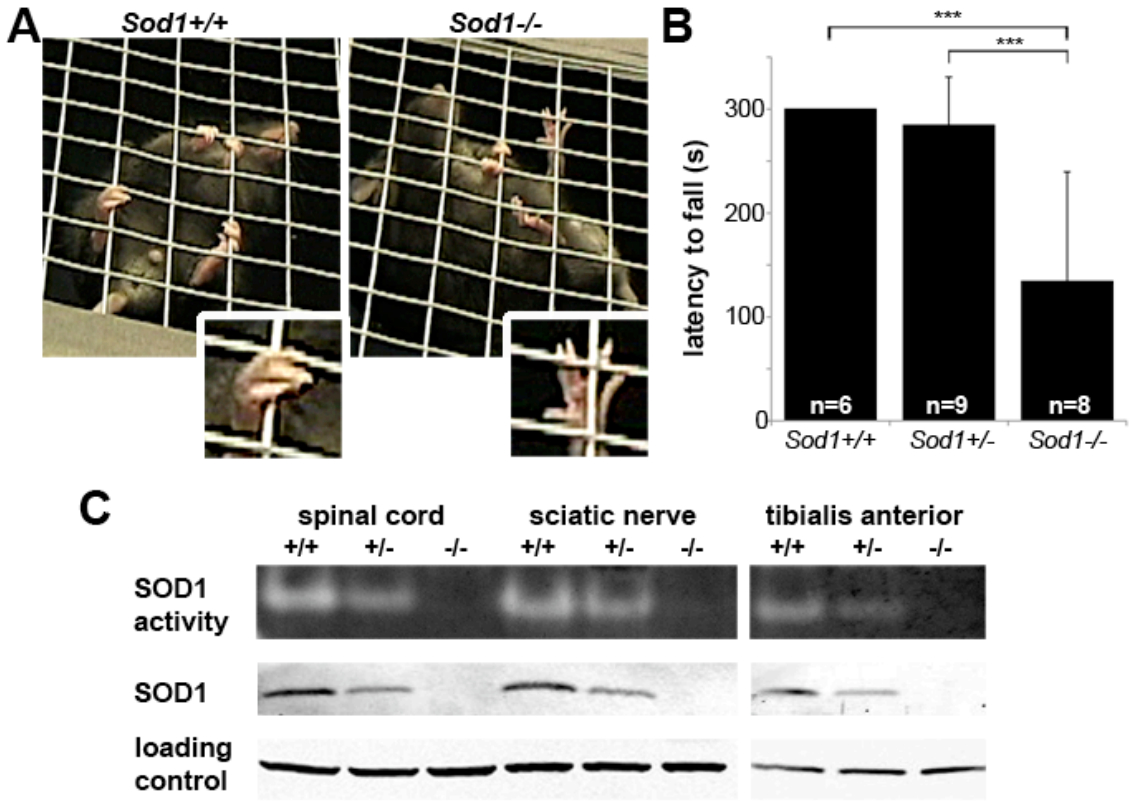

Figure 4.1. Systemic deletion of SOD1 causes a neuromuscular phenotype. **A.** Hindlimb weakness in 12 month-old *Sod1-/-* mice is evidenced by poor performance on a grip strength assay. Mice were given three trials of 300 seconds to remain suspended from a 10 cm x 10 cm wire grid. *Sod1+/+* mice maintained a strong hind-limb grip (inset), whereas *Sod1-/-* mice were unable to achieve a tight grip with their hind-limbs . **B.** The maximum latency to fall over three trials was recorded, and 12 month-old *Sod1-/-* mice showed a significantly shorter latency to fall than age-matched controls (****p<0.001)*. **C.** SOD1 zymography (upper) and western blot (lower) show that SOD1 protein and enzymatic activity are undetectable in spinal cord, sciatic nerve, and tibialis anterior muscle from 12 month-old *Sod1-/-* mice. *Sod1+/-* mice show an intermediate level of expression. Loading controls: β-actin (spinal cord and nerve), EF1α (muscle).

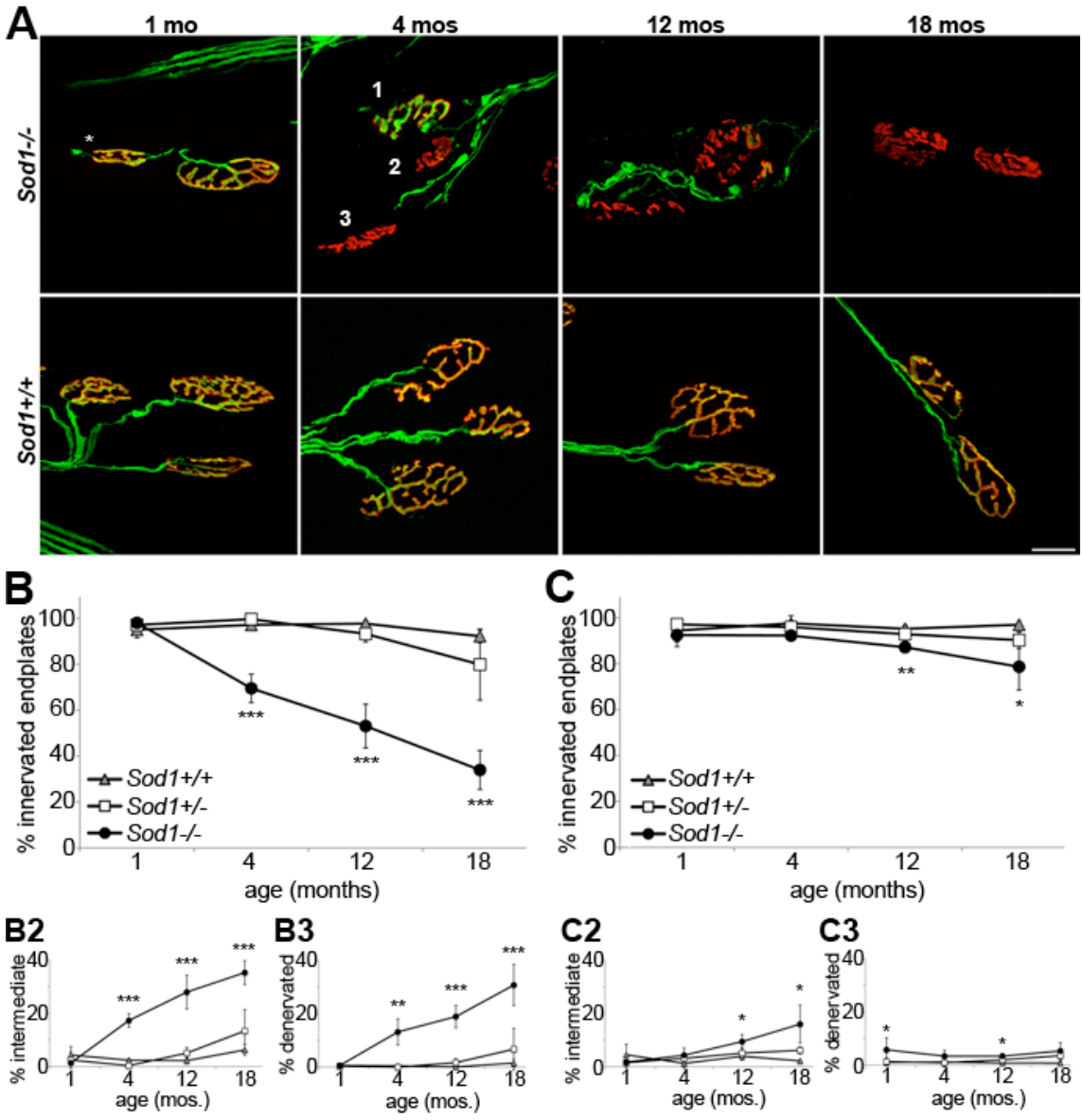

Figure 4.2. *Sod1-/-* mice display progressive denervation of hind limb muscles.

Figure 4.2. *Sod1-/-* mice display progressive denervation of hind limb muscles. **A.** Representative confocal projection of NMJs in tibialis anterior (TA) at 1, 4, 12, and 18 months of age, with motor axons in green (YFP) and endplates in red (bungarotoxin). At one month, *Sod1-/-* NMJs are fully innervated and indistinguishable from *Sod1+/+* mice except for occasional terminal sprouts (*). By 4 months, a significant number of intermediate (*2*) and denervated (*3*) endplates are seen in addition to innervated (*1*) endplates, and denervation continues to progress over time *(scale bar = 25 μm)*. **B.** Comparison of the percent innervated, intermediate, and denervated endplates in TA, a predominantly fast twitch muscle, shows progressive denervation from 4 to 18 months ($p<0.001$ *vs. Sod1+/+*). **C.** Denervation in the soleus muscle, which is predominantly slow twitch, is milder than in TA and does not begin until 12 months (*$p<0.05$, **$p<0.01$ *vs. Sod1+/+)*. In **B-C**, the number of mice is 3-7 animals per group. 898 ± 203 endplates were assessed per TA, and 262 ± 52 endplates per soleus muscle.

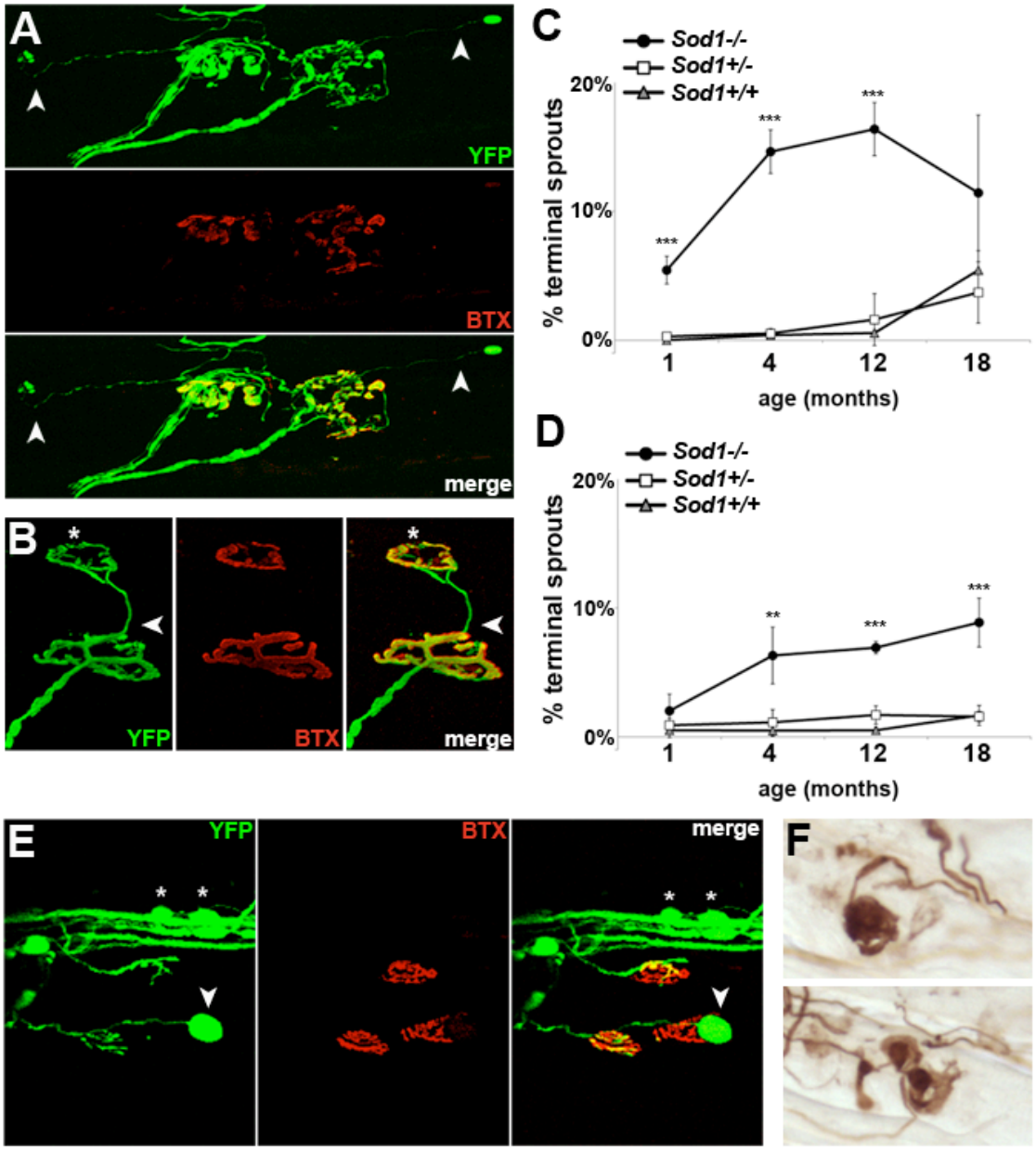

Figure 4.3. Loss of SOD1 causes morphologic abnormalities at the NMJ.

Figure 4.3. Loss of SOD1 causes morphologic abnormalities at the NMJ. **A.** Representative confocal projection of ultraterminal sprouts (➤) arising from innervated NMJs (4 months, TA). **B.** An example of reinnervation of an endplate (*) by a terminal sprout (➤) (4 months, TA). **C.** Quantification of the number of ultraterminal sprouts in TA as a percent of total endplates shows significant sprouting by 1 month of age, prior to the onset of denervation *(***p<0.001 vs. Sod1+/+ and +/-*). **D.** In soleus muscle, significant sprouting is also seen in advance of denervation, by 4 months of age *(**p<0.01, ***p<0.001 vs. Sod1+/+ and +/-*). **E.** Example of terminal axon swellings (➤) commonly seen at 4 months of age in *Sod1-/-* TA but rare in controls. Note also smaller varicosities involving the intramuscular nerve bundle (*). **F.** Immunostaining with SMI-31 antibody shows dense accumulation of phosphorylated neurofilament in terminal axon swellings (4 months, TA).

We also observed prominent terminal axon swellings at NMJs of *Sod1-/-* TA starting at 4 months of age (Fig. 3E), and to a lesser extent in soleus. These swellings most commonly involved motor axon terminals, but smaller varicosities were also seen along the intramuscular nerve fibers in *Sod1-/-* mice, which were rare in control animals. The terminal swellings showed dense accumulation of phosphorylated NF (Fig. 3F), which is also seen in other models of motor neuropathy (Cifuentes-Diaz et al., 2002), and in Wallerian degeneration (Glass and Griffin, 1991).

Lack of proximal pathology

Previous studies reported no difference in the number of spinal motor neurons (Shefner, 1999) or ventral and dorsal root axons (Flood, 1999), in *Sod1-/-* mice out to 17 and 19 months, respectively. We examined Nissl-stained motor neurons in the ventral horn of lumbar spinal cord at 4 and 18 months (Fig. 4A) and also saw no evidence of overt motor neuron loss, vacuolation or chromatolysis. Similarly, we saw no degenerating axons in L4 ventral and dorsal roots, sciatic nerve, tibial nerve, and sural nerve in 18 month-old *Sod1-/-* mice (Fig. 4B and not shown).

To screen for more subtle evidence of pathology, we stained lumbar spinal cord from 4 and 18 month-old *Sod1-/-* and *Sod1+/+* mice (n=3 per group) for a number of markers associated with neurodegeneration (Fig. 4C). No accumulation of phosphorylated NF was seen in motor neurons or proximal axons at either time point. A mild increase in GFAP-positive astrocytes was seen in *Sod1-/-* mice at 4 and 18 months of age, but no microgliosis was seen. Spinal cords were also probed for ubiquitin- or TDP-43-positive inclusions, which were absent. Thus, consistent with previous reports,

we found no evidence to indicate proximal motor pathology in *Sod1-/-* mice, and saw little evidence of reactive changes in the lumbar spinal cord, even in 18 month-old animals.

Sparing of distal sensory fibers

Since *Sod1-/-* motor pathology appears to be restricted to the distal axon, we investigated whether distal sensory fibers may be similarly affected. Epidermal nerve fibers of the plantar footpads are innervated by the sciatic nerve (Hsieh et al., 2000). Therefore, they course through a similar environment and are similar (or longer) in length compared to motor axons innervating hind limb muscles. At 4 and 18 months of age, we assessed the morphology (Fig. 5A) and density (Fig. 5B) of epidermal nerve fibers. *Sod1*+/- and +/+ mice were identical at both time points, so were combined. No difference in fiber density between *Sod1-/-* mice and controls was seen. *Sod1*-/- mice had a subtle increase in epidermal nerve fiber branching at 18 months, but this would have been unlikely to affect quantification, as only those fibers entering the epidermis, not intra-epidermal branches, were counted. Sparing of distal sensory axons in this model, in contrast to motor axons, suggests that distal motor axons are inherently more sensitive to oxidative stress than sensory axons, or may be exposed to higher levels of oxidative stress *in vivo.*

Oxidative stress in peripheral nerve

Oxidative stress has not been previously measured in peripheral nerve of *Sod1-/-* mice. To address the hypothesis that motor axonopathy in *Sod1-/-* mice is due to

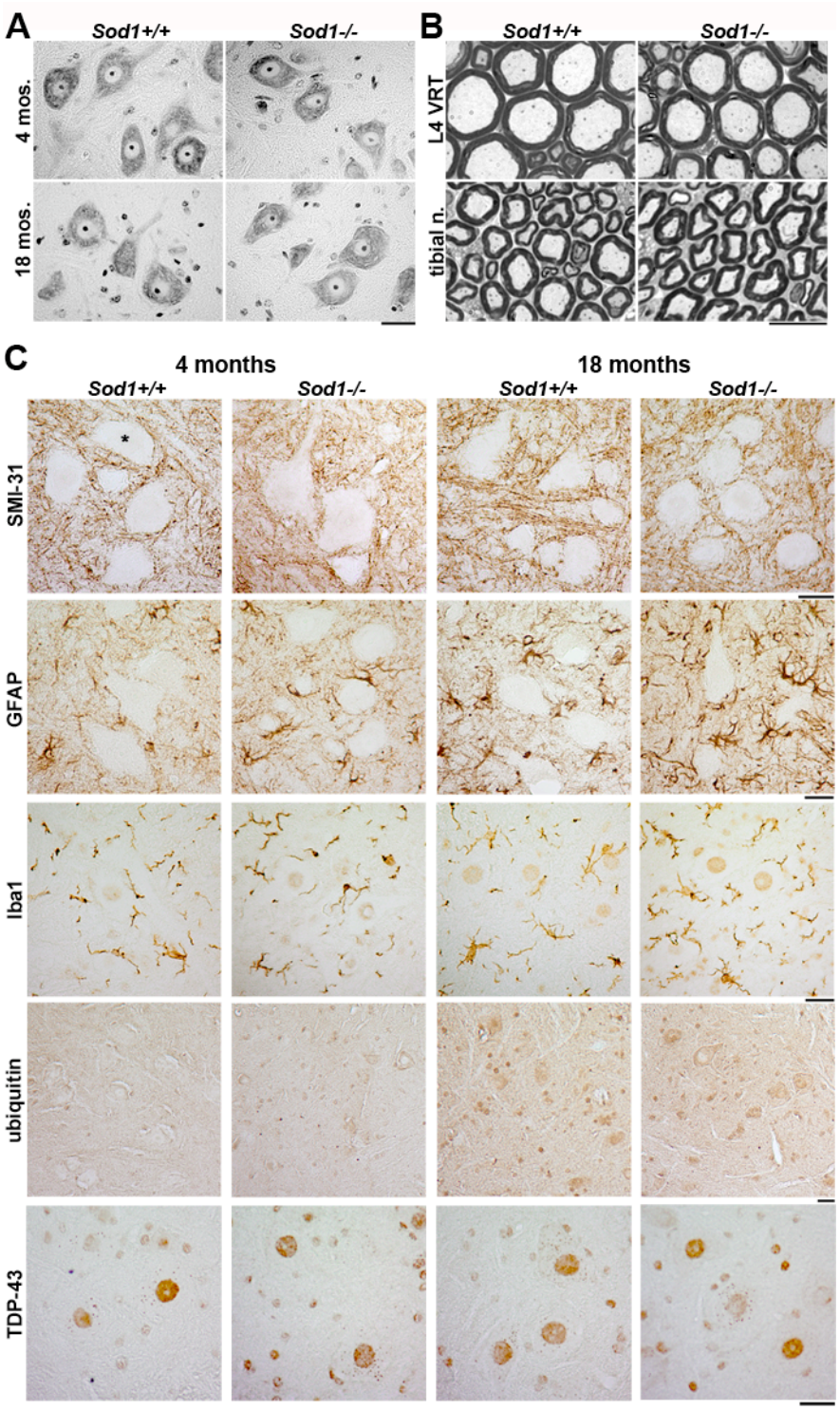

Figure 4.4. *Sod1-/-* mice lack pathologic involvement of lumbar spinal cord and proximal axons.

Figure 4.4. *Sod1-/-* mice lack pathologic involvement of lumbar spinal cord and proximal axons. **A.** Nissl-stained motor neurons in *Sod1-/-* lumbar spinal cord appear identical to wild type at 4 and 18 months of age (*scale bar = 25 μm*). **B.** No degenerating axons are seen in *Sod1-/-* L4 ventral root and tibial nerve at 18 months of age (*scale bar = 10 μm*). **C.** Immunohistochemical staining shows little evidence for pathologic involvement of *Sod1-/-* lumbar spinal cord (representative light micrographs of ventral horn are shown; motor neuron cell bodies are not counterstained in these sections). Phosphorylated neurofilament (NF-H/NF-M) does not accumulate in motor neuron cell bodies (*) or proximal axons (SMI-31 antibody). A mild increase in GFAP-positive astrocytes in *Sod1-/-* mice is seen at both 4 and 18 months of age, but no apparent microgliosis (Iba1). No ubiquitin- or TDP-43-positive inclusions are present, and nuclear TDP-43 localization appears similar in *Sod1-/-* mice and controls (*scale bars = 25 μm*).

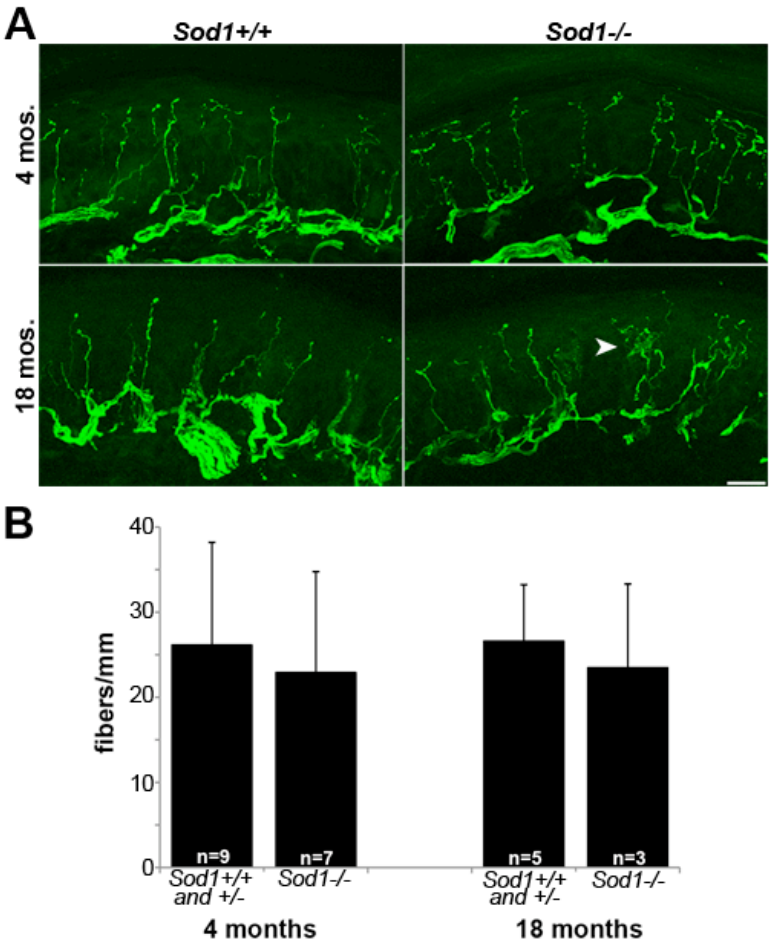

Figure 4.5. Distal sensory fibers do not degenerate in *Sod1-/-* mice. **A.** Representative confocal projection of PGP9.5-labelled epidermal nerve fibers from the plantar footpad, demonstrating that sensory fibers of *Sod1-/-* mice remain intact at 4 and 18 months of age. A subtle increase in intra-epidermal branching (➤) is present in 18 month-old *Sod1-/-* mice (*scale bar = 20 µm*). **B.** Epidermal nerve fiber density, expressed as the number of fibers/mm of epidermis, is equivalent in *Sod1-/-* mice and controls. No difference in *Sod1+/+* and *Sod1+/-* mice was seen, so they were combined for the purpose of this analysis.

oxidative stress, we measured the steady-state GSH redox potential in tibial nerve and MGC muscle at 4 months of age, the earliest time point at which we saw denervation. GSH, a major thiol antioxidant, is a principal redox buffer in cells and is routinely used as a representative indicator of the intracellular redox state (Schafer and Buettner, 2001; Jones, 2002; Jones et al., 2004). E_h typically ranges from -230 to -260 mV in proliferating cells, -190 to -220 mV in differentiated cells, and -140 to -180 mV in apoptotic cells (Jones, 2006b). Perturbations causing oxidation and/or depletion of the GSH pool are reflected by higher (more positive) values of E_h.

We found significant oxidation of the GSH/GSSG pool in *Sod1-/-* tibial nerve, but not gastrocnemius muscle, at 4 months (Fig. 6). The concentration of reduced GSH in *Sod1-/-* tibial nerve (n=14) was 26% lower than age-matched *Sod1+/-* mice (n=13) and 46% lower than *Sod1+/+* mice (n=7) (Fig. 6A). *Sod1-/-* tibial nerve showed a concomitant increase in oxidized GSSG (Fig. 6B). Using the Nernst equation, we calculated a redox potential (E_h) of -215 mV for *Sod1+/+* tibial nerve and -211 mV for *Sod1+/-* tibial nerve, compared to -192 mV in *Sod1-/-* tibial nerve ($p<0.001$) (Fig. 6C). In contrast, GSH, GSSG, and E_h in *Sod1-/-* MGC, which is innervated by tibial nerve and significantly denervated at 4 months, did not differ from controls (Fig. 6D-F). Given that these measurements are from tissue homogenates, we cannot separate changes in axons from those in surrounding cells such as Schwann cells. Still, these data suggest that axon pathology in *Sod1-/-* mice correlates most closely with oxidative stress in peripheral nerve.

Antioxidant rescue of axon outgrowth in primary motor neurons

To test for intrinsic motor axon defects in the *Sod1-/-* model, and determine the effectiveness of antioxidant protection, we cultured primary motor neurons from E12.5 mice in media free of standard antioxidant supplements (Fig. 7). *Sod1-/-* motor neurons were short-lived compared to controls. No viable cells remained at 72 hours in culture (not shown). At 24 hours, *Sod1-/-* motor neurons had markedly shorter axons compared to controls (Fig. 7B). Mean axon length in *Sod1-/-* cells was 50 μm at 24 hours, compared to 93 μm and 83 μm for *Sod1+/+* and *Sod1+/-* cells, respectively ($p<0.001$).

To verify that this defect is mediated by oxidative stress, we treated cells with the antioxidant NAC. NAC is hydrolyzed to cysteine inside cells, where it can act as a precursor for GSH synthesis, in addition to free radical-scavenging capabilities and GSH-independent effects on the cellular thiol/disulfide status (Jones et al., 1995; Schafer and Buettner, 2001; Jones et al., 2004). When NAC was added to primary motor neurons at the time of plating, a dose-dependent rescue of axon outgrowth was observed (Fig. 7C). Axons treated with high-dose (5 mM) NAC were indistinguishable from wild-type cells at 24 hours. This supports the hypothesis that axonal degeneration in the *Sod1-/-* model is caused by oxidative stress, and reinforces the idea that oxidation of the GSH/GSSG pool may contribute to axon pathology in this model.

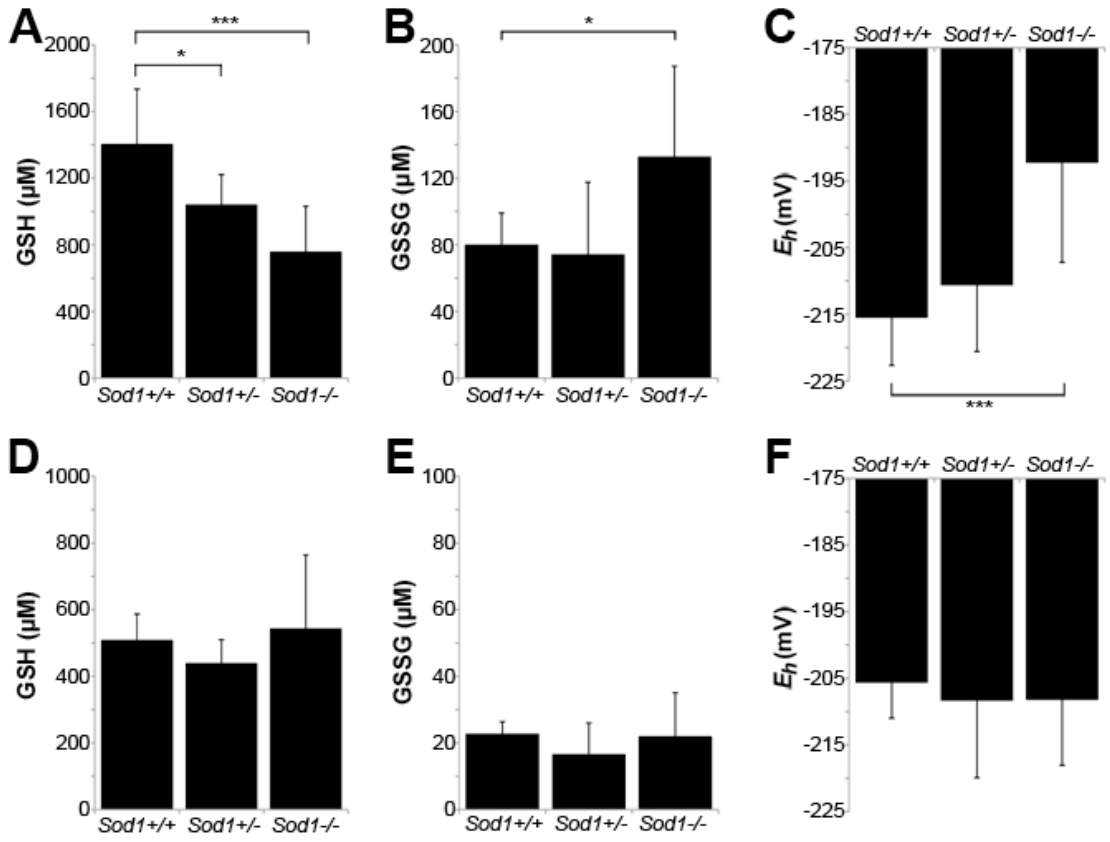

Figure 4.6. Loss of SOD1 leads to a more oxidized GSH redox state in peripheral nerve, but not muscle, at 4 months. **A.** HPLC measurement of GSH in tibial nerve homogenates from 4 month old mice shows a 26% decrease in *Sod1+/-* mice (n=13) compared to *Sod1+/+* mice (n=7) *(*p<0.05*) and a 46% decrease in *Sod1-/-* mice (n=14) *(***p<0.001*). **B.** A concomitant increase in the oxidized form, GSSG, was observed in *Sod1-/-* tibial nerve *(*p<0.05).* **C.** The GSH redox potential (E_h) was calculated using the Nernst equation (E_h, in mV = E_0 + (2.303RT/nF)*log([GSSG]/[GSH]^2). *Sod1-/-* tibial nerve is ~20 mV more oxidized than controls, indicated by a more positive value of E_h *(***p<0.001).* **D.-F.** No difference in GSH (D), GSSG (E), or E_h (F) was seen in MGC muscle from these same animals, which is innervated by tibial nerve, and significantly denervated by this time point.

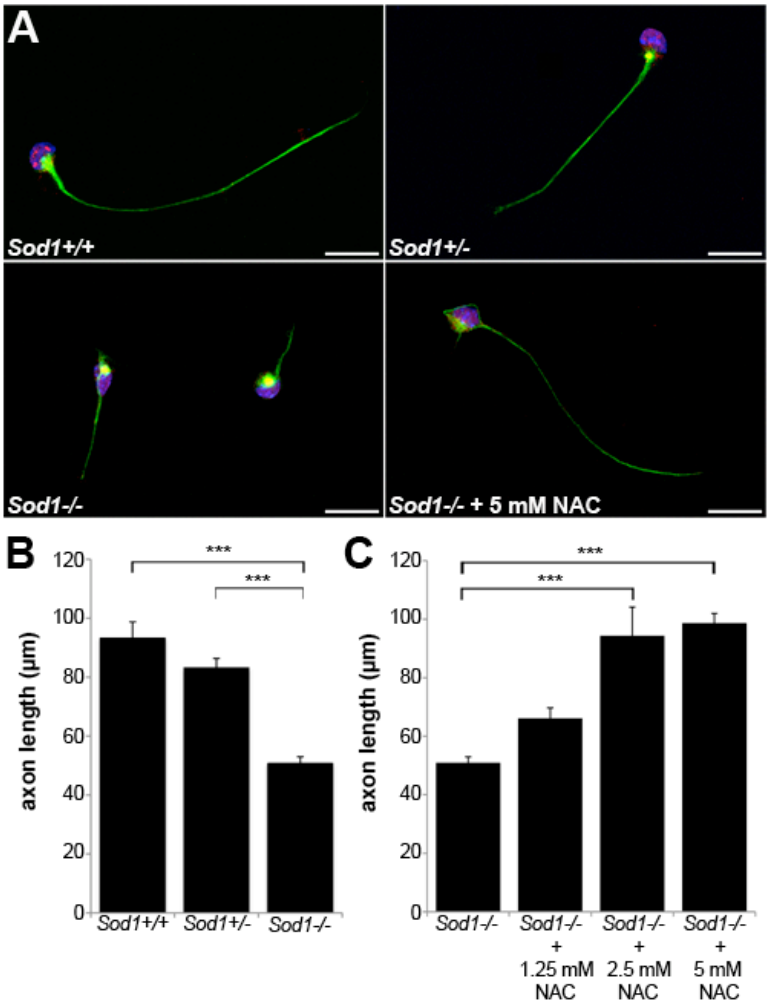

Figure 4.7. Poor axon outgrowth in *Sod1-/-* primary motor neurons is rescued by antioxidant treatment.

Figure 4.7. Poor axon outgrowth in *Sod1-/-* primary motor neurons is rescued by antioxidant treatment. **A.** Representative confocal images of *Sod1+/+, +/-,* and -/- primary motor neurons at 24 hrs in culture, labeled with phosphorylated neurofilament (NF160 antibody, in green), Hb9 (red), and DAPI (blue). *Sod1-/-* motor neurons show significantly shorter axons than controls at 24 hrs. Treatment with 5 mM NAC restores *Sod1-/-* axons to wild-type length (*scale bar = 20 μm*). **B.** Axon measurements verify that *Sod1-/-* axons are ~50% shorter on average than *Sod1+/+* and *Sod1+/-* motor neurons at 24 hours *(***p<0.001*). Mean ± SEM from 4 independent experiments is shown. A total of approximately 500-600 neurons per group were measured (see methods). **C.** Treatment with NAC provides dose-dependent rescue of axon outgrowth in *Sod1-/-* neurons at 24 hours *(***p<0.001).*

Discussion

The question of whether oxidative stress is a cause, propagating factor, or a secondary effect of neurodegeneration has been difficult to resolve in neurodegenerative diseases (Andersen, 2004). Here, we confirm and extend prior reports of motor abnormalities in *Sod1-/-* mice (Flood et al., 1999; Shefner et al., 1999; Muller et al., 2006), and provide the first direct measurement of oxidative stress in peripheral nerves that is associated with conclusive morphologic evidence of motor axonopathy and denervation. *Sod1-/-* mice are far from normal, as commonly represented in the ALS literature, and we contend that the axonal pathology in this model shares much in common with other animal models of motor neuron disease. Moreover, the presence of a motor axonopathy in mice lacking a major antioxidant enzyme demonstrates that chronic oxidative stress is sufficient to trigger distal axonal degeneration *in vivo.*

A review of current ALS literature would suggest that the *Sod1-/-* mouse lacks a neuromuscular phenotype, based primarily on the 1996 study by Reaume and colleagues. The authors followed *Sod1-/-* mice for 6 months, and found no evidence of motor deficits, motor neuron loss, or oxidative stress in brain. However, subsequent studies, including a 1999 follow-up study by Flood, Reaume and colleagues, reported motor abnormalities when animals were followed to later time points. A recent report described age-dependent sarcopenia in *Sod1-/-* mice, acknowledging the potential contribution of denervation, but focusing on oxidative damage to proteins, lipids, and DNA in muscle that was increased by 5 months (Muller et al., 2006). This contrasts with our finding that the GSH redox potential was normal in *Sod1-/-* MGC at 4 months. We also saw no difference in E_h between TA, MGC, and soleus despite differences in denervation (not

shown). The reason for the discrepancy is unclear; data from peripheral nerve were not reported by Muller *et al.* for comparison with muscle. The question of the relative contributions of muscle and nerve to human sarcopenia, and the causes of these abnormalities remains a major question in studies of human aging (Ling et al., 2009). Our current findings demonstrate that distal motor axonopathy in *Sod1-/-* mice correlates most closely with oxidative stress in peripheral nerve.

Along with progressive denervation of hindlimb muscles, we observed robust sprouting in *Sod1-/-* mice that occurred prior to evidence of denervation. This seems contrary to reported electrophysiological data that did not show an increase in motor unit sizes to compensate for loss of motor units (Shefner et al., 1999), suggesting that *Sod1-/-* mice show an additional deficit in sprouting or remodeling. Our demonstration of robust sprouting at *Sod1-/-* NMJs raises the question of whether these sprouts are ineffective, possibly because the reinnervation is short-lived or that the synaptic connection is too weak to create a functional NMJ. Alternatively, sprouting may not be a response to denervation, and may instead be a direct result of oxidative stress, a hypothesis that is supported by the finding of terminal sprouting prior to denervation. Oxidative stress has been postulated to inhibit vesicle release at the NMJ through oxidative damage to SNAP-25 (Giniatullin et al., 2006). This is analogous to the sprout-inducing mechanism of botulinum toxin A (Blasi et al., 1993). Phosphorylation of GAP-43, which promotes spontaneous sprouting at the NMJ *in vivo* (Aigner et al., 1995), is also controlled by a redox-sensitive mechanism (Gopalakrishna et al., 2008). It is unclear whether chronic sprouting alone can promote denervation, although transgenic mice that overexpress GAP-43 do develop motor abnormalities (Aigner et al., 1995).

To address intrinsic susceptibility to oxidative stress and test the effect of antioxidant treatment, we cultured motor neurons from *Sod1-/-* mice. Primary motor neurons from *Sod1-/-* mice were short-lived (no viable cells remained at 72 hours), a finding that is consistent with data from spinal cord slice cultures (Rothstein et al., 1994), and PC12 cells (Troy and Shelanski, 1994), showing that knockdown of SOD1 causes cell death. At 24 hours, the most obvious difference between *Sod1-/-* motor neurons and controls was significantly shorter axons. The deficit in axonal outgrowth was rescued by treatment with NAC, supporting the contention that motor axonopathy is due to oxidative stress. While axon outgrowth *in vitro* is not analogous to denervation at the NMJ *in vivo,* shorter axons have also been reported in primary motor neurons derived from progressive motor neuronopathy (*pmn*) mice (Bömmel et al., 2002), spinal muscular atrophy mice (Rossoll et al., 2003), and in stem cell-derived motor neurons expressing mutant SOD1 (Karumbayaram et al., 2009). This *in vitro* paradigm provides an efficient system for testing mechanistic hypotheses, and importantly, rescue of axon outgrowth *in vitro* has been shown to predict motor axon protection *in vivo* (Oprea et al., 2008; chapter VI).

We found that the age-related distal axonopathy in *Sod1-/-* mice did not involve distal sensory fibers in the epidermis. Previously, we demonstrated that DRG sensory neurons cultured from *Sod1-/-* mice showed poor axon outgrowth and spontaneous axon degeneration *in vitro* (chapter III). It is unclear why sensory axon degeneration is observed *in vitro*, but not *in vivo,* but may relate to the comparatively harsh conditions *in vitro*. In support of this, we found that that degeneration of DRG axons was ameliorated by culturing at physiologic oxygen levels, and by treatment with BME to augment cysteine uptake for GSH synthesis, a role carried out by glia *in vivo* (Sagara et al., 1993).

Another hypothesis is that motor axons are exposed to higher levels of ROS *in vivo* than sensory axons, perhaps by proximity to skeletal muscle. Release of ROS during muscle contraction is a well-described phenomenon (reviewed in Reid and Durham, 2002), that could account for preferential degeneration of motor axons in *Sod1-/-* mice.

Survival of motor axons is one of numerous vital roles for SOD1 that have been identified in SOD1 knockout models. Lack of SOD1 causes a 30% reduction in lifespan in mice (Elchuri et al., 2005) and 80% in *Drosophila* (Phillips et al., 1989). *Sod1-/-* mice have a high incidence of hepatocellular carcinoma late in life (Elchuri et al., 2005). Impaired female fertility (Ho et al., 1998), accelerated age-dependent cataract formation (Reddy et al., 2004), retinal degeneration (Hashizume et al., 2008), and cochlear hair cell loss (McFadden et al., 1999), are also seen, as well as increased susceptibility to noise-induced hearing loss (Ohlemiller et al., 1999). Vascular dysfunction and elevated vascular superoxide levels have also been reported (Didion et al., 2002). Finally, *Sod1-/-* neurons are more vulnerable to cell death due to facial nerve axotomy (Reaume et al., 1996), ischemia (Kondo et al., 1997), and glutamate excitotoxicity (Schwartz et al., 1998).

Motor axon degeneration in *Sod1-/-* mice is unlikely to be a secondary phenomenon caused by ischemia, cachexia, or a paraneoplastic phenomenon. Denervation was present in these mice long before liver tumors were observed at 18 months, and systemic abnormalities cannot account for the abnormalities demonstrated in primary motor neuron cultures. Also, re-introduction of SOD1 specifically to neurons is sufficient to prevent muscle atrophy in these animals (Flood et al., 1999).

There are previous reports of axonal degeneration associated with measures of oxidative stress using *in vitro* models (Press and Milbrandt, 2008; Zherebitskaya et al., 2009). These studies were done in cultured dorsal root ganglia, and studied axonal degeneration in response to mitochondrial and microtubular toxins (Press and Milbrandt, 2008), or a high glucose environment (Zherebitskaya et al., 2009). Assessment of oxidative stress was done with indirect fluorescent indicators of oxidative stress. Our data reported here are the first direct measurements of the GSH redox state in mouse peripheral nerve, and support the findings of previous *in vitro* studies in a model of oxidative stress that does not rely on the use of exogenous toxins.

Potential relevance to mutant SOD1-mediated ALS

Mutations in SOD1 are the cause of approximately 20% of familial ALS, though the mechanisms leading to disease remain unknown (reviewed in Rothstein, 2009). Overexpression of mutant human SOD1 in mice also causes motor neuron disease in rodents, in which the severity depends on the specific mutation and the level of expression of the mutant protein. The deleterious effects of mutant SOD1 in these models are likely due to a toxic gain of function rather than loss of function, given that many of the mutant enzymes retain some degree of dismutase activity (Borchelt et al., 1994), and disease occurs despite super-normal levels of enzyme activity in affected tissues (Turner et al., 2003). However, oxidative stress is a major theme in these ALS models as well as in human ALS (Barber et al., 2006), and a role for oxidative stress in this neurodegenerative disease is likely.

Our findings of motor neuropathy in *Sod1-/-* mice are certainly milder than those reported in mutant SOD1 models of ALS, however it seems unlikely to be a coincidence that both mutation and deletion of SOD1 cause motor deficits that share behavioral and pathologic features. These include early involvement of distal motor axons (Fischer et al., 2004), preferential involvement of motor versus sensory fibers (Fischer et al., 2005), and early, selective denervation of fast-fatigable muscle fibers (Frey et al., 2000; Pun et al., 2006; Hegedus et al., 2007). Our current findings in *Sod1-/-* mice do not contradict the gain of function hypothesis for mutant SOD1. Rather, they raise the question of whether oxidative stress associated with perturbations in SOD1 may underlie motor axon pathology in both models. Numerous mechanisms have been proposed for how mutant SOD1 may cause oxidative stress, including participation in aberrant redox reactions that generate rather than neutralize free radicals (Barber et al., 2006). Mutant SOD1 also has a propensity to aggregate in the cytosol and in mitochondria (Johnston et al., 2000; Vijayvergiya et al., 2005), which has unknown consequences for local SOD1 activity and oxidative stress within axons. Thus, we propose that whether by loss or gain of function, oxidative stress associated with perturbations in SOD1 may be particularly detrimental to distal motor axons.

CHAPTER V. *Wld*^{S} does not protect against oxidative stress-mediated axonal degeneration in the SOD1 knockout model

Introduction

Axonal degeneration is an early and common pathologic entity in peripheral neuropathy and neurodegenerative disease and an important therapeutic target (Coleman and Perry, 2002; Raff et al., 2002). Studies in mouse models of ALS and Parkinson's disease have shown that protection against cell death alone, without protecting axons, does not slow disease progression (Eberhardt et al., 2000; Gould et al., 2006; Rouaux et al., 2007; Suzuki et al., 2007). Currently there are no therapies to treat axonal degeneration in human disease, although studies in cell and animal models have identified several potential strategies (reviewed in Coleman, 2005).

One promising approach is based on a spontaneous mouse mutation, 'slow Wallerian degeneration' (*Wld*^{S}*),* that confers prolonged survival of injured axons (Lunn et al., 1989). Following nerve transection, distal axons of *Wld*^{S} mice survive for up to 4 weeks (Glass and Griffin, 1991; Glass et al., 1993) and support action potentials and axonal transport for 2 weeks (Lunn et al., 1989; Smith and Bisby, 1993; Glass and Griffin, 1994). *Wld*^{S} also protects against genetic (Frey et al., 2000; Mi et al., 2002; Samsam et al., 2003) and toxic (Wang et al., 2002) neuropathies, suggesting the mechanism of action is effective against different types of insults.

Wld^S codes for a novel chimeric protein containing the first 70 amino acids of the E4 ubiquitin ligase *Ube4b*, fused by an 18 amino acid domain (W18) to the NAD+-synthesizing enzyme nicotinamide mononucleotide adenylyl transferase (*Nmnat1)*

(Conforti et al., 2000). The minimum elements needed for the full *Wld*^{S} phenotype are the N-terminal 16 amino acids of *Ube4b*, containing a binding region for valosin-containing protein (VCP), and full-length *Nmnat1* (Avery et al., 2009; Conforti et al., 2009). Enzymatic activity of NMNAT1 is also required, suggesting the mechanism is NAD+-mediated. Still, the critical role of VCP binding, which accounts for at least 35% of the potency of *Wld*^{S} in *Drosophila* (Avery et al., 2009), and is critical for the *Wld*^{S} phenotype in mice (Conforti et al., 2009), remains to be determined. VCP-mediated subcellular targeting or regulation of NMNAT1 turnover may be involved.

In this study, we evaluated the protectiveness of *Wld*^{S} against oxidative stress-mediated axonal degeneration, a mechanism commonly implicated in the pathogenesis of peripheral neuropathy and adult-onset neurodegenerative disease (Barber et al., 2006; Halliwell, 2006; Figueroa-Romero et al., 2008). *Nmnat1* overexpression was previously shown to delay oxidative stress-mediated degeneration of DRG axons *in vitro*, due to the mitochondrial toxin rotenone (Press and Milbrandt, 2008), but the full-length Wld^S protein was not tested in that study, nor was protectiveness investigated *in vivo*. We crossed *Wld*^{S} mice with the Cu,Zn-superoxide dismutase (SOD1) knockout mouse, which shows preferential degeneration of distal motor axons *in vivo* (chapter IV), and robust degeneration of sensory and motor axons *in vitro* (chapter III, IV).

We found that *Wld*^{S} did not prevent hind limb denervation or morphologic abnormalities in *Sod1-/-* distal motor axons by 4 months of age, even though robust axonal protection was still observed after acute axotomy. We also investigated protection of DRG axons *in vitro.* Again, no benefit was seen, either in *Sod1-/-* DRG neurons or in *Wld*^{S} DRGs exposed to the superoxide-generating herbicide, paraquat (PQ) (Sandy et al.,

1986). We conclude that *Wld*^{S} is not effective against axonal degeneration due to loss of SOD1 or increased superoxide. Alterations in the expression level or localization of Wld^S protein may be needed to improve the outcome in oxidative stress-mediated pathology.

Results

Wld^S *does not prevent denervation or morphologic changes at Sod1-/- NMJs*

To test whether *Wld*^{S} protects against oxidative stress-mediated motor axonopathy *in vivo*, we carried out a two-step breeding process to generate *Sod1-/-*, *Wld*^{S} mice. First, *Sod1-/-* males were mated with *Wld*^{S} females, to generate F1 heterozygotes of the genotype *Sod1+/-, Wld*^{S}. These mice were then crossed to generate *Sod1-/-, Wld*^{S} mice and littermate controls. Because the protective effect of *Wld*^{S} in motor axon terminals at the NMJ diminishes with age (Gillingwater et al., 2002), only 4 month-old mice were used in this study. Pathologic changes at *Sod1-/-* NMJs are sufficiently severe by this age to determine if *Wld*^{S} has any effect on the initiation of progressive axonopathy.

Innervation of hindlimb muscles was determined by quantitative morphologic analysis in MGC, TA, and soleus muscles (fig. 1). As previously demonstrated, *Sod1-/-* mice show significant denervation of predominantly fast twitch (type II) muscles by 4 months, whereas no denervation is seen in soleus muscle, which has a higher proportion of slow twitch (type I) fibers. *Sod1-/-, Wld*^{S} mice showed an identical pattern. In MGC, 74% of endplates were fully innervated in *Sod1-/-* mice, compared to 71% in *Sod1-/-, Wld*^{S} mice ($p<0.001$ vs. wild-type). In TA, 69.5% of endplates were fully innervated in *Sod1-/-*mice, compared to 70.2% in *Sod1-/-, Wld*^{S} mice ($p<0.001$ vs. wild-type). Soleus

muscle remained fully innervated in both groups. Thus, *Wld*^{S} was insufficient to slow the onset of denervation in the *Sod1-/-* model.

Next, we examined whether *Wld*^{S} expression attenuated the morphologic abnormalities seen in distal motor axons of *Sod1-/-* mice at 4 months, including sprouting and axonal swellings (fig. 2). No difference was seen in the percent of NMJs with ultraterminal nerve sprouts in *Sod1-/-, Wld*^{S} and *Sod1-/-* mice. Approximately 15% of endplates in MGC and TA had ultraterminal sprouts in both groups ($p<0.001$ vs. wild-type), and both groups had sprouting at approximately 5% of NMJs in soleus ($p>0.05$ vs. wild-type). Large terminal axon swellings were frequently observed in MGC and TA of *Sod1-/-, Wld*^{S} mice, identical to those in *Sod1-/-* mice. In both groups, axonal swellings also involved axons in the intramuscular nerve bundles. Thus, from a morphologic standpoint, *Wld*^{S} had no effect on distal motor axon pathology in young *Sod1-/-* mice.

Sod1-/-, Wld^S *mice retain the 'slow Wallerian degeneration' phenotype*

Given the lack of protection by *Wld*^{S} in young *Sod1-/-* mice, we carried out an acute Wallerian degeneration study to verify that the absence of SOD1 did not somehow interfere with the protectiveness of Wld^S. Unilateral sciatic nerve axotomy was performed in a separate cohort of *Sod1-/-* and *Sod1-/-, Wld*^{S} mice (and corresponding controls). After three days, animals were sacrificed and the morphology of the distal stump of the cut nerve was compared to the uncut side (fig. 3). Robust protection against Wallerian degeneration was observed in *Sod1-/-, Wld*^{S} mice, identical to that seen in *Sod1+/+, Wld*^{S} controls, indicating that lack of SOD1 does not interfere with the classic 'slow Wallerian degeneration' phenotype conferred by expression of *Wld*^{S}.

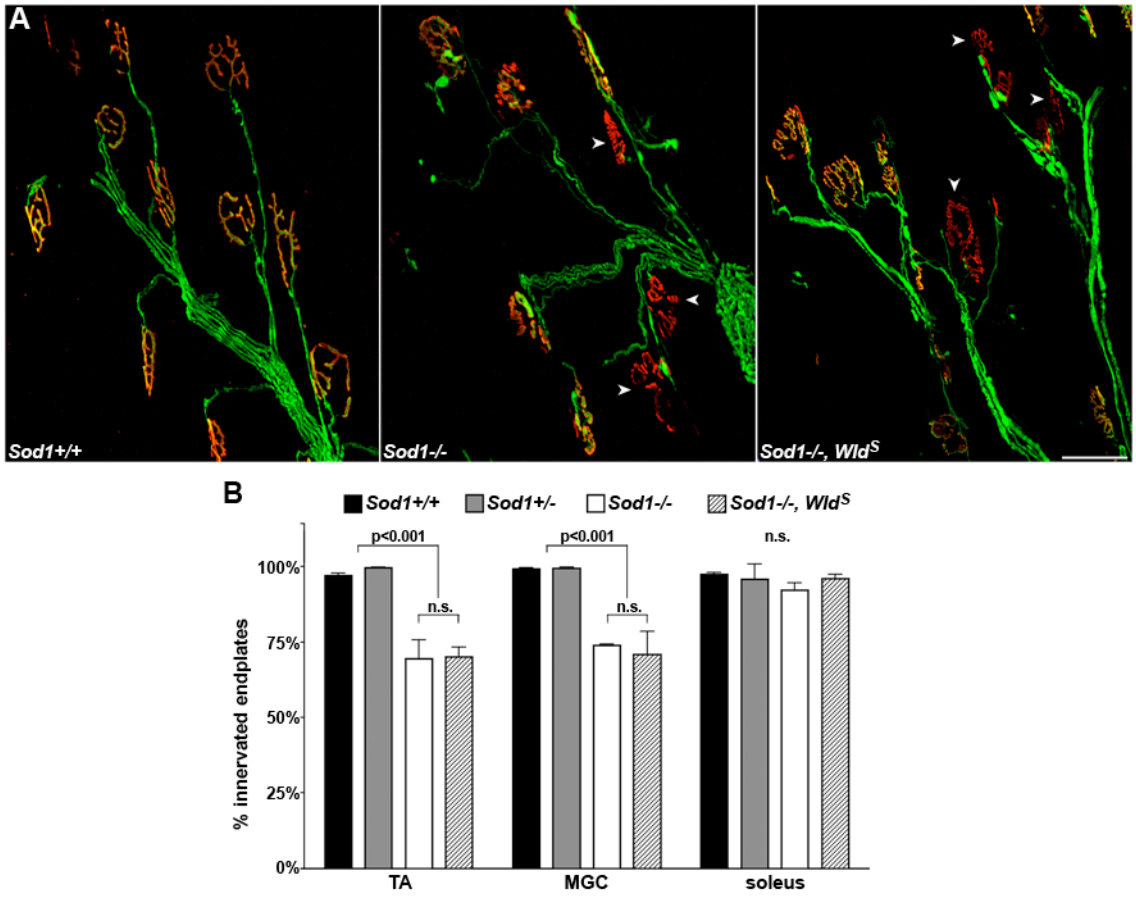

Figure 5.1. *Wld*^{S} does not prevent the onset of denervation in *Sod1-/-* mice. **A.** Denervation (➤) at hind limb NMJs of *Sod1-/-* mice is apparent by four months of age, and is not attenuated by expression of *Wld*^{S}. Representative images of TA are shown, with α-bungarotoxin-labeled motor endplates in red and YFP-positive motor axon terminals in green (*scale bar = 50 μm*). **B.** Quantification of percent innervation in TA, MGC, and soleus muscle at four months of age shows significant denervation in TA and MGC of *Sod1-/-, Wld*^{S} mice, identical to that seen in *Sod1-/-* littermates.

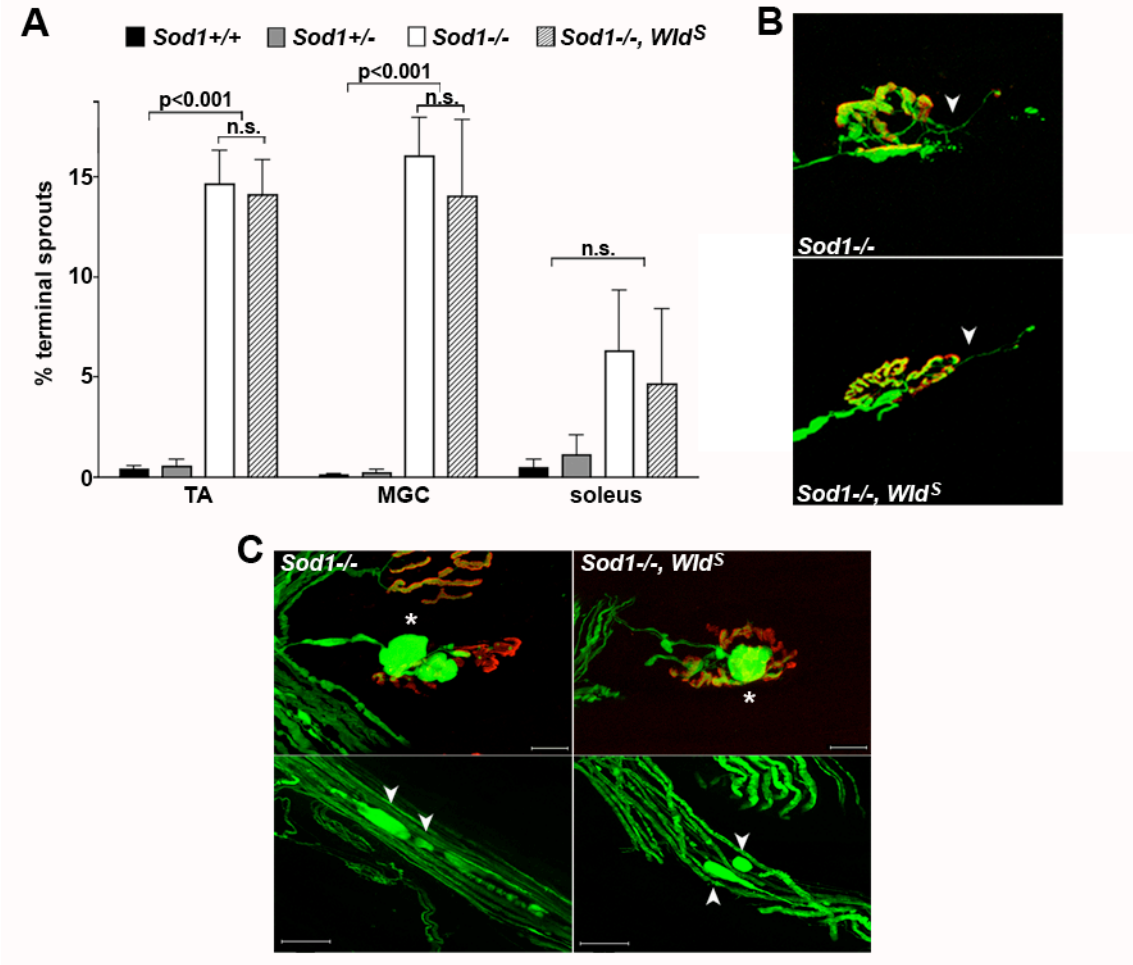

Figure 5.2. *Wld*^{S} does not prevent development of morphologic abnormalities in distal motor axons of *Sod1-/-* mice by four months of age. **A.** The percent of NMJs with ultraterminal sprouts is equivalent in *Sod1-/-* and *Sod1-/-, Wld*^{S} mice at four months. **B.** Ultraterminal sprouts arising from innervated endplates in TA. **C**. Representative images of large axon swellings in motor axon terminals (*) and intramuscular nerve fibers (➤) of *Sod1-/-* and *Sod1-/-, Wld*^{S} mice *(scale bars = 20 µm (upper) and 50 µm (lower))*.

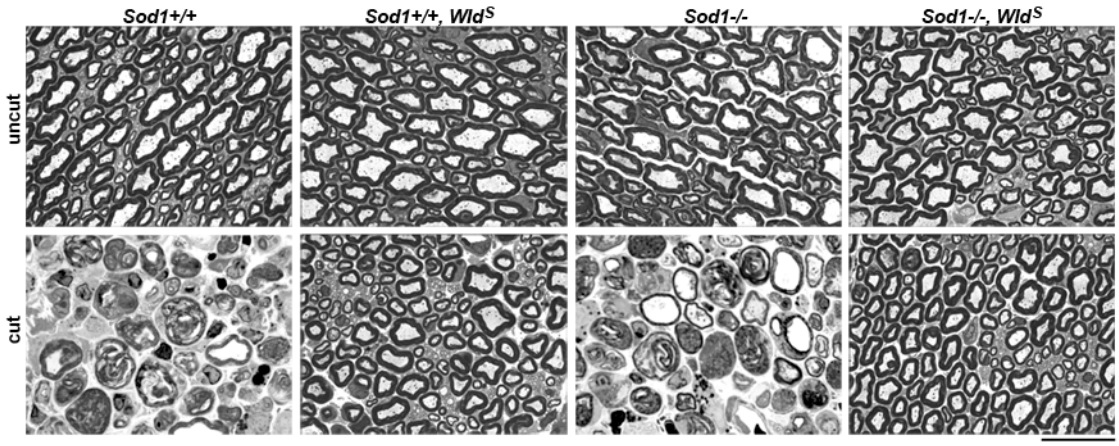

Figure 5.3. *Sod1-/-, Wld*^{S} mice retain the 'slow Wallerian degeneration' phenotype. Toluidine blue-stained cross sections of sciatic nerve are shown three days after unilateral sciatic nerve axotomy. Note robust protection against axon degeneration in the distal stump of cut nerves from *Sod1+/+, Wld*^{S} and *Sod1-/-, Wld*^{S} mice (*scale bar = 20 μm*).

Wld^S *does not alter oxidative stress in Sod1-/- peripheral nerve*

Though we saw no protection by *Wld^S* against distal axonal degeneration in the *Sod1-/-* mouse, we also tested whether *Wld^S* had an effect on oxidative stress in *Sod1-/-* mice. Reduced (GSH) and oxidized (GSSG) glutathione were measured by HPLC in tibial nerve and MGC, and the Nernst equation was used to derive the GSH redox potential (E_h), a well-established indicator of the intracellular redox state (Schafer and Buettner, 2001; Jones, 2002). *Sod1-/-, Wld^S* tissues had an identical redox potential to *Sod1-/-* mice (fig. 4). Tibial nerves from both groups were approximately 20 mV more oxidized than controls ($p<0.01$ vs. wild-type), whereas no significant differences were seen among genotypes in the redox potential of MGC. Thus, *Wld^S* had no effect on the steady-state redox potential of *Sod1-/-* tissues.

Wld^S *fails to protect axons against oxidative stress in vitro*

Next, we used the *Sod1-/-* DRG model (chapter III) to test whether *Wld^S* protects against oxidative stress-mediated axon degeneration outside of the context of the NMJ. DRGs from *Sod1-/-, Wld^S* mice were cultured and total DRG area was measured over time compared to DRGs from *Sod1+/+, Sod1+/-, and Sod1-/-* littermates (fig. 5). *Wld^S* did not confer protection against axonal degeneration by this assay. Immunostaining for Wld^S protein confirmed prominent nuclear expression of Wld^S in *Sod1-/-, Wld^S* neurons, which is consistent with previous reports (Mack et al., 2001; Samsam et al., 2003). Thus, *Wld^S* is insufficient to protect DRG axons against degeneration due to loss of SOD1 *in vitro*.

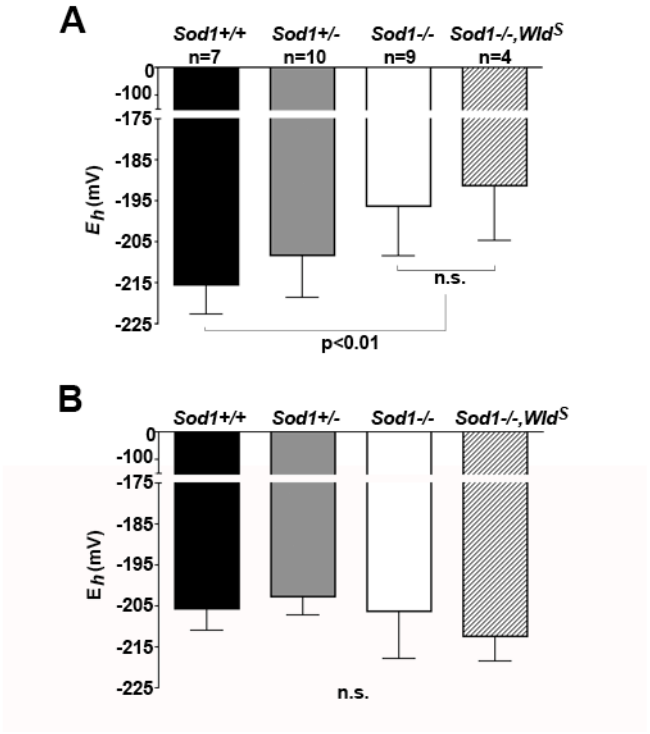

Figure 5.4. *Wld*^{S} does not alter the redox potential (E_h) in *Sod1-/-* tissue, calculated from HPLC measurement of GSH and GSSG. **A.** The redox potential in tibial nerve homogenates from four month-old *Sod1-/-, Wld*^{S} mice is equivalent to that seen in *Sod1-/-* mice. Both are ~20 mV higher (i.e. more oxidized) than *Sod1*+/+ mice ($p < 0.01$). **B.** E_h in medial gastrocnemius muscle of *Sod1-/-* and *Sod1-/-, Wld*^{S} mice is equivalent to controls at four months.

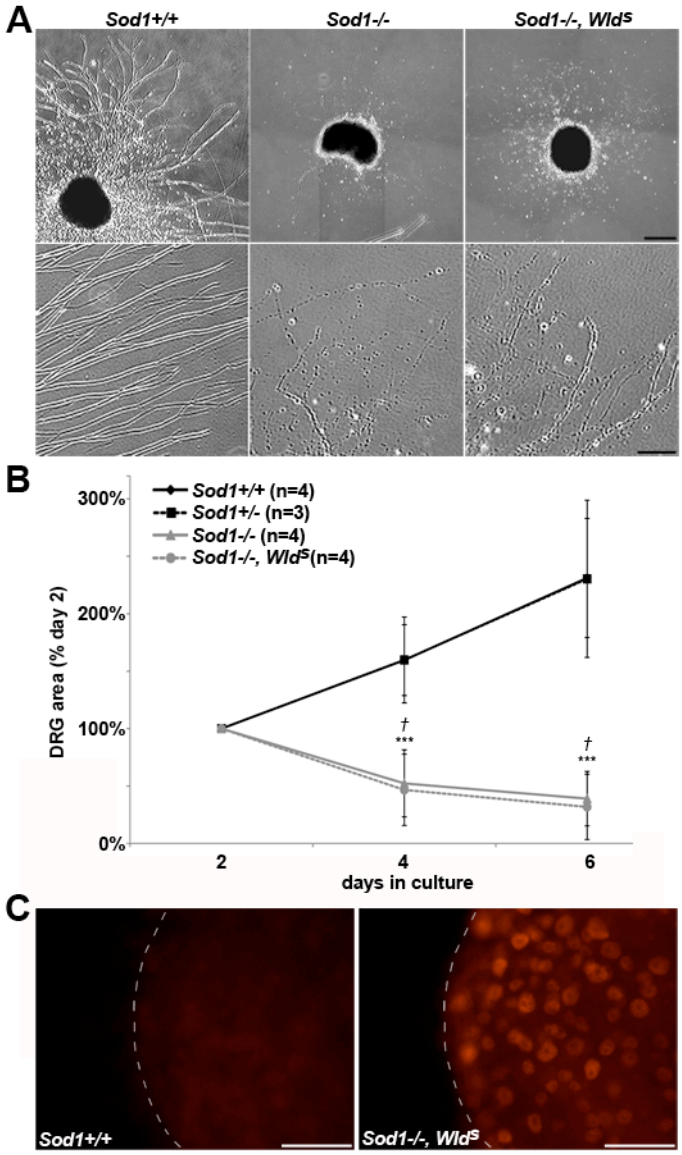

Figure 5.5. *Wld*^{S} fails to protect *Sod1-/-* DRG axons. **A**. By day 6 in culture, *Sod1-/-* and *Sod1-/-, Wld*^{S} DRGs show extensive axonal degeneration not seen in DRGs from *Sod1+/+* mice (*scale bars = 100 µm (upper) and 10 µm (lower)*). **B**. *Wld*^{S} does not prevent loss of DRG area in *Sod1-/-* DRGs. N=number of mice. 4-8 DRGs were measured per animal ($^{***}p$<0.001, *Sod1-/-* vs. *Sod1+/+*; $^{\dagger}p$<0.001, *Sod1-/-, Wld*^{S} vs. *Sod1+/+)*. **C**. *Sod1-/-, Wld*^{S} DRG neurons show characteristic nuclear expression of Wld^S protein (W18 antibody). Dotted line denotes border of DRG explant (*scale bar = 50 µm*).

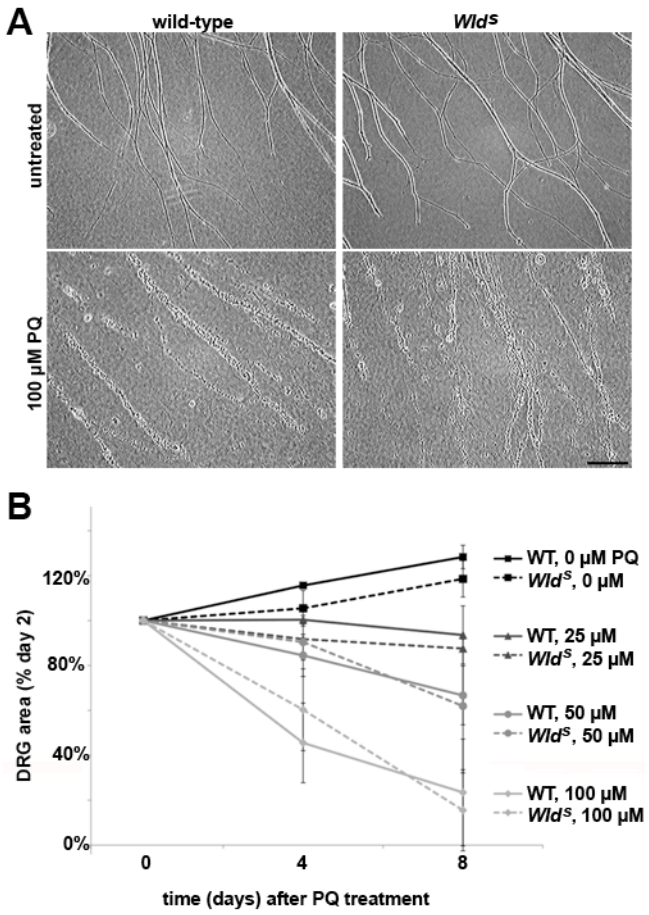

Figure 5.6. *Wld*^{S} fails to protect DRG axons against oxidative stress due to treatment with the redox-cycling herbicide, paraquat (PQ). **A**. Administration of PQ to mature DRGs (two weeks in culture) causes degeneration of wild-type and *Wld*^{S} axons. Representative images of DRG axons after 8 days of treatment with 100 µM PQ are shown (*scale bar = 50 µM*). **B**. Susceptibility of *Wld*^{S} DRGs to PQ toxicity is identical to wild-type DRGs over a range of doses.

To address whether *Wld*^{S} is protective against oxidative stress outside of the *Sod1-/-* model, we treated DRGs from *Wld*^{S} mice with paraquat (PQ), a redox-cycling herbicide that generates superoxide within cells (fig. 6) (Sandy et al., 1986). Wild-type (WT) and *Wld*^{S} DRGs were maintained in culture for two weeks, followed by a single dose of 25 μM, 50 μM, or 100 μM PQ. DRG area was measured at 4 and 8 days after PQ administration, and each DRG normalized to its own area on day 0 (day of PQ administration). We observed dose-dependent degeneration of both WT and *Wld*^{S} axons over this time period. *Wld*^{S} DRGs did not show protection at any dose. This supports our conclusion that *Wld*^{S} does not protect against axonal degeneration due to oxidative stress, due to loss of SOD1 or an excess of superoxide.

Discussion

Oxidative stress may trigger and/or propagate axonal degeneration in motor neuron disease, diabetic neuropathy, neuropathy of aging, and other forms of peripheral neuropathy. In this study, we tested the effectiveness of *Wld*^{S} as a strategy for protecting against axon degeneration in the *Sod1-/-* mouse. *Wld*^{S} failed to attenuate denervation in this model, and had no effect on sprouting or formation of large axonal swellings, despite a previous demonstration of protection against axonal spheroid pathology in the CNS (Mi et al., 2005). Acute axotomy showed that loss of SOD1 did not abolish the function of Wld^S protein, since slowing of Wallerian degeneration was as robust in *Sod1-/-, Wld*^{S} mice as in *Sod1+/+, Wld*^{S} controls.

Lack of protection at the NMJ in *Sod1-/-* mice is consistent with studies showing that *Wld*^{S}-mediated protection at the NMJ is short-lived compared to the rest of the axon

(Ribchester et al., 1995). This parallels the course of Wallerian degeneration in wild-type mice, in which motor axon terminals degenerate more quickly than non-terminal regions (Miledi and Slater, 1970). *Wld*^{S} terminal motor axons remain intact for a period of 3 days to 2 weeks following nerve transection (Ribchester et al., 1995), long enough to delay muscle atrophy (Brown et al., 1991), but transient compared to non-terminal axonal protection which lasts 4 weeks (Glass et al., 1993). Additionally, protection at the synapse in *Wld*^{S} mice is lost with age (Gillingwater et al., 2002), whereas axonal protection persists, even out to 16 months of age (Crawford et al., 1995). Gillingwater and colleagues demonstrated slowly progressive synapse withdrawal after axotomy in 2 month-old *Wld*^{S} mice, but by 4 months, there is a mix of slow and fast synapse loss, and by 7 months, axotomy causes rapid, synchronous degeneration at the NMJ, equivalent to wild-type mice (2002). Since axonal pathology in the *Sod1-/-* mouse is limited to motor axon terminals at the NMJ, and is still in early stages at 4 months (chapter IV), the lack of protection we observed may, in fact, reflect the transient nature of *Wld*^{S} protection at the NMJ. We also found only transient protection at the NMJ by *Wld*^{S} in the SOD1-G93A model of familial ALS (Fischer et al., 2005), and no protection was seen in mouse models of spinal muscular atrophy, a disease that primarily targets NMJs (Rose et al., 2008; Kariya et al., 2009).

To test axonal protection independent of the NMJ, we tested *Wld*^{S} in *Sod1-/-* DRG cultures, and in DRG cultures exposed to PQ. No protection was observed in either rmodel. This is surprising given that *Wld*^{S} has typically shown robust protection of DRG axons in other models. In fact, DRG cultures showed a protective effect in *Nmnat1*-only studies (Araki et al., 2004; Wang et al., 2005; Sasaki et al., 2006) where no protection

was observed in mice *in vivo* (Conforti et al., 2007b). Transected *Wld*^{S} DRG axons survive for an extended period of time compared to wild-type axons (Glass et al., 1993), and *Wld*^{S} DRG axons are resistant to vincristine (Wang et al., 2001b; Wang et al., 2001a) and paclitaxel toxicity (Wang et al., 2002). The doses of vincristine and paclitaxel used in those studies caused axon degeneration over a similar time period as that caused by PQ in the current study (~1 week), but no protection was observed against PQ.

These data suggest that *Wld*^{S} may be somehow ineffective in protecting against oxidative stress-mediated axon degeneration. Mechanistic studies demonstrate that NMNAT-mediated NAD+ production is required for *Wld*^{S}-mediated axon protection (Avery et al., 2009; Conforti et al., 2009). NAD+ participates in numerous metabolic pathways, ranging from ATP production to regulation of Ca^{2+} signaling to DNA repair (reviewed in Braidy et al., 2008). For example, repair of oxidatively damaged DNA by poly (ADP-ribose) polymerase-1 (PARP-1) depends on NAD+, and hyperactivation of PARP due to oxidative stress can rapidly deplete NAD+. This process is important for repair of DNA damage in the nucleus, but PARP-1 and other PARP family members are also expressed in mitochondria (Du et al., 2003). Preferential inhibition of mitochondrial PARP preserved mitochondrial function and prevented cell death in cultured cortical neurons exposed to $ONOO^-$, demonstrating that mitochondrial NAD+ depletion due to oxidative stress is detrimental to neurons. Inhibition of PARP also provided modest protection against Wallerian degeneration in DRG cultures, suggesting this pathway is relevant to axon survival (Araki et al., 2004).

To our knowledge, NAD+ depletion has not been tested in the *Sod1-/-* model. However, rapid oxidative stress-mediated depletion of NAD+ could theoretically

overwhelm the protective capacity of *Wld*^{S}. This is speculation, although there are data to suggest that oxidative damage due to loss of SOD1 preferentially targets mitochondria (Elchuri et al., 2005; Aquilano et al., 2006; Muller et al., 2007; Yanase et al., 2009, and see chapter VI). If lack of protection by *Wld*^{S} in *Sod1-/-* mice is due to oxidative stress-mediated NAD+ depletion, increasing the dose of Wld^S protein or altering the localization may be beneficial. In mice, protection by *Wld*^{S} is dose-dependent (Mack et al., 2001; Samsam et al., 2003). Up to 4 gene copies of *Wld*^{S} can currently be introduced by breeding *Wld*^{S} mice with *Wld*-transgenic mice (Mack et al., 2001). Deletion of the *Wld*^{S} nuclear localization signal (NLS) was also recently shown to increase Wld^S protein expression in axons and improve NMJ protection (Beirowski et al., 2009). The effect of ΔNLS-*Wld*^{S} may therefore be useful to test in the *Sod1-/-* model. Overexpression of the mitochondrial isoform of NMNAT, NMNAT3, was also shown to be as effective as *Wld*^{S} in *Drosophila* (Avery et al., 2009) and in mice (Yahata et al., 2009). If mitochondrial NAD+ depletion is responsible for the lack of protection against oxidative stress, NMNAT3 overexpression may be a useful strategy to pursue.

In summary, we demonstrated that *Wld*^{S} did not attenuate oxidative stress-mediated axonal degeneration due to loss of SOD1 or exposure to PQ. *Wld*^{S} still protected against acute Wallerian degeneration, suggesting that the protein is present and active in *Sod1-/-*, *Wld*^{S} mice, but incapable of preventing distal axonal denervation. This could be related to the transient effect of *Wld*^{S} at the NMJ that diminishes with age (Ribchester et al., 1995; Gillingwater et al., 2002). Or, there may be a mechanistic explanation for failure of *Wld*^{S}, such as oxidative stress-mediated NAD+ depletion (Du et al., 2003). Strategies to increase *Wld*^{S} expression in axons, and specifically in

mitochondria, may be useful for protecting against oxidative stress-mediated axonal degeneration.

CHAPTER VI: Targeted expression of SOD1 in the mitochondrial intermembrane space is sufficient to prevent motor axonopathy in the SOD1 knockout mouse

Introduction

Mice lacking the antioxidant enzyme Cu,Zn-superoxide dismutase (SOD1) develop a progressive distal motor axonopathy associated with oxidative stress in peripheral nerve (chapter IV). SOD1 is therefore required for maintenance of distal motor axons and intact neuromuscular junctions (NMJ). The source of oxidative stress responsible for axonal degeneration in *Sod1-/-* mice and the precise role of SOD1 in axon survival are unknown.

SOD1 is one of three mammalian SOD enzymes that convert superoxide ($O_2\cdot^-$) to H_20_2 and O_2 (McCord and Fridovich, 1969). SOD1 is localized throughout the cytosol and nucleus, and is also found in the mitochondrial intermembrane space (IMS) (Weisiger and Fridovich, 1973; Sturtz et al., 2001; Iñarrea, 2002), while SOD2 is found exclusively in the mitochondrial matrix and SOD3 is a secreted protein (reviewed in Zelko et al., 2002). SOD enzymes neutralize $O_2\cdot^-$ produced by the mitochondrial electron transport chain, located along the mitochondrial inner membrane and considered to be the primary source of intracellular $O_2\cdot^-$. Complex I releases $O_2\cdot^-$ into the mitochondrial matrix, whereas complex III releases $O_2\cdot^-$ bidirectionally into the matrix and IMS (Han et al., 2001; Lambert and Brand, 2004; Muller et al., 2004). Thus, even though SOD1 is traditionally considered to be the "cytoplasmic" SOD, localization in the IMS suggests SOD1 also plays an important role in mitochondria.

The idea that SOD1 protects against oxidative stress in mitochondria is supported

by studies demonstrating mitochondrial damage due to knockdown or deletion of SOD1. SOD1 knockdown in SH-SY5Y cells caused oxidation of mitochondrial and not cytosolic proteins, loss of mitochondrial membrane potential, and decreased ATP production (Aquilano et al., 2006). Inactivation of aconitase, a surrogate marker of $O_2\cdot^-$ levels, was observed in both the cytosolic and in mitochondrial compartments of liver from SOD1 KO mice (Elchuri et al., 2005). Increased mitochondrial ROS generation due to loss of SOD1 has also been reported in *Sod1-/-* mice (Muller et al., 2007) and *C. elegans* (Yanase et al., 2009). Still, the importance of IMS SOD1 for protecting against oxidative stress-mediated pathology remains an open question.

We hypothesized that mitochondrial $O_2\cdot^-$ may contribute to distal axonal degeneration in the *Sod1-/-* mouse. To test this hypothesis, we crossed *Sod1-/-* mice with transgenic mice expressing wild-type human SOD1 targeted to the mitochondrial IMS (in collaboration with Anissa Igoudjil and Giovanni Manfredi, Cornell University). IMS-SOD1 rescued axon outgrowth and restored mitochondrial density in axons from *Sod1-/-* primary motor neurons. *In vivo,* IMS-SOD1 was sufficient for long-term preservation of innervated NMJs, and prevented the development of morphologic abnormalities in distal motor axons. These data suggest that localization of SOD1 in the IMS is critical for survival of motor axons, and implicate mitochondria as a source of $O_2\cdot^-$ leading to motor axon degeneration in the *Sod1-/-* mouse.

Results

Targeting of wild-type human SOD1 to the mitochondrial IMS

To study the function of SOD1 in the IMS, transgenic *IMS-SOD1* mice were

generated that express wild-type human SOD1 targeted to the mitochondrial IMS. SOD1 was fused to mitochondrial targeting elements derived from mitofilin, a transmembrane protein of the mitochondrial inner membrane (Gieffers et al., 1997) (fig. 1, courtesy of A. Igoudjil). The 21-amino acid mitofilin presequence directs the N-terminal portion of the polypeptide to be threaded into the mitochondrial matrix, where the presequence is cleaved by mitochondrial processing peptidase (MPP, indicated in fig. 1A). The transmembrane domain remains embedded in the mitochondrial inner membrane, with the C-terminal portion, containing SOD1, extending out into the IMS (fig. 1B). Transgene expression was via MoPrp.Xho, a well-characterized vector for prion promoter-mediated expression in central and peripheral nervous tissues, with variable expression in heart, liver, kidney, and skeletal muscle (Borchelt et al., 1996). Measurement of SOD1 activity in isolated brain mitochondria from *IMS-SOD1* mice showed a two-fold increase in mitochondrial SOD1 activity (fig. 1C). The restricted expression of wild-type human SOD1 in the IMS was verified by subcellular fractionization, and alkaline extraction studies demonstrated that the IMS-SOD1 protein is membrane bound (A. Igoudjil, not shown). There were no differences in body weight or rotarod performance between *IMS-SOD1* mice and non-transgenic littermates when observed out to 8 months of age (A. Igoudjil, not shown).

To generate mice expressing SOD1 only in the mitochondrial IMS, *IMS-SOD1* mice were crossed with *Sod1-/-* mice in a two-step breeding process (fig. 2A). The offspring of interest from this breeding are double transgenic *IMS-SOD1, Sod1-/-* mice. Littermate *IMS-SOD1, Sod1+/+* and *Sod1+/+* mice were used as controls. F2 heterozygotes were discarded since no difference was seen between *Sod1+/+* and

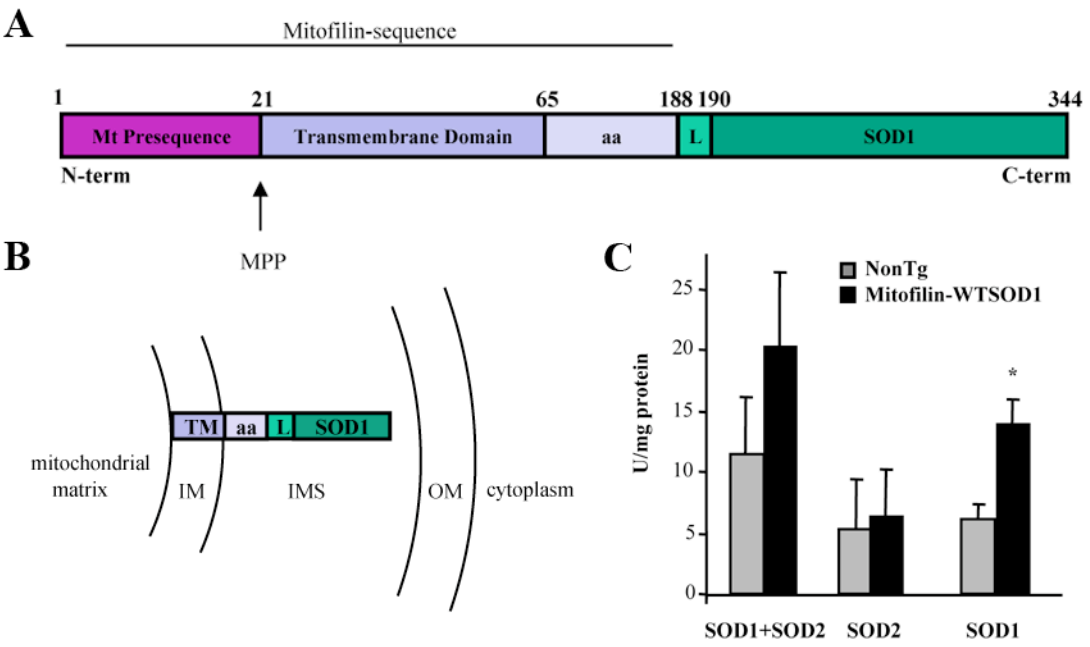

Fig. 6.1. Generation of *IMS-SOD1* transgenic mice. **A.** The mitofilin-WTSOD1 fusion protein consists of the mitofilin mitochondrial targeting sequence ('Mt presequence'), transmembrane domain, and 123 amino acids ('aa', 65-188) of the mitofilin protein, fused in-frame to wild-type human SOD1 by a 2 amino acid linker ('L'). Note the site of cleavage by mitochondrial processing peptidase (MPP). **B.** Expected localization of wild-type human SOD1, tethered to the outer face of the mitochondrial inner membrane (presequence has been cleaved) (IM = inner membrane; IMS = intermembrane space; OM = outer membrane). **C.** SOD enzyme activity in isolated brain mitochondria from mitofilin-WTSOD1 mice was measured by a standard colorimetric assay. Mitofilin-WTSOD1 mice show a two-fold increase in mitochondrial SOD activity compared to non-transgenic (Non-Tg) littermates. Cyanide-mediated inhibition of SOD1 (but not SOD2), was used to distinguish the activity of the two enzymes. The difference in total SOD activity was due to an increase in SOD1 activity, whereas SOD2 activity was unchanged.

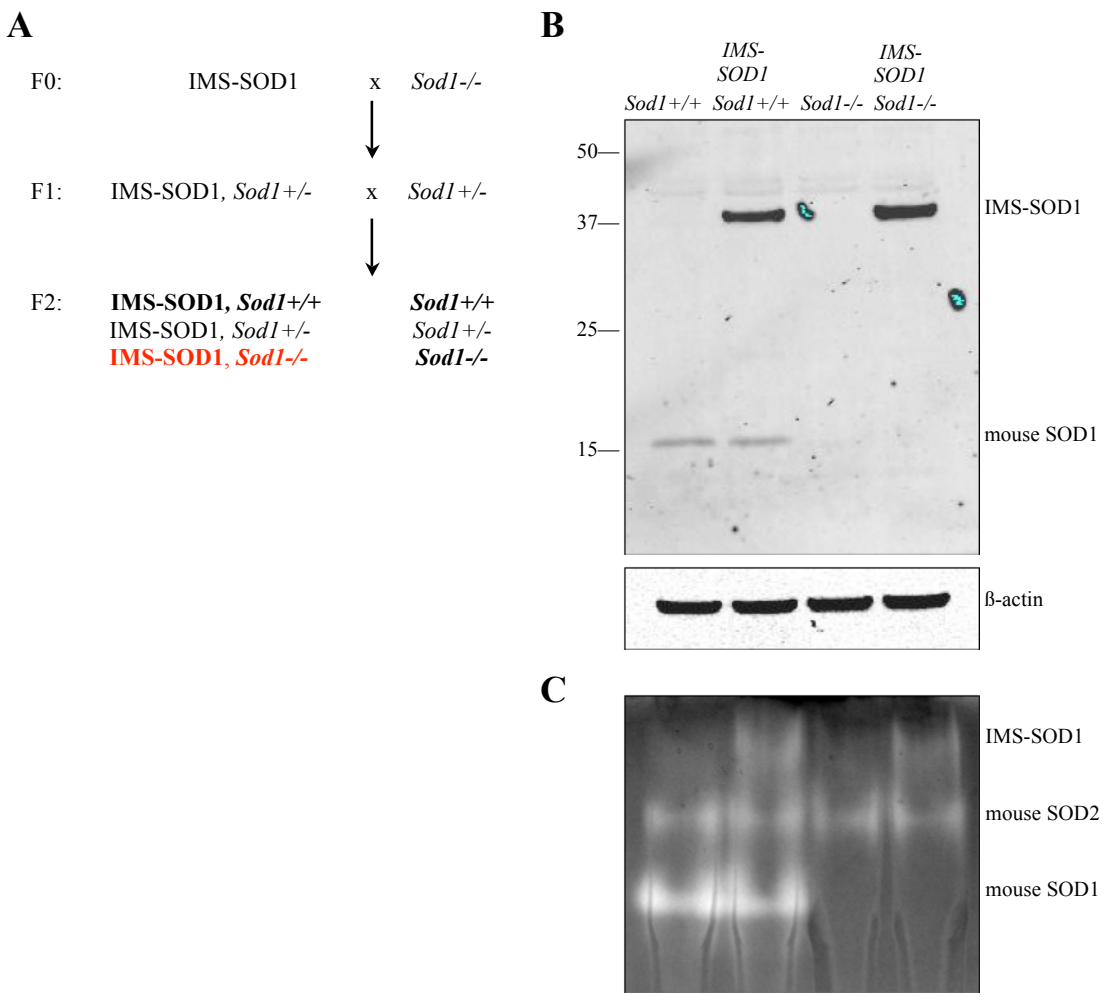

Fig. 6.2. Breeding of *IMS-SOD1* and *Sod1-/-* mice. **A.** Two-step breeding strategy used to generate mice of the target genotype: *IMS-SOD1, Sod1-/-* (in red) and littermate controls (in bold). F2 heterozygotes were omitted from the analysis. **B.** Western blot of lumbar spinal cord homogenates, probed with an antibody that recognizes mouse and human SOD1 (Calbiochem). **C.** SOD1 zymography from these same spinal cords showing expected levels of mouse SOD1 and SOD2 activity, and an additional band putatively corresponding to IMS-SOD1.

Sod1+/- mice at the ages used in this study (chapter IV). Western blot analysis of SOD1 protein in spinal cord homogenates showed the expected expression of mouse and human SOD1 for each genotype (fig. 2B). Analysis of SOD1 enzyme activity by native PAGE showed the presence of an additional band in *IMS- SOD1, Sod1+/+* and *IMS-SOD1, Sod1-/-* mice (fig. 2C), suggesting that SOD1 anchored to the mitochondrial inner membrane in these mice is enzymatically active.

IMS-SOD1 localization and rescue of axon outgrowth in primary motor neurons

Primary motor neurons were cultured from *IMS-SOD1, Sod1-/-* mice, and mitochondrial localization of human SOD1 was verified by immunocytochemistry (fig. 3A). Staining with a monoclonal antibody specific for human SOD1 revealed a punctate distribution. This staining was absent in cells negative for the *IMS-SOD1* transgene (not shown). Double labeling with Mitotracker Red CM-H_2XRos revealed precise colocalization of SOD1 staining with mitochondria (fig. 3A, overlay).

To obtain a preliminary readout of the effect of *IMS-SOD1,* axon outgrowth was measured in primary motor neurons at 24 and 48 hours (fig. 3B). *Sod1-/-* motor neurons extended shorter axons than controls, consistent with previous data (chapter IV). *IMS-SOD1* showed a robust protective effect in *IMS-SOD1, Sod1-/-* motor neurons, restoring growth characteristics and axon length to wild-type levels. Axon length at 24 hours (mean ± SEM) in *Sod1-/-* motor neurons was 47.1 ± 4.4 μm, compared to 78.07 ± 5.9 μm in *IMS-SOD1, Sod1-/-* motor neurons ($p<0.05$). At 48 hours, *Sod1-/-* motor axons decreased to 34.6 ± 2.0 μm in length, while *IMS-SOD1, Sod1-/-* motor axons doubled in length to 168.8 ± 19.2 μm ($p<0.001$). Thus, *in vitro,* IMS-SOD1 was properly localized

to mitochondria and rescued axon outgrowth in *Sod1-/-* motor neurons.

IMS-SOD1 normalizes mitochondrial density in motor axons

To determine if mitochondrial density is altered in *Sod1-/-* primary motor neurons, mitochondria were labeled with Mitotracker Red- CM-H_2XRos after 24 hours in culture, fixed, and the cumulative length of mitochondria (in μm) was compared to the total length of the axon (fig. 4A). A 40% decrease in mitochondrial density was observed in *Sod1-/-* axons compared to *Sod1+/+* axons ($p<0.05$), which was normalized by IMS-SOD1 (fig. 4B).

Sod1-/- motor neurons had significantly shorter axons on average than the other groups. To determine whether differences in axon length may have biased the data, short (≤ 100 μM) versus long (>100 μM) axons were compared (fig. 4C). Mitochondrial density did not differ based on axon length, and the magnitude of the decrease in *Sod1-/-* mice remained constant (although the standard error increased for *Sod1-/-* axons >100 μm due to the low n). This supports the conclusion that mitochondrial density is primarily a function of genotype.

IMS-SOD1 preserves NMJ integrity in vivo

Cohorts of *Sod1-/-* and *IMS-SOD1, Sod1-/-* mice (and littermate controls) were followed to 4 and 8 months of age for assessment of NMJ pathology. Morphologic analysis of innervation in tibialis anterior (TA) showed a robust protective effect of *IMS-SOD1* that did not diminish over time (fig. 5A-B). At 4 months, 55% ± 8% of *Sod1-/-* NMJs were fully innervated, compared to >92% in *IMS-SOD1, Sod1-/-* mice and controls

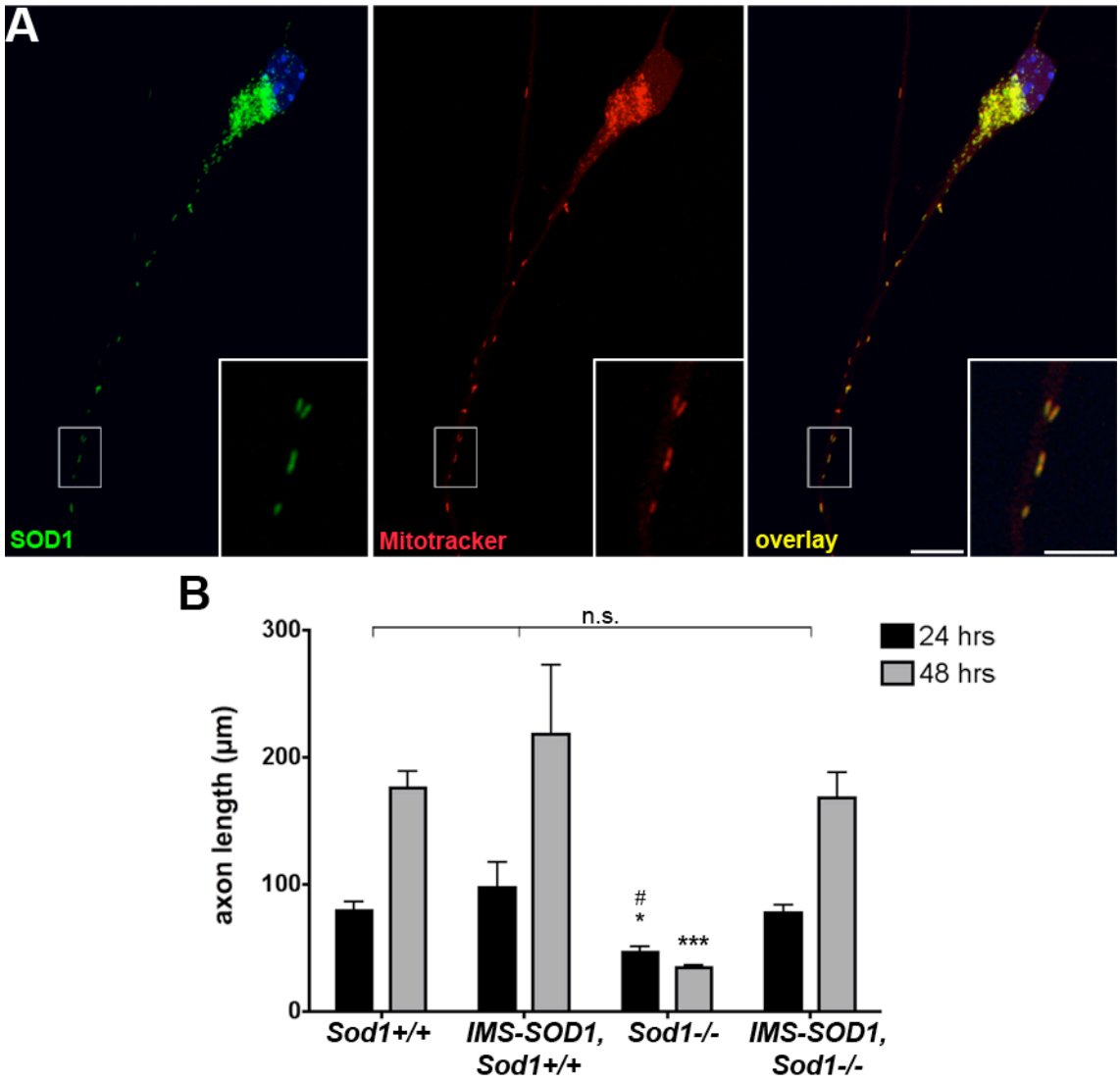

Fig. 6.3. *IMS-SOD1* rescues axon outgrowth in *Sod1-/-* primary motor neurons. **A.** Mitochondrial localization of IMS-SOD1 was verified by double labeling for human SOD1 (Sigma antibody, in green) and Mitotracker Red CM-H_2XRos. A representative image of a *IMS-SOD1,Sod1-/-* motor neuron (24 hrs) is shown. Scale bar = 10 µm (inset 5 µm). **B.** Axon length at 24 and 48 hours in culture. Mean ± SEM is shown from six independent experiments, needed to generate ≥ three replicates per genotype (24 hours: **p*<0.05 vs. *Sod1+/+* and *IMS-SOD1,Sod1-/-; #p*<0.01 vs. *IMS-SOD1, Sod1+/+*. 48 hours: ****p*<0.001 vs. all other genotypes).

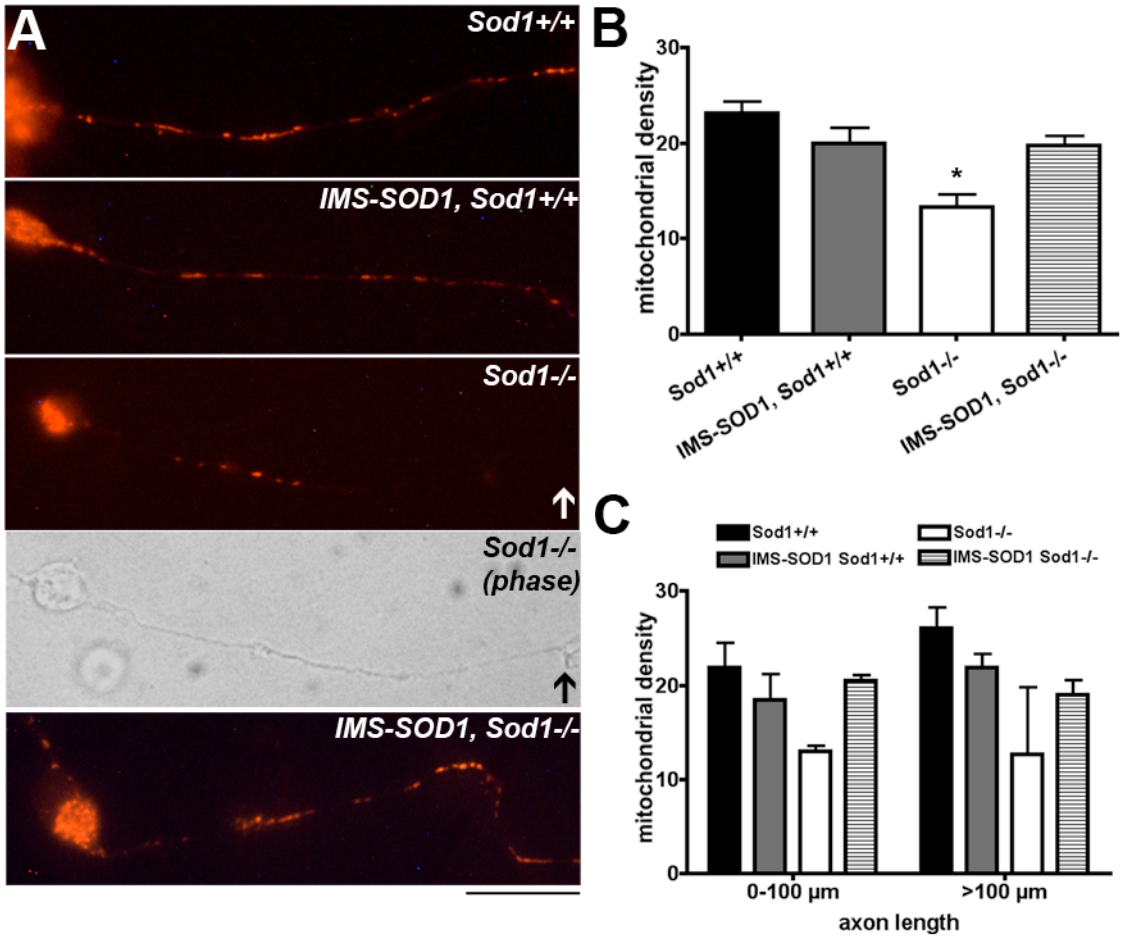

Fig. 6.4. IMS-SOD1 normalizes mitochondrial density in motor axons. **A.** Representative ~100 µm axons labeled with Mitotracker Red CM-H_2XRos (24 hrs). A phase contrast image is also shown for the *Sod1-/-* motor neuron to visualize the full length of the axon (the terminal is marked with an arrow). Scale bar = 25 µm. **B.** Mitochondrial density (mean ± SEM) expressed as total µm mitochondria / µm axon length (*p<0.05 vs. controls). At least three independent replicates (n=25 axons) were performed per genotype. **C.** Comparison of mitochondrial density in short (≤ 100 µm) versus long (>100 µm) axons shows that differences in mitochondrial density are primarily due to genotype, and not axon length.

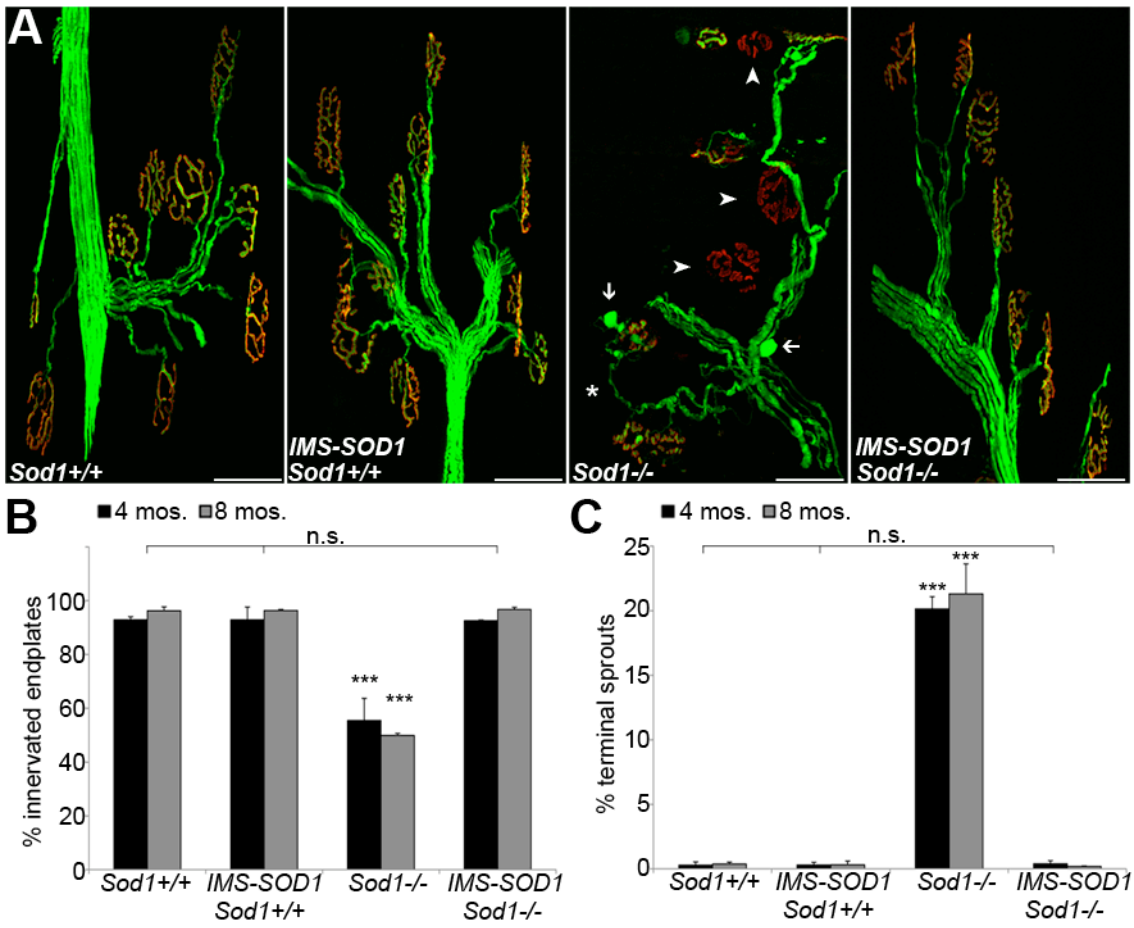

Fig. 6.5. IMS-SOD1 is sufficient for long-term maintenance of NMJ innervation and morphology *in vivo.* **A.** Representative images of NMJs from TA at 8 months. *Sod1-/-* muscle shows denervated endplates (➤), axon swellings (➔), and a chain of endplates typical of reinnervation (*). These features are absent in control mice, as well as in *IMS-SOD1, Sod1-/-* mice (scale bar = 50 μm). **B.** Percent of fully innervated endplates in TA muscle at 4 and 8 months of age. **C.** Percent of NMJs with ultraterminal nerve sprouts at 4 and 8 months of age (***$p < 0.001$ vs. all other genotypes, n.s. = not significant). In **B-C**, mean ± SD is shown, n=3 mice per genotype. NMJs evaluated per TA: 954±109 (4 mos); 974±102 (8 mos).

($p<0.001$). By 8 months, denervation had progressed slightly in *Sod1-/-* animals (consistent with the slow progression reported in chapter IV), but *IMS-SOD1, Sod1-/-* NMJs remained fully innervated.

Axonal and terminal sprouting, typical of *Sod1-/-* mice by 4 months, were also prevented (fig. 5C). Ultra-terminal nerve sprouts were seen at 20.1% ± 1% and 21.3% ± 2.5% of *Sod1-/-* NMJs at 4 and 8 months, respectively, compared to < 1% in *IMS-SOD1, Sod1-/-* mice and controls ($p<0.001$). These data demonstrate that *IMS-SOD1* is sufficient to prevent the development of motor axonopathy in *Sod1-/-* mice, and protection persists over time.

Discussion

Altered mitochondrial function and dynamics are emerging as a major cause of axonal degeneration in peripheral neuropathy and motor neuron disease (Baloh, 2008; Magrané and Manfredi, 2009; Shi et al., 2009). Here, we investigated how wild-type SOD1 expression in the mitochondrial IMS influences the survival of motor axons, based on the hypothesis that mitochondria are a major source of $O_2{\cdot}^-$ causing axonal degeneration in the *Sod1-/-* mouse. Our primary goal was to establish whether or not IMS SOD1 protects *Sod1-/-* axons, *in vitro* and *in vivo*. A protective function for IMS SOD1 has been suggested by reports of mitochondrial oxidative stress and/or oxidative damage due to deletion of SOD1 (Elchuri et al., 2005; Aquilano et al., 2006; Muller et al., 2007; Yanase et al., 2009). However, one group reported increased ROS generation by IMS SOD1 in the context of excess $O_2{\cdot}^-$ production (Goldsteins et al., 2008). None of these previous studies addressed the functional effect of IMS SOD1 on oxidative stress-

mediated pathology.

We found *in vitro* and *in vivo* that IMS-SOD1 is sufficient to rescue motor axon defects associated with loss of SOD1. Robust protection by IMS-SOD1, in the absence of SOD1 in other compartments, suggests that SOD1 in the IMS is critical for regulating physiologic $O_2{\cdot}^-$ levels. Given the consensus that negatively charged $O_2{\cdot}^-$ cannot diffuse across membranes without access to anion channels (Han et al., 2003), it stands to reason that SOD activity in the IMS is required to neutralize $O_2{\cdot}^-$ released by mitochondrial electron transport. Still, H_2O_2 and other $O_2{\cdot}^-$-derived ROS such as ·OH can freely cross membranes and could potentially lead to cross-compartmental damage. We investigated the redox state of thioredoxin-2, a thiol antioxidant in the mitochondrial matrix (Hansen et al., 2006; He et al., 2008), and found no oxidation in spinal cord, sciatic nerve, or tibialis anterior due to loss of SOD1 (data not shown). Therefore oxidative stress in mitochondria due to loss of SOD1 is unlikely to affect the mitochondrial matrix, or is adequately compensated for. Further investigation is needed to address whether IMS-SOD1 protects motor axons by neutralization of $O_2{\cdot}^-$ within the IMS, or prevents release of $O_2{\cdot}^-$ and other ROS from mitochondria into the cytoplasm.

Native (endogenous) SOD1, like other IMS proteins such cytochrome c, lacks a canonical mitochondrial-targeting signal. The mechanisms governing mitochondrial import of unfolded SOD1 have not been fully elucidated. Partitioning of SOD1 between the mitochondria and the cytoplasm depends on the level of copper-chaperone for SOD1 (CCS) in mitochondria, which in turn depends on oxygen levels and import via the Mia40/Erv1 disulfide relay system (Kawamata and Manfredi, 2008; Reddehase et al., 2009). Alteration of SOD1 levels in the IMS via manipulation of CCS suggests that the

CCS-mediated folding state of SOD1 is what determines mitochondrial import (Son et al., 2007; Kawamata and Manfredi, 2008). However, this means that mitochondrial localization of endogenous SOD1 cannot be experimentally manipulated without also influencing the mitochondrial localization of other proteins (Reddehase et al., 2009).

An artificial targeting approach was therefore required for the current study. The mitofilin targeting sequence was chosen because it creates an integral membrane protein, anchoring SOD1 to the outer face of the inner mitochondrial membrane and trapping SOD1 in the IMS. IMS SOD1 is normally free-floating, and is released from mitochondria during spontaneous and pathologic opening of the membrane permeability transition pore (Li et al., 2006; Li et al., 2009). Anchoring of SOD1 effectively prevents unwanted release back out into the cytosol (A. Igoudjil, data not shown). Activity assays in isolated (intact) mitochondria and in tissue homogenates showed that IMS-SOD1 is enzymatically active (fig. 1-2); therefore anchoring SOD1 to the inner membrane does not preclude its proper folding and enzymatic activity. Whether SOD1 activity indicates IMS-SOD1 homodimer formation along the inner membrane, or is due to activity of isolated monomers, which retain ~10% activity (Bertini et al., 1994), remains to be determined.

We identified a 40% decrease in mitochondrial density in *Sod1-/-* motor axons that was attenuated by *IMS-SOD1* expression. Further investigation is required to correlate this with NMJ preservation *in vivo*; however, there is evidence linking altered mitochondrial trafficking and distribution in axons with a distal motor axonopathy phenotype. Inactivation of *Drosophila* Miro, a cargo adaptor for anterograde mitochondrial transport, causes accumulation of mitochondria in motor neuron cell

bodies and depletion in axons (Guo et al., 2005). Synaptic boutons at the NMJ in mutant flies show gross morphologic abnormalities and impaired synaptic transmission, and muscle atrophy in this model is corrected by replacement of Miro in neurons. Studies in mutant SOD1 models of familial ALS, in which axonal degeneration is a primary feature (Fischer et al., 2004), demonstrate decreased mitochondrial density in axons, slowed mitochondrial transport and abnormal clustering of mitochondria (De Vos et al., 2007; Magrané et al., 2009; Sotelo-Silveira et al., 2009). Aberrant regulation of mitochondrial fission and fusion is also implicated in hereditary peripheral neuropathy. Mutations in *MFN2* and *GDAP1*, regulators of mitochondrial fission and fusion, alter mitochondrial trafficking and architecture in models of Charcot Marie Tooth disease (Niemann et al., 2005; Baloh et al., 2007). Additional studies are warranted to determine whether the decreased mitochondrial density in *Sod1-/-* axons is due to alterations in transport or altered fission and fusion. Since accumulation of Mitotracker Red CM-H_2XRos in mitochondria depends on membrane potential, mitochondrial dysfunction, rather than altered trafficking, may be another explanation for our findings.

In summary, we demonstrated that targeted expression of SOD1 in the mitochondrial IMS is sufficient for robust, long-term rescue of motor axonopathy in *Sod1-/-* mice. These data suggest that the functional requirement for SOD1, at least in motor axons, is based on a protective role in mitochondria. Moreover, mitochondrial damage may be the underlying cause of distal motor axonopathy in *Sod1-/-* mice.

CHAPTER VII: Summary and future directions

The question of cause and effect regarding the role of oxidative stress in neurodegenerative disease has been particularly challenging to resolve, given that oxidative stress is also a downstream consequence of neurodegeneration (Ischiropoulos and Beckman, 2003; Andersen, 2004). For this reason, studies in postmortem tissues, and animal models where numerous destructive pathways converge to cause neuronal death, are poorly suited for isolating the role of oxidative stress.

Here, we focused on the SOD1 KO mouse, an extreme case of loss of an antioxidant enzyme, with no known correlate to human disease. However, the SOD1 KO model carries a distinct advantage for resolving the issue of cause and effect. Our studies demonstrating axon degeneration in this model provide conclusive evidence that chronic oxidative stress is sufficient to cause a progressive distal motor axonopathy *in vivo.* Moreover, we show that susceptibility is highest in motor axon terminals, suggesting that distal motor axons may be inherently susceptible to oxidative injury, or may be exposed to higher levels of oxidative stress *in vivo*.

In the course of these studies, we also uncovered new data regarding the normal role of SOD1. Rescue of SOD1 KO pathology by IMS-SOD1 suggests that the requirement for SOD1 in axons may be related to its role in mitochondria, rather than in the cytoplasm. This finding raises a number of additional questions. One question is whether IMS-SOD1 provides local protection in the IMS, or limits ROS release from mitochondria out into the cytoplasm. We are currently in the process of cloning and testing redox-sensitive YFP constructs targeted to the mitochondrial matrix, IMS, and cytoplasm, for use as tools to address this issue (Hu et al., 2008). Another question

regards the effect of manipulation of IMS-SOD1 on mitochondrial function and trafficking. Motor axon terminals at the NMJ have a high density of mitochondria, so alterations in mitochondrial energy production or Ca^{2+}-buffering may be particularly detrimental. If mitochondrial trafficking or fission and fusion are compromised, this could also cause localized defects at the NMJ, as evidenced by the "extreme" scenario in the Drosophila *Miro* mutants (Guo et al., 2005).

Another question is, will increasing expression of SOD1 in the mitochondrial IMS be protective against other pathologic insults, such as Wallerian degeneration or exposure to toxic agents? Studies in mice that overexpress wild-type human SOD1 systemically show that too much SOD1 is also detrimental, perhaps due to overproduction of H_2O_2 (Peled-Kamar et al., 1997; Jaarsma et al., 2000). However, if mitochondrial defects are central to oxidative stress-mediated axon degeneration, then other therapeutic approaches aimed at mitochondria, such as NMNAT3 overexpression or mitochondrial PARP-inhibition, may be feasible alternatives to antioxidants for conferring axonal protection.

Finally, a major question raised by this study is whether axon defects in SOD1 KO mice inform us about the mechanism of distal axonal degeneration in disease caused by SOD1 mutations. Pathology in the SOD1 KO progresses much more slowly than in SOD1 mutant mice, and never reaches full-blown paralysis. Moreover, pathology remains isolated at the NMJ in the SOD1 KO, whereas in the SOD1 mutant, pathology progresses in a distal to proximal pattern, ultimately resulting in the death of spinal motor neurons. Still, there are parallels, such as the preferential denervation of fast-twitch muscle fibers, and the preferential effect on motor versus sensory fibers. Perhaps oxidative stress due to perturbation of SOD1 (loss of function on one hand, and a gain of

pro-oxidative function on the other hand) may cause distal axonal defects in both models. Mutant SOD1 also appears to be particularly detrimental to mitochondria (Magrané et al., 2009). Control of SOD1 partitioning between mitochondria and the cytosol, and the functional relevance of IMS-SOD1 for axon survival, may be an important point of convergence between these two models. Future investigations in this area may yield new insights into pathogenic mechanism(s) of oxidative stress-mediated axon degeneration in human disease.

References:

Adalbert R, Nógrádi A, Szabó A, Coleman MP (2006) The slow Wallerian degeneration gene in vivo protects motor axons but not their cell bodies after avulsion and neonatal axotomy. Eur J Neurosci 24:2163-2168.

Adamec E, Mohan P, Vonsattel J, Nixon R (2002) Calpain activation in neurodegenerative diseases: confocal immunofluorescence study with antibodies specifically recognizing the active form of calpain 2. Acta Neuropathologica 104:92-104.

Afifi AK, Aleu FP, Goodgold J, MacKay B (1966) Ultrastructure of atrophic muscle in amyotrophic lateral sclerosis. Neurology 16:475-481.

Aggarwal A, Nicholson G (2002) Detection of preclinical motor neurone loss in SOD1 mutation carriers using motor unit number estimation. J Neurol Neurosurg Psychiatr 73:199-201.

Aigner L, Arber S, Kapfhammer JP, Laux T, Schneider C, Botteri F, Brenner HR, Caroni P (1995) Overexpression of the neural growth-associated protein GAP-43 induces nerve sprouting in the adult nervous system of transgenic mice. Cell 83:269-278.

Akude E, Zherebitskaya E, Roy Chowdhury S, Girling K, Fernyhough P (2009) 4-Hydroxy-2-Nonenal Induces Mitochondrial Dysfunction and Aberrant Axonal Outgrowth in Adult Sensory Neurons that Mimics Features of Diabetic Neuropathy. Neurotox Res. DOI 10.1007/s12640-009-9074-5.

Al-Kateb H et al. (2008) Multiple superoxide dismutase 1/splicing factor serine alanine 15 variants are associated with the development and progression of diabetic

nephropathy: the Diabetes Control and Complications Trial/Epidemiology of Diabetes Interventions and Complications Genetics study. Diabetes 57:218-228.

Alvarez B, Radi R (2003) Peroxynitrite reactivity with amino acids and proteins. Amino Acids 25:295-311.

Amiri M, Hollenbeck PJ (2008) Mitochondrial biogenesis in the axons of vertebrate peripheral neurons. Dev Neurobiol 68:1348-1361.

Andersen JK (2004) Oxidative stress in neurodegeneration: cause or consequence? Nat Med 10 Suppl:S18-25.

Andersen PM, Nilsson P, Forsgren L, Marklund SL (1998) CuZn-superoxide dismutase, extracellular superoxide dismutase, and glutathione peroxidase in blood from individuals homozygous for Asp90Ala CuZu-superoxide dismutase mutation. J Neurochem 70:715-720.

Andrus PK, Fleck TJ, Gurney ME, Hall ED (1998) Protein oxidative damage in a transgenic mouse model of familial amyotrophic lateral sclerosis. J Neurochem 71:2041-2048.

Aquilano K, Vigilanza P, Rotilio G, Ciriolo MR (2006) Mitochondrial damage due to SOD1 deficiency in SH-SY5Y neuroblastoma cells: a rationale for the redundancy of SOD1. FASEB J 20:1683-1685.

Araki T, Sasaki Y, Milbrandt J (2004) Increased nuclear NAD biosynthesis and SIRT1 activation prevent axonal degeneration. Science 305:1010-1013.

Arce V, Garces A, de Bovis B, Filippi P, Henderson C, Pettmann B, deLapeyrière O (1999) Cardiotrophin-1 requires LIFRbeta to promote survival of mouse motoneurons purified by a novel technique. J Neurosci Res 55:119-126.

Arendt T (2009) Synaptic degeneration in Alzheimer's disease. Acta Neuropathologica 118:167-179.

Armon C, Brandstater ME (1999) Motor unit number estimate-based rates of progression of ALS predict patient survival. Muscle Nerve 22:1571-1575.

Atsumi T (1981) The ultrastructure of intramuscular nerves in amyotrophic lateral sclerosis. Acta Neuropathologica 55:193-198.

Avery MA, Sheehan AE, Kerr KS, Wang J, Freeman MR (2009) Wld S requires Nmnat1 enzymatic activity and N16-VCP interactions to suppress Wallerian degeneration. The Journal of Cell Biology 184:501-513.

Baldereschi M, Inzitari M, Di Carlo A, Farchi G, Scafato E, Inzitari D, Group IW (2007) Epidemiology of distal symmetrical neuropathies in the Italian elderly. Neurology 68:1460-1467.

Baloh RH (2008) Mitochondrial dynamics and peripheral neuropathy. The Neuroscientist 14:12-18.

Baloh RH, Schmidt RE, Pestronk A, Milbrandt J (2007) Altered axonal mitochondrial transport in the pathogenesis of Charcot-Marie-Tooth disease from mitofusin 2 mutations. J Neurosci 27:422-430.

Barber SC, Mead RJ, Shaw PJ (2006) Oxidative stress in ALS: a mechanism of neurodegeneration and a therapeutic target. Biochim Biophys Acta 1762:1051-1067.

Bartus RT, Elliott PJ, Hayward NJ, Dean RL, Harbeson S, Straub JA, Li Z, Powers JC (1995) Calpain as a novel target for treating acute neurodegenerative disorders. Neurol Res 17:249-258.

Beal MF, Ferrante RJ, Browne SE, Matthews RT, Kowall NW, Brown RH (1997) Increased 3-nitrotyrosine in both sporadic and familial amyotrophic lateral sclerosis. Ann Neurol 42:644-654.

Beauchamp C, Fridovich I (1971) Superoxide dismutase: improved assays and an assay applicable to acrylamide gels. Anal Biochem 44:276-287.

Beckman JS, Beckman TW, Chen J, Marshall PA, Freeman BA (1990) Apparent hydroxyl radical production by peroxynitrite: implications for endothelial injury from nitric oxide and superoxide. Proc Natl Acad Sci USA 87:1620-1624.

Beckman KB, Ames BN (1998) The free radical theory of aging matures. Physiol Rev 78:547-581.

Beirowski B, Babetto E, Coleman MP, Martin KR (2008) The WldS gene delays axonal but not somatic degeneration in a rat glaucoma model. Eur J Neurosci 28:1166-1179.

Beirowski B, Babetto E, Gilley J, Mazzola F, Conforti L, Janeckova L, Magni G, Ribchester RR, Coleman MP (2009) Non-nuclear Wld(S) determines its neuroprotective efficacy for axons and synapses in vivo. J Neurosci 29:653-668.

Beretta S, Sala G, Mattavelli L, Ceresa C, Casciati A, Ferri A, Carrì MT, Ferrarese C (2003) Mitochondrial dysfunction due to mutant copper/zinc superoxide dismutase associated with amyotrophic lateral sclerosis is reversed by N-acetylcysteine. Neurobiol Dis 13:213-221.

Berliocchi L, Fava E, Leist M, Horvat V, Dinsdale D, Read D, Nicotera P (2005) Botulinum neurotoxin C initiates two different programs for neurite degeneration and neuronal apoptosis. The Journal of Cell Biology 168:607-618.

Berridge MV, Tan AS (1993) Characterization of the cellular reduction of 3-(4,5-dimethylthiazol-2-yl)-2,5-diphenyltetrazolium bromide (MTT): subcellular localization, substrate dependence, and involvement of mitochondrial electron transport in MTT reduction. Arch Biochem Biophys 303:474-482.

Bertini I, Piccioli M, Viezzoli MS, Chiu CY, Mullenbach GT (1994) A spectroscopic characterization of a monomeric analog of copper, zinc superoxide dismutase. Eur Biophys J 23:167-176.

Blasi J, Chapman ER, Link E, Binz T, Yamasaki S, De Camilli P, Südhof TC, Niemann H, Jahn R (1993) Botulinum neurotoxin A selectively cleaves the synaptic protein SNAP-25. Nature 365:160-163.

Blondet B, Carpentier G, Aït-Ikhlef A, Murawsky M, Rieger F (2002) Motoneuron morphological alterations before and after the onset of the disease in the wobbler mouse. Brain Research 930:53-57.

Blough N, Zafiriou O (1985) Reaction of superoxide with nitric oxide to form peroxonitrite in alkaline aqueous solution. Inorganic Chemistry 24:3502-3504.

Bogdanov M, Brown RH, Matson W, Smart R, Hayden D, O'Donnell H, Flint Beal M, Cudkowicz M (2000) Increased oxidative damage to DNA in ALS patients. Free Radic Biol Med 29:652-658.

Bömmel H, Xie G, Rossoll W, Wiese S, Jablonka S, Boehm T, Sendtner M (2002) Missense mutation in the tubulin-specific chaperone E (Tbce) gene in the mouse mutant progressive motor neuronopathy, a model of human motoneuron disease. J Cell Biol 159:563-569.

Bonneh-Barkay D, Langston WJ, Di Monte D (2005) Toxicity of redox cycling pesticides in primary mesencephalic cultures. Antioxid Redox Signal 7:649-653.

Borchelt DR, Guarnieri M, Wong PC, Lee MK, Slunt HS, Xu ZS, Sisodia SS, Price DL, Cleveland DW (1995) Superoxide dismutase 1 subunits with mutations linked to familial amyotrophic lateral sclerosis do not affect wild-type subunit function. J Biol Chem 270:3234-3238.

Borchelt DR, Lee MK, Slunt HS, Guarnieri M, Xu ZS, Wong PC, Brown RH, Price DL, Sisodia SS, Cleveland DW (1994) Superoxide dismutase 1 with mutations linked to familial amyotrophic lateral sclerosis possesses significant activity. Proc Natl Acad Sci USA 91:8292-8296.

Borchelt DR, Davis J, Fischer M, Lee MK, Slunt HH, Ratovitsky T, Regard J, Copeland NG, Jenkins NA, Sisodia SS, Price DL (1996) A vector for expressing foreign genes in the brains and hearts of transgenic mice. Genet Anal 13:159-163.

Borthwick GM, Johnson MA, Ince PG, Shaw PJ, Turnbull DM (1999) Mitochondrial enzyme activity in amyotrophic lateral sclerosis: implications for the role of mitochondria in neuronal cell death. Ann Neurol 46:787-790.

Boveris A, Chance B (1973) The mitochondrial generation of hydrogen peroxide. General properties and effect of hyperbaric oxygen. Biochem J 134:707-716.

Bowling AC, Schulz JB, Brown RH, Beal MF (1993) Superoxide dismutase activity, oxidative damage, and mitochondrial energy metabolism in familial and sporadic amyotrophic lateral sclerosis. J Neurochem 61:2322-2325.

Bowling AC, Barkowski EE, McKenna-Yasek D, Sapp P, Horvitz HR, Beal MF, Brown RH (1995) Superoxide dismutase concentration and activity in familial amyotrophic lateral sclerosis. J Neurochem 64:2366-2369.

Bradley WG, Good P, Rasool CG, Adelman LS (1983) Morphometric and Biochemical Studies of Peripheral Nerves in Amyotrophic Lateral Sclerosis. Annals of Neurology 14:267-277.

Braidy N, Guillemin G, Grant R (2008) Promotion of cellular NAD(+) anabolism: therapeutic potential for oxidative stress in ageing and Alzheimer's disease. Neurotox Res 13:173-184.

Brown MC, Booth CM, Lunn ER, Perry VH (1991) Delayed response to denervation in muscles of C57BL/Ola mice. Neuroscience 43:279-283.

Burne JF, Staple JK, Raff MC (1996) Glial cells are increased proportionally in transgenic optic nerves with increased numbers of axons. J Neurosci 16:2064-2073.

Bus JS, Aust SD, Gibson JE (1974) Superoxide- and singlet oxygen-catalyzed lipid peroxidation as a possible mechanism for paraquat (methyl viologen) toxicity. Biochem Biophys Res Commun 58:749-755.

Cajal SR (1928) Degeneration and Regeneration of the Nervous System: Oxford University Press.

Carlsson LM, Jonsson J, Edlund T, Marklund SL (1995) Mice lacking extracellular superoxide dismutase are more sensitive to hyperoxia. Proc Natl Acad Sci USA 92:6264-6268.

Carrì MT, Ferri A, Battistoni A, Famhy L, Gabbianelli R, Poccia F, Rotilio G (1997) Expression of a Cu,Zn superoxide dismutase typical of familial amyotrophic lateral sclerosis induces mitochondrial alteration and increase of cytosolic Ca2+ concentration in transfected neuroblastoma SH-SY5Y cells. FEBS Lett 414:365-368.

Casoni F, Basso M, Massignan T, Gianazza E, Cheroni C, Salmona M, Bendotti C, Bonetto V (2005) Protein nitration in a mouse model of familial amyotrophic lateral sclerosis: possible multifunctional role in the pathogenesis. J Biol Chem 280:16295-16304.

Cavalli V, Kujala P, Klumperman J, Goldstein LSB (2005) Sunday Driver links axonal transport to damage signaling. The Journal of Cell Biology 168:775-787.

Cavanagh JB (1964) The significance of the "dying back" process in experimental and human neurological disease. International review of experimental pathology 3:219-267.

Ceballos D, Cuadras J, Verdú E, Navarro X (1999) Morphometric and ultrastructural changes with ageing in mouse peripheral nerve. J Anat 195 (Pt 4):563-576.

Chance B, Sies H, Boveris A (1979) Hydroperoxide metabolism in mammalian organs. Physiol Rev 59:527-605.

Chiu AY, Zhai P, Dal Canto MC, Peters TM, Kwon YW, Prattis SM, Gurney ME (1995) Age-dependent penetrance of disease in a transgenic mouse model of familial amyotrophic lateral sclerosis. Mol Cell Neurosci 6:349-362.

Chung CY, Koprich JB, Siddiqi H, Isacson O (2009) Dynamic changes in presynaptic and axonal transport proteins combined with striatal neuroinflammation precede

dopaminergic neuronal loss in a rat model of AAV alpha-synucleinopathy. J Neurosci 29:3365-3373.

Cifuentes-Diaz C, Nicole S, Velasco ME, Borra-Cebrian C, Panozzo C, Frugier T, Millet G, Roblot N, Joshi V, Melki J (2002) Neurofilament accumulation at the motor endplate and lack of axonal sprouting in a spinal muscular atrophy mouse model. Hum Mol Genet 11:1439-1447.

Cleveland DW, Rothstein JD (2001) From Charcot to Lou Gehrig: deciphering selective motor neuron death in ALS. Nat Rev Neurosci 2:806-819.

Cleveland DW, Laing N, Hurse PV, Brown RH (1995) Toxic mutants in Charcot's sclerosis. Nature 378:342-343.

Cohen O, Kohen R, Lavon E, Abramsky O, Steiner I (1996) Serum Cu/Zn superoxide dismutase activity is reduced in sporadic amyotrophic lateral sclerosis patients. J Neurol Sci 143:118-120.

Coleman M (2005) Axon degeneration mechanisms: commonality amid diversity. Nat Rev Neurosci 6:889-898.

Coleman M, Perry VH (2002) Axon pathology in neurological disease: a neglected therapeutic target. Trends Neurosci 25:532-537.

Conforti L, Adalbert R, Coleman MP (2007a) Neuronal death: where does the end begin? Trends in Neurosciences 30:159-166.

Conforti L, Tarlton A, Mack TGA, Mi W, Buckmaster EA, Wagner D, Perry VH, Coleman MP (2000) A Ufd2/D4Cole1e chimeric protein and overexpression of Rbp7 in the slow Wallerian degeneration (Wld^{s}) mouse. Proceedings of the National Academy of Sciences USA 97:11377-11382.

Conforti L, Fang G, Beirowski B, Wang MS, Sorci L, Asress S, Adalbert R, Silva A, Bridge K, Huang XP, Magni G, Glass JD, Coleman MP (2007b) NAD(+) and axon degeneration revisited: Nmnat1 cannot substitute for Wld(S) to delay Wallerian degeneration. Cell Death Differ 14:116-127.

Conforti L, Wilbrey A, Morreale G, Janeckova L, Beirowski B, Adalbert R, Mazzola F, Di Stefano M, Hartley R, Babetto E, Smith T, Gilley J, Billington RA, Genazzani AA, Ribchester RR, Magni G, Coleman M (2009) Wld S protein requires Nmnat activity and a short N-terminal sequence to protect axons in mice. The Journal of Cell Biology 184:491-500.

Cookson MR, Thatcher NM, Ince PG, Shaw PJ (1996) Selective loss of neurofilament proteins after exposure of differentiated human IMR-32 neuroblastoma cells to oxidative stress. Brain Research 738:162-166.

Crawford TO, Hsieh ST, Schryer BL, Glass JD (1995) Prolonged axonal survival in transected nerves of C57BL/Ola mice is independent of age. J Neurocytol 24:333-340.

Crow J, Calingasan N, Chen J, Hill J, Beal M (2005) Manganese porphyrin given at symptom onset markedly extends survival of ALS mice. Ann Neurol 58:258-265.

Crow JP, Sampson JB, Zhuang Y, Thompson JA, Beckman JS (1997) Decreased zinc affinity of amyotrophic lateral sclerosis-associated superoxide dismutase mutants leads to enhanced catalysis of tyrosine nitration by peroxynitrite. J Neurochem 69:1936-1944.

Curti D, Rognoni F, Alimonti D, Malaspina A, Feletti F, Tessera S, Finotti N, Rehak L, Mazzini L, Zerbi F, Poloni TE, Ceroni M (2002) SOD1 activity and protective

factors in familial ALS patients with L84F SOD1 mutation. Amyotroph Lateral Scler Other Motor Neuron Disord 3:115-122.

Dalton TP, Dieter MZ, Yang Y, Shertzer HG, Nebert DW (2000) Knockout of the mouse glutamate cysteine ligase catalytic subunit (Gclc) gene: embryonic lethal when homozygous, and proposed model for moderate glutathione deficiency when heterozygous. Biochem Biophys Res Commun 279:324-329.

Damiano M, Starkov AA, Petri S, Kipiani K, Kiaei M, Mattiazzi M, Flint Beal M, Manfredi G (2006) Neural mitochondrial Ca2+ capacity impairment precedes the onset of motor symptoms in G93A Cu/Zn-superoxide dismutase mutant mice. J Neurochem 96:1349-1361.

Dauer W, Przedborski S (2003) Parkinson's disease: mechanisms and models. Neuron 39:889-909.

De Vos KJ, Chapman AL, Tennant ME, Manser C, Tudor EL, Lau KF, Brownlees J, Ackerley S, Shaw PJ, McLoughlin DM, Shaw CE, Leigh PN, Miller CC, Grierson AJ (2007) Familial amyotrophic lateral sclerosis-linked SOD1 mutants perturb fast axonal transport to reduce axonal mitochondria content. Human Molecular Genetics 16:2720-2728.

Deckwerth TL, Johnson EM (1994) Neurites can remain viable after destruction of the neuronal soma by programmed cell death (apoptosis). Developmental Biology 165:63-72.

DeRubertis FR, Craven PA, Melhem MF (2007) Acceleration of diabetic renal injury in the superoxide dismutase knockout mouse: effects of tempol. Metab Clin Exp 56:1256-1264.

Didion SP, Ryan MJ, Didion LA, Fegan PE, Sigmund CD, Faraci FM (2002) Increased superoxide and vascular dysfunction in CuZnSOD-deficient mice. Circ Res 91:938-944.

Du L, Zhang X, Han YY, Burke NA, Kochanek PM, Watkins SC, Graham SH, Carcillo JA, Szabó C, Clark RSB (2003) Intra-mitochondrial poly(ADP-ribosylation) contributes to NAD+ depletion and cell death induced by oxidative stress. J Biol Chem 278:18426-18433.

Dubois-Dauphin M, Frankowski H, Tsujimoto Y, Huarte J, Martinou JC (1994) Neonatal motoneurons overexpressing the bcl-2 protooncogene in transgenic mice are protected from axotomy-induced cell death. Proc Natl Acad Sci USA 91:3309-3313.

Eberhardt O, Coelln RV, Kugler S, Lindenau J, Rathke-Hartlieb S, Gerhardt E, Haid S, Isenmann S, Gravel C, Srinivasan A, Bahr M, Weller M, Dichgans J, Schulz JB (2000) Protection by synergistic effects of adenovirus-mediated X-chromosome-linked inhibitor of apoptosis and glial cell line-derived neurotrophic factor gene transfer in the 1-methyl-4-phenyl-1,2,3,6-tetrahydropyridine model of Parkinson's disease. J Neurosci 20:9126-9134.

Echtay KS, Murphy MP, Smith RA, Talbot DA, Brand MD (2002) Superoxide activates mitochondrial uncoupling protein 2 from the matrix side. Studies using targeted antioxidants. J Biol Chem 277:47129-47135.

Elchuri S, Oberley TD, Qi W, Eisenstein RS, Jackson Roberts L, Van Remmen H, Epstein CJ, Huang T-T (2005) CuZnSOD deficiency leads to persistent and

widespread oxidative damage and hepatocarcinogenesis later in life. Oncogene 24:367-380.

Estévez AG, Crow JP, Sampson JB, Reiter C, Zhuang Y, Richardson GJ, Tarpey MM, Barbeito L, Beckman JS (1999) Induction of nitric oxide-dependent apoptosis in motor neurons by zinc-deficient superoxide dismutase. Science 286:2498-2500.

Ezzi SA, Urushitani M, Julien J-P (2007) Wild-type superoxide dismutase acquires binding and toxic properties of ALS-linked mutant forms through oxidation. J Neurochem 102:170-178.

Feng G, Mellor RH, Bernstein M, Keller-Peck C, Nguyen QT, Wallace M, Nerbonne JM, Lichtman JW, Sanes JR (2000) Imaging neuronal subsets in transgenic mice expressing multiple spectral variants of GFP. Neuron 28:41-51.

Ferrante RJ, Browne SE, Shinobu LA, Bowling AC, Baik MJ, MacGarvey U, Kowall NW, Brown RH, Beal MF (1997) Evidence of increased oxidative damage in both sporadic and familial amyotrophic lateral sclerosis. J Neurochem 69:2064-2074.

Ferri A, Sanes J, Coleman M, Cunningham JM, Kato AC (2003) Inhibiting axon degeneration and synapse loss attenuates apoptosis and disease progression in a mouse model of motoneuron disease. Curr Biol 13:669-673.

Ferri A, Cozzolino M, Crosio C, Nencini M, Casciati A, Gralla EB, Rotilio G, Valentine JS, Carrì MT (2006) Familial ALS-superoxide dismutases associate with mitochondria and shift their redox potentials. Proc Natl Acad Sci USA 103:13860-13865.

Figueroa-Romero C, Sadidi M, Feldman EL (2008) Mechanisms of disease: the oxidative stress theory of diabetic neuropathy. Rev Endocr Metab Disord 9:301-314.

Finn JT, Weil M, Archer F, Srinivasan A, Raff MC (2000) Evidence That Wallerian Degeneration and Localized Axon Degeneration Induced by Local Neurotrophin Deprivation Do Not Involve Caspases. The Journal of Neuroscience 20:1333-1341.

Fischer LR, Glass J (2007) Axonal degeneration in motor neuron disease. Neurodegener Dis 4:431-442.

Fischer LR, Culver D, Tennant P, Davis A, Wang M, Castellano-Sanchez A, Khan J, Polak MA, Glass J (2004) Amyotrophic lateral sclerosis is a distal axonopathy: evidence in mice and man. Exp Neurol 185:232-240.

Fischer LR, Culver D, Davis A, Tennant P, Wang M, Coleman M, Asress S, Adalbert R, Alexander GM, Glass J (2005) The WldS gene modestly prolongs survival in the SOD1G93A fALS mouse. Neurobiol Dis 19:293-300.

Fiszman ML, Borodinsky LN, Ricart KC, Sanz OP, Sica RE (1999) Cu/Zn superoxide dismutase activity at different ages in sporadic amyotrophic lateral sclerosis. J Neurol Sci 162:34-37.

Flekac M, Skrha J, Hilgertova J, Lacinova Z, Jarolimkova M (2008) Gene polymorphisms of superoxide dismutases and catalase in diabetes mellitus. BMC Med Genet 9:30.

Flint DH, Tuminello JF, Emptage MH (1993) The inactivation of Fe-S cluster containing hydro-lyases by superoxide. J Biol Chem 268:22369-22376.

Flood DG, Reaume AG, Gruner JA, Hoffman EK, Hirsch JD, Lin YG, Dorfman KS, Scott RW (1999) Hindlimb motor neurons require Cu/Zn superoxide dismutase for maintenance of neuromuscular junctions. Am J Pathol 155:663-672.

Fordel E, Thijs L, Martinet W, Lenjou M, Laufs T, Van Bockstaele D, Moens L, Dewilde S (2006) Neuroglobin and cytoglobin overexpression protects human SH-SY5Y neuroblastoma cells against oxidative stress-induced cell death. Neurosci Lett 410:146-151.

Frey D, Schneider C, Xu L, Borg J, Spooren W, Caroni P (2000) Early and selective loss of neuromuscular synapse subtypes with low sprouting competence in motoneuron diseases. J Neurosci 20:2534-2542.

Fridovich I (1995) Superoxide radical and superoxide dismutases. Annu Rev Biochem 64:97-112.

Fujita K, Yamauchi M, Shibayama K, Ando M, Honda M, Nagata Y (1996) Decreased cytochrome c oxidase activity but unchanged superoxide dismutase and glutathione peroxidase activities in the spinal cords of patients with amyotrophic lateral sclerosis. J Neurosci Res 45:276-281.

Garcia I, Martinou I, Tsujimoto Y, Martinou JC (1992) Prevention of programmed cell death of sympathetic neurons by the bcl-2 proto-oncogene. Science 258:302-304.

Gardner PR, Fridovich I (1991) Superoxide sensitivity of the Escherichia coli aconitase. J Biol Chem 266:19328-19333.

Gélinas S, Chapados C, Beauregard M, Gosselin I, Martinoli MG (2000) Effect of oxidative stress on stability and structure of neurofilament proteins. Biochem Cell Biol 78:667-674.

Gieffers C, Korioth F, Heimann P, Ungermann C, Frey J (1997) Mitofilin is a transmembrane protein of the inner mitochondrial membrane expressed as two isoforms. Experimental Cell Research 232:395-399.

Gillingwater T, Thomson D, Mack TG, Soffin EM, Mattison RJ, Coleman M, Ribchester R (2002) Age-dependent synapse withdrawal at axotomised neuromuscular junctions in Wld(s) mutant and Ube4b/Nmnat transgenic mice. The Journal of Physiology 543:739-755.

Giniatullin AR, Darios F, Shakirzyanova A, Davletov B, Giniatullin R (2006) SNAP25 is a pre-synaptic target for the depressant action of reactive oxygen species on transmitter release. J Neurochem 98:1789-1797.

Giorgio M, Trinei M, Migliaccio E, Pelicci PG (2007) Hydrogen peroxide: a metabolic by-product or a common mediator of ageing signals? Nat Rev Mol Cell Biol 8:722-728.

Glass J, Griffin JW (1991) Neurofilament redistribution in transected nerves: evidence for bidirectional transport of neurofilaments. J Neurosci 11:3146-3154.

Glass JD (2002) Pathophysiology of Nerve and Root Disorders. In: Diseases of the Nervous System: Clinical Neuroscience and Therapeutic Principles, 3rd Edition (Asbury A, McKhann G, McDonald WI, Goadsby P, McArthur J, eds), pp 1075-1091. Cambridge: Cambridge University Press.

Glass JD, Griffin JW (1994) Retrograde transport of radiolabeled cytoskeletal proteins in transected nerves. Journal of Neuroscience 14:3915-3921.

Glass JD, Brushart TM, George EB, Griffin JW (1993) Prolonged survival of transected nerve fibres in C57BL/Ola mice is an intrinsic characteristic of the axon. J Neurocytol 22:311-321.

Goldsteins G, Keksa-Goldsteine V, Ahtoniemi T, Jaronen M, Arens E, Akerman K, Chan PH, Koistinaho J (2008) Deleterious role of superoxide dismutase in the mitochondrial intermembrane space. J Biol Chem 283:8446-8452.

Gopalakrishna R, Gundimeda U, Schiffman JE, McNeill TH (2008) A direct redox regulation of protein kinase C isoenzymes mediates oxidant-induced neuritogenesis in PC12 cells. J Biol Chem 283:14430-14444.

Gould TW, Buss RR, Vinsant S, Prevette D, Sun W, Knudson CM, Milligan CE, Oppenheim RW (2006) Complete dissociation of motor neuron death from motor dysfunction by Bax deletion in a mouse model of ALS. J Neurosci 26:8774-8786.

Gowers WR (1902) A Lecture on Abiotrophy. The Lancet:1003-1007.

Griffin JW (2007) Augustus Waller and the case of the disappearing axon. Nature Clinical Practice Neurology 3:355.

Griffin JW, Höke A, Nguyen TT (2006) Axon degeneration and rescue. Textbook of neural repair and rehabilitation:293-302.

Guo X, Macleod G, Wellington A, Hu F, Panchumarthi S, Schoenfield M, Marin L, Charlton M, Atwood H, Zinsmaier K (2005) The GTPase dMiro Is Required for Axonal Transport of Mitochondria to Synapses. Neuron 47:379-393.

Gurney ME, Pu H, Chiu AY, Dal Canto MC, Polchow CY, Alexander DD, Caliendo J, Hentati A, Kwon YW, Deng HX (1994) Motor neuron degeneration in mice that express a human Cu,Zn superoxide dismutase mutation. Science 264:1772-1775.

Gus'kova RA, Ivanov II, Kol'tover VK, Akhobadze VV, Rubin AB (1984) Permeability of bilayer lipid membranes for superoxide (O2-.) radicals. Biochim Biophys Acta 778:579-585.

Hafezparast M et al. (2003) Mutations in dynein link motor neuron degeneration to defects in retrograde transport. Science 300:808-812.

Hall ED, Andrus PK, Oostveen JA, Fleck TJ, Gurney ME (1998) Relationship of oxygen radical-induced lipid peroxidative damage to disease onset and progression in a transgenic model of familial ALS. J Neurosci Res 53:66-77.

Halliwell B (2006) Oxidative stress and neurodegeneration: where are we now? J Neurochem 97:1634-1658.

Halliwell B, Gutteridge JM (1990) Role of free radicals and catalytic metal ions in human disease: an overview. Meth Enzymol 186:1-85.

Halliwell B, Gutteridge JM (1992) Biologically relevant metal ion-dependent hydroxyl radical generation. An update. FEBS Lett 307:108-112.

Han D, Williams E, Cadenas E (2001) Mitochondrial respiratory chain-dependent generation of superoxide anion and its release into the intermembrane space. Biochem J 353:411-416.

Han D, Antunes F, Canali R, Rettori D, Cadenas E (2003) Voltage-dependent anion channels control the release of the superoxide anion from mitochondria to cytosol. J Biol Chem 278:5557-5563.

Hansen J, Klass M, Harris C, Csete M (2007) A reducing redox environment promotes C2C12 myogenesis: Implications for regeneration in aged muscle. Cell Biol Int 31:546-553.

Hansen JM, Zhang H, Jones DP (2006) Mitochondrial thioredoxin-2 has a key role in determining tumor necrosis factor-alpha-induced reactive oxygen species generation, NF-kappaB activation, and apoptosis. Toxicol Sci 91:643-650.

Hansen S, Ballantyne JP (1978) A quantitative electrophysiological study of motor neurone disease. J Neurol Neurosurg Psychiatr 41:773-783.

Harman D (1956) Aging: a theory based on free radical and radiation chemistry. Journal of gerontology 11:298-300.

Harraz MM, Marden JJ, Zhou W, Zhang Y, Williams A, Sharov VS, Nelson K, Luo M, Paulson H, Schöneich C, Engelhardt JF (2008) SOD1 mutations disrupt redox-sensitive Rac regulation of NADPH oxidase in a familial ALS model. J Clin Invest 118:659-670.

Hasbani DM, O'Malley KL (2006) Wld(S) mice are protected against the Parkinsonian mimetic MPTP. Experimental Neurology 202:93-99.

Hashizume K, Hirasawa M, Imamura Y, Noda S, Shimizu T, Shinoda K, Kurihara T, Noda K, Ozawa Y, Ishida S, Miyake Y, Shirasawa T, Tsubota K (2008) Retinal dysfunction and progressive retinal cell death in SOD1-deficient mice. Am J Pathol 172:1325-1331.

He M, Cai J, Go YM, Johnson JM, Martin WD, Hansen JM, Jones DP (2008) Identification of thioredoxin-2 as a regulator of the mitochondrial permeability transition. Toxicological Sciences 105:44-50.

Hegedus J, Putman CT, Gordon T (2007) Time course of preferential motor unit loss in the SOD1 G93A mouse model of amyotrophic lateral sclerosis. Neurobiol Dis 28:154-164.

Henderson CE, Bloch-Gallego E, Camu W (1995) Purified Embryonic Motoneurons. In: Neural Cell Culture (Cohen J, Wilkin G, eds), pp 69-81. Oxford: Oxford University Press.

Higgins CMJ, Jung C, Ding H, Xu Z (2002) Mutant Cu, Zn superoxide dismutase that causes motoneuron degeneration is present in mitochondria in the CNS. J Neurosci 22:RC215.

Hirano A, Donnenfeld H, Sasaki S, Nakano I (1984) Fine structural observations of neurofilamentous changes in amyotrophic lateral sclerosis. J Neuropathol Exp Neurol 43:461-470.

Ho YS, Gargano M, Cao J, Bronson RT, Heimler I, Hutz RJ (1998) Reduced fertility in female mice lacking copper-zinc superoxide dismutase. J Biol Chem 273:7765-7769.

Ho YS, Magnenat JL, Bronson RT, Cao J, Gargano M, Sugawara M, Funk CD (1997) Mice deficient in cellular glutathione peroxidase develop normally and show no increased sensitivity to hyperoxia. J Biol Chem 272:16644-16651.

Hodgson EK, Fridovich I (1975) The interaction of bovine erythrocyte superoxide dismutase with hydrogen peroxide: inactivation of the enzyme. Biochemistry 14:5294-5299.

Höke A (2006) Neuroprotection in the peripheral nervous system: rationale for more effective therapies. Arch Neurol 63:1681-1685.

Höke A, Cornblath DR (2004) Peripheral neuropathies in human immunodeficiency virus infection. Supplements to Clinical neurophysiology 57:195-210.

Holtmann B, Zielasek J, Toyka KV, Sendtner M (1999) Comparative analysis of motoneuron loss and functional deficits in PMN mice: implications for human motoneuron disease. J Neurol Sci 169:140-147.

Howland DS, Liu J, She Y, Goad B, Maragakis NJ, Kim B, Erickson J, Kulik J, DeVito L, Psaltis G, DeGennaro LJ, Cleveland DW, Rothstein JD (2002) Focal loss of the glutamate transporter EAAT2 in a transgenic rat model of SOD1 mutant-mediated amyotrophic lateral sclerosis (ALS). Proc Natl Acad Sci USA 99:1604-1609.

Hsieh ST, Chiang HY, Lin WM (2000) Pathology of nerve terminal degeneration in the skin. J Neuropathol Exp Neurol 59:297-307.

Hu J, Dong L, Outten CE (2008) The redox environment in the mitochondrial intermembrane space is maintained separately from the cytosol and matrix. J Biol Chem 283:29126-29134.

Huang TT, Yasunami M, Carlson EJ, Gillespie AM, Reaume AG, Hoffman EK, Chan PH, Scott RW, Epstein CJ (1997) Superoxide-mediated cytotoxicity in superoxide dismutase-deficient fetal fibroblasts. Arch Biochem Biophys 344:424-432.

Ihara Y, Mori A, Hayabara T, Kawai M, Namba R, Nobukuni K, Sato K, Kibata M (1995) Superoxide dismutase and free radicals in sporadic amyotrophic lateral sclerosis: relationship to clinical data. J Neurol Sci 134:51-56.

Iñarrea P (2002) Purification and determination of activity of mitochondrial cyanide-sensitive superoxide dismutase in rat tissue extract. Meth Enzymol 349:106-114.

Iñarrea P, Moini H, Rettori D, Han D, Martínez J, García I, Fernández-Vizarra E, Iturralde M, Cadenas E (2005) Redox activation of mitochondrial intermembrane space Cu,Zn-superoxide dismutase. Biochem J 387:203.

Ischiropoulos H, Beckman JS (2003) Oxidative stress and nitration in neurodegeneration: cause, effect, or association? Journal of Clinical Investigation 111:163-169.

Ishii T, Bannai S, Sugita Y (1981) Mechanism of growth stimulation of L1210 cells by 2-mercaptoethanol in vitro. Role of the mixed disulfide of 2-mercaptoethanol and cysteine. J Biol Chem 256:12387-12392.

Jaarsma D, Haasdijk ED, Grashorn JA, Hawkins R, van Duijn W, Verspaget HW, London J, Holstege JC (2000) Human Cu/Zn superoxide dismutase (SOD1) overexpression in mice causes mitochondrial vacuolization, axonal degeneration, and premature motoneuron death and accelerates motoneuron disease in mice expressing a familial amyotrophic lateral sclerosis mutant SOD1. Neurobiol Dis 7:623-643.

Jensen PK (1966) Antimycin-insensitive oxidation of succinate and reduced nicotinamide-adenine dinucleotide in electron-transport particles. I. pH dependency and hydrogen peroxide formation. Biochim Biophys Acta 122:157-166.

Johnston JA, Dalton MJ, Gurney ME, Kopito RR (2000) Formation of high molecular weight complexes of mutant Cu, Zn-superoxide dismutase in a mouse model for familial amyotrophic lateral sclerosis. Proc Natl Acad Sci USA 97:12571-12576.

Jones DP (2002) Redox potential of GSH/GSSG couple: assay and biological significance. Meth Enzymol 348:93-112.

Jones DP (2006a) Disruption of mitochondrial redox circuitry in oxidative stress. Chem Biol Interact 163:38-53.

Jones DP (2006b) Extracellular redox state: refining the definition of oxidative stress in aging. Rejuvenation Res 9:169-181.

Jones DP (2006c) Redefining oxidative stress. Antioxid Redox Signal 8:1865-1879.

Jones DP, Maellaro E, Jiang S, Slater AF, Orrenius S (1995) Effects of N-acetyl-L-cysteine on T-cell apoptosis are not mediated by increased cellular glutathione. Immunol Lett 45:205-209.

Jones DP, Go YM, Anderson CL, Ziegler TR, Kinkade JM, Kirlin WG (2004) Cysteine/cystine couple is a newly recognized node in the circuitry for biologic redox signaling and control. FASEB J 18:1246-1248.

Jonsson PA, Ernhill K, Andersen PM, Bergemalm D, Brännström T, Gredal O, Nilsson P, Marklund SL (2004) Minute quantities of misfolded mutant superoxide dismutase-1 cause amyotrophic lateral sclerosis. Brain 127:73-88.

Jung C, Higgins CMJ, Xu Z (2002) Mitochondrial electron transport chain complex dysfunction in a transgenic mouse model for amyotrophic lateral sclerosis. J Neurochem 83:535-545.

Kabashi E, Valdmanis PN, Dion P, Rouleau GA (2007) Oxidized/misfolded superoxide dismutase-1: the cause of all amyotrophic lateral sclerosis? Ann Neurol 62:553-559.

Kanai K, Kuwabara S, Misawa S, Tamura N, Ogawara K, Nakata M, Sawai S, Hattori T, Bostock H (2006) Altered axonal excitability properties in amyotrophic lateral sclerosis: impaired potassium channel function related to disease stage. Brain 129:953-962.

Kariya S, Mauricio R, Dai Y, Monani UR (2009) The neuroprotective factor Wld(s) fails to mitigate distal axonal and neuromuscular junction (NMJ) defects in mouse models of spinal muscular atrophy. Neuroscience Letters 449:246-251.

Kariya S, Park G-H, Maeno-Hikichi Y, Leykekhman O, Lutz C, Arkovitz MS, Landmesser LT, Monani UR (2008) Reduced SMN protein impairs maturation of the neuromuscular junctions in mouse models of spinal muscular atrophy. Human Molecular Genetics 17:2552-2569.

Karumbayaram S, Kelly TK, Paucar AA, Roe AJ, Umbach JA, Charles A, Goldman S, Kornblum HI, Wiedau-Pazos M (2009) Human embryonic stem cell-derived motor neurons expressing SOD1 mutants exhibit typical signs of motor neuron degeneration linked to ALS. Dis Model Mech 2:189-195.

Kasai H (2002) Chemistry-based studies on oxidative DNA damage: formation, repair, and mutagenesis. Free Radic Biol Med 33:450-456.

Kasarskis EJ, Tandon L, Lovell MA, Ehmann WD (1995) Aluminum, calcium, and iron in the spinal cord of patients with sporadic amyotrophic lateral sclerosis using laser microprobe mass spectroscopy: a preliminary study. J Neurol Sci 130:203-208.

Kato M, Aoki M, Ohta M, Nagai M, Ishizaki F, Nakamura S, Itoyama Y (2001) Marked reduction of the Cu/Zn superoxide dismutase polypeptide in a case of familial amyotrophic lateral sclerosis with the homozygous mutation. Neuroscience Letters 312:165-168.

Katsuno M, Adachi H, Minamiyama M, Waza M, Tokui K, Banno H, Suzuki K, Onoda Y, Tanaka F, Doyu M, Sobue G (2006) Reversible Disruption of Dynactin 1-Mediated Retrograde Axonal Transport in Polyglutamine-Induced Motor Neuron Degeneration. J Neurosci 26:12106-12117.

Kawamata H, Manfredi G (2008) Different regulation of wild-type and mutant Cu,Zn superoxide dismutase localization in mammalian mitochondria. Human Molecular Genetics 17:3303-3317.

Kennel PF, Finiels F, Revah F, Mallet J (1996) Neuromuscular function impairment is not caused by motor neuron loss in FALS mice: an electromyographic study. Neuroreport 7:1427-1431.

Kieran D (2005) A mutation in dynein rescues axonal transport defects and extends the life span of ALS mice. The Journal of Cell Biology 169:561-567.

Kieran D, Hafezparast M, Bohnert S, Dick JRT, Martin JE, Schiavo G, Fisher EMC, Greensmith L (2005) A mutation in dynein rescues axonal transport defects and extends the life span of ALS mice. The Journal of Cell Biology 169:561-567.

Kim N, Jeong M, Choi S, Hoonkang J (2004) Oxidative modification of neurofilament-L by the Cu,Zn-superoxide dismutase and hydrogen peroxide system. Biochimie 86:553-559.

Kirkinezos IG, Bacman SR, Hernandez D, Oca-Cossio J, Arias LJ, Perez-Pinzon MA, Bradley WG, Moraes CT (2005) Cytochrome c association with the inner mitochondrial membrane is impaired in the CNS of G93A-SOD1 mice. J Neurosci 25:164-172.

Kondo T, Reaume AG, Huang TT, Carlson E, Murakami K, Chen SF, Hoffman EK, Scott RW, Epstein CJ, Chan PH (1997) Reduction of CuZn-superoxide dismutase activity exacerbates neuronal cell injury and edema formation after transient focal cerebral ischemia. J Neurosci 17:4180-4189.

Kong J, Xu Z (1998) Massive mitochondrial degeneration in motor neurons triggers the onset of amyotrophic lateral sclerosis in mice expressing a mutant SOD1. J Neurosci 18:3241-3250.

Kong L, Wang X, Choe DW, Polley M, Burnett BG, Bosch-Marcé M, Griffin JW, Rich MM, Sumner CJ (2009) Impaired synaptic vesicle release and immaturity of neuromuscular junctions in spinal muscular atrophy mice. J Neurosci 29:842-851.

Kriscenski-Perry E, Durham HD, Sheu SS, Figlewicz DA (2002) Synergistic effects of low level stressors in an oxidative damage model of spinal motor neuron degeneration. Amyotroph Lateral Scler Other Motor Neuron Disord 3:151-157.

Kruman II, Pedersen WA, Springer JE, Mattson MP (1999) ALS-linked Cu/Zn-SOD mutation increases vulnerability of motor neurons to excitotoxicity by a mechanism involving increased oxidative stress and perturbed calcium homeostasis. Experimental Neurology 160:28-39.

Kumar N (2007) Nutritional neuropathies. Neurologic clinics 25:209-255.

Kwan AC, Dietz SB, Webb WW, Harris-Warrick RM (2009) Activity of Hb9 interneurons during fictive locomotion in mouse spinal cord. J Neurosci 29:11601-11613.

Lambert AJ, Brand MD (2004) Inhibitors of the quinone-binding site allow rapid superoxide production from mitochondrial NADH:ubiquinone oxidoreductase (complex I). J Biol Chem 279:39414-39420.

Lamonte B, Wallace KE, Holloway BA, Shelly SS, Ascaño J, Tokito M, Van Winkle T, Howland DS, Holzbaur EL (2002) Disruption of dynein/dynactin inhibits axonal

transport in motor neurons causing late-onset progressive degeneration. Neuron 34:715-727.

Laser H, Conforti L, Morreale G, Mack TG, Heyer M, Haley JE, Wishart T, Beirowski B, Walker SA, Haase G, Celik A, Adalbert R, Wagner D, Grumme D, Ribchester R, Plomann M, Coleman M (2006) The slow Wallerian degeneration protein, WldS, binds directly to VCP/p97 and partially redistributes it within the nucleus. Mol Biol Cell 17:1075-1084.

Lebovitz R (1996) Neurodegeneration, myocardial injury, and perinatal death in mitochondrial superoxide dismutase-deficient mice. Proc Natl Acad Sci USA 93:9782-9787.

Li H, Li SH, Yu ZX, Shelbourne P, Li XJ (2001) Huntingtin aggregate-associated axonal degeneration is an early pathological event in Huntington's disease mice. J Neurosci 21:8473-8481.

Li Q, Sato EF, Zhu X, Inoue M (2009) A simultaneous release of SOD1 with cytochrome c regulates mitochondria-dependent apoptosis. Mol Cell Biochem 322:151-159.

Li Q, Sato EF, Kira Y, Nishikawa M, Utsumi K, Inoue M (2006) A possible cooperation of SOD1 and cytochrome c in mitochondria-dependent apoptosis. Free Radic Biol Med 40:173-181.

Liedtke W, Leman EE, Fyffe REW, Raine CS, Schubart UK (2002) Stathmin-deficient mice develop an age-dependent axonopathy of the central and peripheral nervous systems. Am J Pathol 160:469-480.

Lin A, Holt C (2008) Function and regulation of local axonal translation. Current Opinion in Neurobiology 18:60-68.

Ling SM, Conwit RA, Ferrucci L, Metter EJ (2009) Age-associated changes in motor unit physiology: observations from the Baltimore Longitudinal Study of Aging. Arch Phys Med Rehabil 90:1237-1240.

Liu J, Lillo C, Jonsson PA, Vande Velde C, Ward CM, Miller TM, Subramaniam JR, Rothstein JD, Marklund S, Andersen PM, Brännström T, Gredal O, Wong PC, Williams DS, Cleveland DW (2004) Toxicity of familial ALS-linked SOD1 mutants from selective recruitment to spinal mitochondria. Neuron 43:5-17.

Loschen G, Flohé L, Chance B (1971) Respiratory chain linked H(2)O(2) production in pigeon heart mitochondria. FEBS Lett 18:261-264.

Loschen G, Azzi A, Richter C, Flohé L (1974) Superoxide radicals as precursors of mitochondrial hydrogen peroxide. FEBS Lett 42:68-72.

Lourenssen S, Miller KG, Blennerhassett MG (2009) Discrete responses of myenteric neurons to structural and functional damage by neurotoxins in vitro. Am J Physiol Gastrointest Liver Physiol 297:G228-239.

Lunn E, Perry V, Brown M, Rosen H, Gordon S (1989) Absence of Wallerian Degeneration does not Hinder Regeneration in Peripheral Nerve. Eur J Neurosci 1:27-33.

Ly CV, Verstreken P (2006) Mitochondria at the synapse. The Neuroscientist : a review journal bringing neurobiology, neurology and psychiatry 12:291-299.

Lynch RE, Fridovich I (1978) Effects of superoxide on the erythrocyte membrane. J Biol Chem 253:1838-1845.

Lyons TJ, Liu H, Goto JJ, Nersissian A, Roe JA, Graden JA, Café C, Ellerby LM, Bredesen DE, Gralla EB, Valentine JS (1996) Mutations in copper-zinc

superoxide dismutase that cause amyotrophic lateral sclerosis alter the zinc binding site and the redox behavior of the protein. Proc Natl Acad Sci USA 93:12240-12244.

MacInnis BL, Campenot RB (2005) Regulation of Wallerian degeneration and nerve growth factor withdrawal-induced pruning of axons of sympathetic neurons by the proteasome and the MEK/Erk pathway. Mol Cell Neurosci 28:430-439.

Mack TG, Reiner M, Beirowski B, Mi W, Emanuelli M, Wagner D, Thomson D, Gillingwater T, Court F, Conforti L, Fernando FS, Tarlton A, Andressen C, Addicks K, Magni G, Ribchester RR, Perry VH, Coleman MP (2001) Wallerian degeneration of injured axons and synapses is delayed by a Ube4b/Nmnat chimeric gene. Nat Neurosci 4:1199-1206.

Magrané J, Manfredi G (2009) Mitochondrial function, morphology, and axonal transport in amyotrophic lateral sclerosis. Antioxid Redox Signal 11:1615-1626.

Magrané J, Hervias I, Henning M, Damiano M, Kawamata H, Manfredi G (2009) Mutant SOD1 in neuronal mitochondria causes toxicity and mitochondrial dynamics abnormalities. Human Molecular Genetics DOI: 10.1093/hmg/ddp421.

Marklund SL (1982) Human copper-containing superoxide dismutase of high molecular weight. Proc Natl Acad Sci USA 79:7634-7638.

Masè G, Ros S, Gemma A, Bonfigli L, Carraro N, Cazzato G, Rolfo M, Zanconati F, Sepcic J, Jurjevic A, Pirulli D, Boniotto M, Zezlina S, Crovella S, Amoroso A (2001) ALS with variable phenotypes in a six-generation family caused by leu144phe mutation in the SOD1 gene. J Neurol Sci 191:11-18.

Mattiazzi M, D'Aurelio M, Gajewski CD, Martushova K, Kiaei M, Beal MF, Manfredi G (2002) Mutated human SOD1 causes dysfunction of oxidative phosphorylation in mitochondria of transgenic mice. J Biol Chem 277:29626-29633.

Mattson MP (2007) Calcium and neurodegeneration. Aging Cell 6:337-350.

Matzuk MM, Dionne L, Guo Q, Kumar TR, Lebovitz RM (1998) Ovarian function in superoxide dismutase 1 and 2 knockout mice. Endocrinology 139:4008-4011.

McCord JM, Fridovich I (1969) Superoxide dismutase. An enzymic function for erythrocuprein (hemocuprein). J Biol Chem 244:6049-6055.

McFadden S, Ohlemiller K, Ding D, Shero M, Salvi R (2001) The Influence of Superoxide Dismutase and Glutathione Peroxidase Deficiencies on Noise-Induced Hearing Loss in Mice. Noise Health 3:49-64.

McFadden SL, Ding D, Reaume AG, Flood DG, Salvi RJ (1999) Age-related cochlear hair cell loss is enhanced in mice lacking copper/zinc superoxide dismutase. Neurobiol Aging 20:1-8.

McGovern VL, Gavrilina TO, Beattie CE, Burghes AHM (2008) Embryonic motor axon development in the severe SMA mouse. Human Molecular Genetics 17:2900-2909.

Melli G, Keswani SC, Fischer A, Chen W, Höke A (2006) Spatially distinct and functionally independent mechanisms of axonal degeneration in a model of HIV-associated sensory neuropathy. Brain 129:1330-1338.

Menzies FM, Cookson MR, Taylor RW, Turnbull DM, Chrzanowska-Lightowlers ZM, Dong L, Figlewicz DA, Shaw PJ (2002) Mitochondrial dysfunction in a cell culture model of familial amyotrophic lateral sclerosis. Brain 125:1522-1533.

Mi W, Conforti L, Coleman M (2002) Genotyping methods to detect a unique neuroprotective factor (Wld(s)) for axons. Journal of Neuroscience Methods 113:215-218.

Mi W, Beirowski B, Gillingwater TH, Adalbert R, Wagner D, Grumme D, Osaka H, Conforti L, Arnhold S, Addicks K, Wada K, Ribchester RR, Coleman MP (2005) The slow Wallerian degeneration gene, WldS, inhibits axonal spheroid pathology in gracile axonal dystrophy mice. Brain 128:405-416.

Miledi R, Slater CR (1970) On the degeneration of rat neuromuscular junctions after nerve section. The Journal of Physiology 207:507-528.

Miller BR, Press C, Daniels RW, Sasaki Y, Milbrandt J, DiAntonio A (2009) A dual leucine kinase-dependent axon self-destruction program promotes Wallerian degeneration. Nat Neurosci 12:387-389.

Misawa H, Nakata K, Matsuura J, Moriwaki Y, Kawashima K, Shimizu T, Shirasawa T, Takahashi R (2006) Conditional knockout of Mn superoxide dismutase in postnatal motor neurons reveals resistance to mitochondrial generated superoxide radicals. Neurobiology of Disease 23:169-177.

Mitsumoto H, Santella RM, Liu X, Bogdanov M, Zipprich J, Wu H-C, Mahata J, Kilty M, Bednarz K, Bell D, Gordon PH, Hornig M, Mehrazin M, Naini A, Flint Beal M, Factor-Litvak P (2008) Oxidative stress biomarkers in sporadic ALS. Amyotrophic lateral sclerosis 9:177-183.

Miura H, Oda K, Endo C, Yamazaki K, Shibasaki H, Kikuchi T (1993) Progressive degeneration of motor nerve terminals in GAD mutant mouse with hereditary sensory axonopathy. Neuropathol Appl Neurobiol 19:41-51.

Monani UR, Pastore MT, Gavrilina TO, Jablonka S, Le TT, Andreassi C, DiCocco JM, Lorson C, Androphy EJ, Sendtner M, Podell M, Burghes AHM (2003) A transgene carrying an A2G missense mutation in the SMN gene modulates phenotypic severity in mice with severe (type I) spinal muscular atrophy. The Journal of Cell Biology 160:41-52.

Muller F, Song W, Jang Y, Liu Y, Sabia M, Richardson A, Van Remmen H (2007) Denervation-induced skeletal muscle atrophy is associated with increased mitochondrial ROS production. AJP: Regulatory, Integrative and Comparative Physiology 293:R1159-R1168.

Muller F, Song W, Liu Y, Chaudhuri A, Piekedahl S, Strong R, Huang T, Epstein C, Robertsii L, Csete M (2006) Absence of CuZn superoxide dismutase leads to elevated oxidative stress and acceleration of age-dependent skeletal muscle atrophy. Free Radic Biol Med 40:1993-2004.

Muller FL, Liu Y, Van Remmen H (2004) Complex III releases superoxide to both sides of the inner mitochondrial membrane. J Biol Chem 279:49064-49073.

Murakami T, Nagano I, Hayashi T, Manabe Y, Shoji M, Setoguchi Y, Abe K (2001) Impaired retrograde axonal transport of adenovirus-mediated E. coli LacZ gene in the mice carrying mutant SOD1 gene. Neuroscience Letters 308:149-152.

Murphy MP (2009) How mitochondria produce reactive oxygen species. Biochem J 417:1-13.

Murray LM, Thomson D, Conklin A, Wishart TM, Gillingwater TH (2008a) Loss of translation elongation factor (eEF1A2) expression in vivo differentiates between Wallerian degeneration and dying-back neuronal pathology. J Anat 213:633-645.

Murray LM, Comley LH, Thomson D, Parkinson N, Talbot K, Gillingwater T (2008b) Selective vulnerability of motor neurons and dissociation of pre- and post-synaptic pathology at the neuromuscular junction in mouse models of spinal muscular atrophy. Hum Mol Genet 17:949-962.

Naini A, Mehrazin M, Lu J, Gordon P, Mitsumoto H (2007) Identification of a novel D109Y mutation in Cu/Zn superoxide dismutase (sod1) gene associated with amyotrophic lateral sclerosis. J Neurol Sci 254:17-21.

Nakata M, Kuwabara S, Kanai K, Misawa S, Tamura N, Sawai S, Hattori T, Bostock H (2006) Distal excitability changes in motor axons in amyotrophic lateral sclerosis. Clinical Neurophysiology 117:1444-1448.

Newbery HJ, Gillingwater T, Dharmasaroja P, Peters J, Wharton SB, Thomson D, Ribchester R, Abbott CM (2005) Progressive loss of motor neuron function in wasted mice: effects of a spontaneous null mutation in the gene for the eEF1 A2 translation factor. J Neuropathol Exp Neurol 64:295-303.

Niemann A, Ruegg M, La Padula V, Schenone A, Suter U (2005) Ganglioside-induced differentiation associated protein 1 is a regulator of the mitochondrial network: new implications for Charcot-Marie-Tooth disease. The Journal of Cell Biology 170:1067-1078.

Nikolić-Kokić A, Stević Z, Blagojević D, Davidović B, Jones DR, Spasić MB (2006) Alterations in anti-oxidative defence enzymes in erythrocytes from sporadic amyotrophic lateral sclerosis (SALS) and familial ALS patients. Clin Chem Lab Med 44:589-593.

Nishikawa T, Edelstein D, Du XL, Yamagishi S, Matsumura T, Kaneda Y, Yorek MA, Beebe D, Oates PJ, Hammes HP, Giardino I, Brownlee M (2000) Normalizing mitochondrial superoxide production blocks three pathways of hyperglycaemic damage. Nature 404:787-790.

Nixon RA, Saito KI, Grynspan F, Griffin WR, Katayama S, Honda T, Mohan PS, Shea TB, Beermann M (1994) Calcium-activated neutral proteinase (calpain) system in aging and Alzheimer's disease. Ann N Y Acad Sci 747:77-91.

O'Hanlon G, Humphreys P, Goldman R, Halstead S, Bullens R, Plomp J, Ushkaryov Y, Willison H (2003) Calpain inhibitors protect against axonal degeneration in a model of anti-ganglioside antibody-mediated motor nerve terminal injury. Brain 126:2497.

Ohlemiller KK, McFadden SL, Ding DL, Flood DG, Reaume AG, Hoffman EK, Scott RW, Wright JS, Putcha GV, Salvi RJ (1999) Targeted deletion of the cytosolic Cu/Zn-superoxide dismutase gene (Sod1) increases susceptibility to noise-induced hearing loss. Audiol Neurootol 4:237-246.

Olofsson EM, Marklund SL, Behndig A (2009) Enhanced diabetes-induced cataract in copper-zinc superoxide dismutase-null mice. Invest Ophthalmol Vis Sci 50:2913-2918.

Oosthuyse B et al. (2001) Deletion of the hypoxia-response element in the vascular endothelial growth factor promoter causes motor neuron degeneration. Nat Genet 28:131-138.

Oprea GE, Kröber S, McWhorter ML, Rossoll W, Müller S, Krawczak M, Bassell GJ, Beattie CE, Wirth B (2008) Plastin 3 is a protective modifier of autosomal recessive spinal muscular atrophy. Science 320:524-527.

Oteiza PI, Uchitel OD, Carrasquedo F, Dubrovski AL, Roma JC, Fraga CG (1997) Evaluation of antioxidants, protein, and lipid oxidation products in blood from sporadic amyotrophic lateral sclerosis patients. Neurochem Res 22:535-539.

Pasinelli P, Belford ME, Lennon N, Bacskai BJ, Hyman BT, Trotti D, Brown RH (2004) Amyotrophic lateral sclerosis-associated SOD1 mutant proteins bind and aggregate with Bcl-2 in spinal cord mitochondria. Neuron 43:19-30.

Pedersen WA, Fu W, Keller JN, Markesbery WR, Appel S, Smith RG, Kasarskis E, Mattson MP (1998) Protein modification by the lipid peroxidation product 4-hydroxynonenal in the spinal cords of amyotrophic lateral sclerosis patients. Ann Neurol 44:819-824.

Peled-Kamar M, Lotem J, Wirguin I, Weiner L, Hermalin A, Groner Y (1997) Oxidative stress mediates impairment of muscle function in transgenic mice with elevated level of wild-type Cu/Zn superoxide dismutase. Proc Natl Acad Sci USA 94:3883-3887.

Phillips JP, Campbell SD, Michaud D, Charbonneau M, Hilliker AJ (1989) Null mutation of copper/zinc superoxide dismutase in Drosophila confers hypersensitivity to paraquat and reduced longevity. Proc Natl Acad Sci USA 86:2761-2765.

Press C, Milbrandt J (2008) Nmnat delays axonal degeneration caused by mitochondrial and oxidative stress. J Neurosci 28:4861-4871.

Przedborski S, Donaldson D, Jakowec M, Kish SJ, Guttman M, Rosoklija G, Hays AP (1996a) Brain superoxide dismutase, catalase, and glutathione peroxidase activities in amyotrophic lateral sclerosis. Ann Neurol 39:158-165.

Przedborski S, Donaldson DM, Murphy PL, Hirsch O, Lange D, Naini AB, McKenna-Yasek D, Brown RH (1996b) Blood superoxide dismutase, catalase and glutathione peroxidase activities in familial and sporadic amyotrophic lateral sclerosis. Neurodegeneration : a journal for neurodegenerative disorders, neuroprotection, and neuroregeneration 5:57-64.

Puls I, Jonnakuty C, Lamonte B, Holzbaur E, Tokito M, Mann E, Floeter M, Bidus K, Drayna D, Oh S, Brown R, Ludlow C, Fischbeck K (2003) Mutant dynactin in motor neuron disease. Nat Genet 33:455-456.

Pun S, Santos AF, Saxena S, Xu L, Caroni P (2006) Selective vulnerability and pruning of phasic motoneuron axons in motoneuron disease alleviated by CNTF. Nat Neurosci 9:408-419.

Puymirat J, Cossette L, Gosselin F, Bouchard JP (1994) Red blood cell Cu/Zn superoxide dismutase activity in sporadic amyotrophic lateral sclerosis. J Neurol Sci 127:121-123.

Qi X, Lewin AS, Hauswirth WW, Guy J (2003) Optic neuropathy induced by reductions in mitochondrial superoxide dismutase. Invest Ophthalmol Vis Sci 44:1088-1096.

Raff MC, Whitmore AV, Finn JT (2002) Axonal self-destruction and neurodegeneration. Science 296:868-871.

Raha S, Robinson BH (2000) Mitochondria, oxygen free radicals, disease and ageing. Trends Biochem Sci 25:502-508.

Reaume AG, Elliott JL, Hoffman EK, Kowall NW, Ferrante RJ, Siwek DF, Wilcox HM, Flood DG, Beal MF, Brown RH, Scott RW, Snider WD (1996) Motor neurons in Cu/Zn superoxide dismutase-deficient mice develop normally but exhibit enhanced cell death after axonal injury. Nat Genet 13:43-47.

Reddehase S, Grumbt B, Neupert W, Hell K (2009) The disulfide relay system of mitochondria is required for the biogenesis of mitochondrial Ccs1 and Sod1. Journal of Molecular Biology 385:331-338.

Reddy VN, Kasahara E, Hiraoka M, Lin LR, Ho YS (2004) Effects of variation in superoxide dismutases (SOD) on oxidative stress and apoptosis in lens epithelium. Exp Eye Res 79:859-868.

Reid MB, Durham WJ (2002) Generation of reactive oxygen and nitrogen species in contracting skeletal muscle: potential impact on aging. Ann N Y Acad Sci 959:108-116.

Rhee SG, Chae HZ, Kim K (2005) Peroxiredoxins: a historical overview and speculative preview of novel mechanisms and emerging concepts in cell signaling. Free Radic Biol Med 38:1543-1552.

Ribchester RR, Tsao JW, Barry JA, Asgari-Jirhandeh N, Perry VH, Brown MC (1995) Persistence of neuromuscular junctions after axotomy in mice with slow Wallerian degeneration (C57BL/WldS). Eur J Neurosci 7:1641-1650.

Rich MM, Wang X, Cope TC, Pinter MJ (2002) Reduced neuromuscular quantal content with normal synaptic release time course and depression in canine motor neuron disease. Journal of Neurophysiology 88:3305-3314.

Romero FJ, Monsalve E, Hermenegildo C, Puertas FJ, Higueras V, Nies E, Segura-Aguilar J, Roma J (1991) Oxygen toxicity in the nervous tissue: comparison of the antioxidant defense of rat brain and sciatic nerve. Neurochem Res 16:157-161.

Rose FF, Meehan PW, Coady TH, Garcia VB, Garcia ML, Lorson CL (2008) The Wallerian degeneration slow (Wld(s)) gene does not attenuate disease in a mouse model of spinal muscular atrophy. Biochemical and Biophysical Research Communications 375:119-123.

Rosen DR, Siddique T, Patterson D, Figlewicz DA, Sapp P, Hentati A, Donaldson D, Goto J, O'Regan JP, Deng HX (1993) Mutations in Cu/Zn superoxide dismutase gene are associated with familial amyotrophic lateral sclerosis. Nature 362:59-62.

Rossoll W, Jablonka S, Andreassi C, Kröning AK, Karle K, Monani UR, Sendtner M (2003) Smn, the spinal muscular atrophy-determining gene product, modulates axon growth and localization of beta-actin mRNA in growth cones of motoneurons. J Cell Biol 163:801-812.

Rothstein J (2009) Current hypotheses for the underlying biology of amyotrophic lateral sclerosis. Ann Neurol 65 Suppl 1:S3-9.

Rothstein JD, Bristol LA, Hosler B, Brown RH, Kuncl RW (1994) Chronic inhibition of superoxide dismutase produces apoptotic death of spinal neurons. Proc Natl Acad Sci USA 91:4155-4159.

Rouaux C, Panteleeva I, René F, Gonzalez De Aguilar J-L, Echaniz-Laguna A, Dupuis L, Menger Y, Boutillier A-L, Loeffler J-P (2007) Sodium valproate exerts neuroprotective effects in vivo through CREB-binding protein-dependent

mechanisms but does not improve survival in an amyotrophic lateral sclerosis mouse model. J Neurosci 27:5535-5545.

Sagara JI, Miura K, Bannai S (1993) Maintenance of neuronal glutathione by glial cells. J Neurochem 61:1672-1676.

Sagot Y, Dubois-Dauphin M, Tan SA, de Bilbao F, Aebischer P, Martinou JC, Kato AC (1995) Bcl-2 overexpression prevents motoneuron cell body loss but not axonal degeneration in a mouse model of a neurodegenerative disease. J Neurosci 15:7727-7733.

Said G, Goulon-Goeau C, Slama G, Tchobroutsky G (1992) Severe early-onset polyneuropathy in insulin-dependent diabetes mellitus. A clinical and pathological study. N Engl J Med 326:1257-1263.

Sajadi A, Schneider B, Aebischer P (2004) Wlds-Mediated Protection of Dopaminergic Fibers in an Animal Model of Parkinson Disease. Curr Biol 14:326-330.

Samsam M, Mi W, Wessig C, Zielasek J, Toyka KV, Coleman M, Martini R (2003) The Wlds mutation delays robust loss of motor and sensory axons in a genetic model for myelin-related axonopathy. J Neurosci 23:2833-2839.

Sandy MS, Moldeus P, Ross D, Smith MT (1986) Role of redox cycling and lipid peroxidation in bipyridyl herbicide cytotoxicity. Studies with a compromised isolated hepatocyte model system. Biochem Pharmacol 35:3095-3101.

Sango K, McDonald MP, Crawley JN, Mack ML, Tifft CJ, Skop E, Starr CM, Hoffmann A, Sandhoff K, Suzuki K, Proia RL (1996) Mice lacking both subunits of lysosomal beta-hexosaminidase display gangliosidosis and mucopolysaccharidosis. Nat Genet 14:348-352.

Sasaki S, Iwata M (1996) Impairment of fast axonal transport in the proximal axons of anterior horn neurons in amyotrophic lateral sclerosis. Neurology 47:535-540.

Sasaki S, Iwata M (2007) Mitochondrial alterations in the spinal cord of patients with sporadic amyotrophic lateral sclerosis. J Neuropathol Exp Neurol 66:10-16.

Sasaki Y, Araki T, Milbrandt J (2006) Stimulation of Nicotinamide Adenine Dinucleotide Biosynthetic Pathways Delays Axonal Degeneration after Axotomy. Journal of Neuroscience 26:8484-8491.

Schaefer A, Sanes J, Lichtman J (2005) A compensatory subpopulation of motor neurons in a mouse model of amyotrophic lateral sclerosis. J Comp Neurol 490:209-219.

Schafer FQ, Buettner GR (2001) Redox environment of the cell as viewed through the redox state of the glutathione disulfide/glutathione couple. Free Radic Biol Med 30:1191-1212.

Schwartz PJ, Reaume A, Scott R, Coyle JT (1998) Effects of over- and under-expression of Cu,Zn-superoxide dismutase on the toxicity of glutamate analogs in transgenic mouse striatum. Brain Res 789:32-39.

Selkoe DJ (2002) Alzheimer's disease is a synaptic failure. Science 298:789-791.

Sendtner M, Schmalbruch H, Stöckli KA, Carroll P, Kreutzberg GW, Thoenen H (1992) Ciliary neurotrophic factor prevents degeneration of motor neurons in mouse mutant progressive motor neuronopathy. Nature 358:502-504.

Sharma AK, Bajada S, Thomas PK (1980) Age changes in the tibial and plantar nerves of the rat. J Anat 130:417-428.

Shaw IC, Fitzmaurice PS, Mitchell JD, Lynch PG (1995) Studies on cellular free radical protection mechanisms in the anterior horn from patients with amyotrophic lateral sclerosis. Neurodegeneration 4:391-396.

Shefner JM (2001) Motor unit number estimation in human neurological diseases and animal models. Clinical neurophysiology 112:955-964.

Shefner JM, Cudkowicz M, Brown RH (2006) Motor unit number estimation predicts disease onset and survival in a transgenic mouse model of amyotrophic lateral sclerosis. Muscle Nerve 34:603-607.

Shefner JM, Reaume AG, Flood DG, Scott RW, Kowall NW, Ferrante RJ, Siwek DF, Upton-Rice M, Brown RH (1999) Mice lacking cytosolic copper/zinc superoxide dismutase display a distinctive motor axonopathy. Neurology 53:1239-1246.

Shi P, Gal J, Kwinter D, Liu X, Zhu H (2009) Mitochondrial dysfunction in amyotrophic lateral sclerosis. Biochim Biophys Acta DOI: 10.1016/j.bbadis.2009.08.012.

Shibata N, Nagai R, Uchida K, Horiuchi S, Yamada S, Hirano A, Kawaguchi M, Yamamoto T, Sasaki S, Kobayashi M (2001) Morphological evidence for lipid peroxidation and protein glycoxidation in spinal cords from sporadic amyotrophic lateral sclerosis patients. Brain Res 917:97-104.

Siklós L, Engelhardt J, Harati Y, Smith RG, Joó F, Appel SH (1996) Ultrastructural evidence for altered calcium in motor nerve terminals in amyotropic lateral sclerosis. Ann Neurol 39:203-216.

Siklós L, Engelhardt JI, Alexianu ME, Gurney ME, Siddique T, Appel SH (1998) Intracellular calcium parallels motoneuron degeneration in SOD-1 mutant mice. J Neuropathol Exp Neurol 57:571-587.

Silva A, Wang Q, Wang M, Ravula SK, Glass J (2006) Evidence for direct axonal toxicity in vincristine neuropathy. J Peripher Nerv Syst 11:211-216.

Smith RS, Bisby MA (1993) Persistence of axonal transport in isolated axons of the mouse. European Journal of Neuroscience 5:1127-1135.

Son M, Puttaparthi K, Kawamata H, Rajendran B, Boyer PJ, Manfredi G, Elliott JL (2007) Overexpression of CCS in G93A-SOD1 mice leads to accelerated neurological deficits with severe mitochondrial pathology. Proc Natl Acad Sci USA 104:6072-6077.

Song MS, Saavedra L, de Chaves EI (2006) Apoptosis is secondary to non-apoptotic axonal degeneration in neurons exposed to Abeta in distal axons. Neurobiol Aging 27:1224-1238.

Sotelo-Silveira JR, Lepanto P, Elizondo MV, Horjales S, Palacios F, Martinez Palma L, Marin M, Beckman JS, Barbeito L (2009) Axonal mitochondrial clusters containing mutant SOD1 in transgenic models of ALS. Antioxid Redox Signal 11:1-11.

Spencer P, Schaumburg H (1982) The pathogenesis of motor neuron disease: perspectives from neurotoxicology. Advances in neurology 36:249-66.

Spencer PS, Schaumbug HH (1976) Central-Peripheral Distal Axonopathy—The Pathology of Dying-Back Polyneuropathies. Progress in Neuropathology 3:253-295.

Stokin GB, Lillo C, Falzone TL, Brusch RG, Rockenstein E, Mount SL, Raman R, Davies P, Masliah E, Williams DS, Goldstein LSB (2005) Axonopathy and

transport deficits early in the pathogenesis of Alzheimer's disease. Science 307:1282-1288.

Studer L, Csete M, Lee SH, Kabbani N, Walikonis J, Wold B, McKay R (2000) Enhanced proliferation, survival, and dopaminergic differentiation of CNS precursors in lowered oxygen. J Neurosci 20:7377-7383.

Sturtz LA, Diekert K, Jensen LT, Lill R, Culotta VC (2001) A fraction of yeast Cu,Zn-superoxide dismutase and its metallochaperone, CCS, localize to the intermembrane space of mitochondria. A physiological role for SOD1 in guarding against mitochondrial oxidative damage. J Biol Chem 276:38084-38089.

Suzuki M, McHugh J, Tork C, Shelley B, Klein SM, Aebischer P, Svendsen CN (2007) GDNF secreting human neural progenitor cells protect dying motor neurons, but not their projection to muscle, in a rat model of familial ALS. PLoS ONE 2:e689.

Tam SL, Gordon T (2003) Mechanisms controlling axonal sprouting at the neuromuscular junction. J Neurocytol 32:961-974.

Tandan R, Bradley WG (1985) Amyotrophic Lateral Sclerosis: Part 1. Clinical Features, Pathology, and Ethical Issues in Management. Annals of Neurology 18:271-280.

Thomas PK, Tomlinson DR (1993) Diabetic and Hypoglycemic Neuropathy. In: Peripheral Neuropathy, 3rd Edition (Dyck PJ, Thomas PK, Griffin JW, Low PA, Poduslo JF, eds), pp 1219-1250. Philadelphia/London: WB Saunders & Co,.

Tórsdóttir G, Kristinsson J, Gudmundsson G, Snaedal J, Jóhannesson T (2000) Copper, ceruloplasmin and superoxide dismutase (SOD) in amyotrophic lateral sclerosis. Pharmacol Toxicol 87:126-130.

Troncoso JC, Costello AC, Kim JH, Johnson GV (1995) Metal-catalyzed oxidation of bovine neurofilaments in vitro. Free Radic Biol Med 18:891-899.

Troy CM, Shelanski ML (1994) Down-regulation of copper/zinc superoxide dismutase causes apoptotic death in PC12 neuronal cells. Proc Natl Acad Sci USA 91:6384-6387.

Tuncel D, Aydin N, Aribal Kocatürk P, Ozelçi Kavas G, Sarikaya S (2006) Red cell superoxide dismutase activity in sporadic amyotrophic lateral sclerosis. Journal of clinical neuroscience 13:991-994.

Turner B (2003) Neuromuscular accumulation of mutant superoxide dismutase 1 aggregates in a transgenic mouse model of familial amyotrophic lateral sclerosis. Neuroscience Letters 350:132-136.

Turner B, Lopes E, Cheema S (2003) Neuromuscular accumulation of mutant superoxide dismutase 1 aggregates in a transgenic mouse model of familial amyotrophic lateral sclerosis. Neurosci Lett 350:132-136.

Twiss JL, Fainzilber M (2009) Ribosomes in axons--scrounging from the neighbors? Trends in Cell Biology 19:236-243.

Valdmanis PN, Daoud H, Dion PA, Rouleau GA (2009) Recent advances in the genetics of amyotrophic lateral sclerosis. Current neurology and neuroscience reports 9:198-205.

Vande Velde C, Garcia ML, Yin X, Trapp BD, Cleveland D (2004) The neuroprotective factor Wlds does not attenuate mutant SOD1-mediated motor neuron disease. Neuromolecular Med 5:193-203.

Vielhaber S, Kunz D, Winkler K, Wiedemann FR, Kirches E, Feistner H, Heinze HJ, Elger CE, Schubert W, Kunz WS (2000) Mitochondrial DNA abnormalities in skeletal muscle of patients with sporadic amyotrophic lateral sclerosis. Brain 123 (Pt 7):1339-1348.

Vijayvergiya C, Beal MF, Buck J, Manfredi G (2005) Mutant superoxide dismutase 1 forms aggregates in the brain mitochondrial matrix of amyotrophic lateral sclerosis mice. J Neurosci 25:2463-2470.

Vila L, Barrett EF, Barrett JN (2003) Stimulation-induced mitochondrial [Ca2+] elevations in mouse motor terminals: comparison of wild-type with SOD1-G93A. The Journal of Physiology 549:719-728.

Vincent AM, Russell JW, Sullivan KA, Backus C, Hayes JM, McLean LL, Feldman EL (2007) SOD2 protects neurons from injury in cell culture and animal models of diabetic neuropathy. Exp Neurol 208:216-227.

Vinceti M, Bergomi M, Nacci G, Pietrini V, Ferrari A, Fortini K, Guidetti D, Sola P, Rocchi E, Mancia D, Vivoli G (2002) Erythrocyte zinc, copper, and copper/zinc superoxide dismutase and risk of sporadic amyotrophic lateral sclerosis: a population-based case-control study. Amyotroph Lateral Scler Other Motor Neuron Disord 3:208-214.

Vucic S, Kiernan M (2006) Axonal excitability properties in amyotrophic lateral sclerosis. Clinical Neurophysiology 117:1458-1466.

Waller A (1850) Experiments on the section of the glossopharyngeal and hypoglossal nerves of the frog, and observations of the alterations produced thereby in the

structure of their primitive fibres. Philosophical Transactions of the Royal Society of London 140:423-429.

Wang J, Zhai Q, Chen Y, Lin E, Gu W, McBurney MW, He Z (2005) A local mechanism mediates NAD-dependent protection of axon degeneration. The Journal of Cell Biology 170:349-355.

Wang M, Wu Y, Culver DG, Glass J (2000) Pathogenesis of axonal degeneration: parallels between Wallerian degeneration and vincristine neuropathy. J Neuropathol Exp Neurol 59:599-606.

Wang M, Wu Y, Culver DG, Glass J (2001a) The gene for slow Wallerian degeneration (Wld(s)) is also protective against vincristine neuropathy. Neurobiol Dis 8:155-161.

Wang M, Fang G, Culver DG, Davis AA, Rich MM, Glass J (2001b) The WldS protein protects against axonal degeneration: a model of gene therapy for peripheral neuropathy. Ann Neurol 50:773-779.

Wang MS, Davis AA, Culver DG, Glass JD (2002) Wlds Mice are Resistant to Paclitaxel (Taxol) Neuropathy. Annals of Neurology 52:442-447.

Wang MS, Davis AA, Culver DG, Wang Q, Powers JC, Glass JD (2004) Calpain inhibition protects against Taxol-induced sensory neuropathy. Brain 127:671-679.

Warita H, Itoyama Y, Abe K (1999) Selective impairment of fast anterograde axonal transport in the peripheral nerves of asymptomatic transgenic mice with a G93A mutant SOD1 gene. Brain Research 819:120-131.

Watkins PJ, Gayle C, Alsanjari N, Scaravilli F, Zanone M, Thomas PK (1995) Severe sensory-autonomic neuropathy and endocrinopathy in insulin-dependent diabetes. QJM 88:795-804.

Weisiger RA, Fridovich I (1973) Mitochondrial superoxide dismutase. Site of synthesis and intramitochondrial localization. J Biol Chem 248:4793-4796.

Wichterle H, Lieberam I, Porter JA, Jessell TM (2002) Directed differentiation of embryonic stem cells into motor neurons. Cell 110:385-397.

Wiedau-Pazos M, Goto JJ, Rabizadeh S, Gralla EB, Roe JA, Lee MK, Valentine JS, Bredesen DE (1996) Altered reactivity of superoxide dismutase in familial amyotrophic lateral sclerosis. Science 271:515-518.

Wiedemann FR, Manfredi G, Mawrin C, Beal MF, Schon EA (2002) Mitochondrial DNA and respiratory chain function in spinal cords of ALS patients. J Neurochem 80:616-625.

Wiedemann FR, Winkler K, Kuznetsov AV, Bartels C, Vielhaber S, Feistner H, Kunz WS (1998) Impairment of mitochondrial function in skeletal muscle of patients with amyotrophic lateral sclerosis. J Neurol Sci 156:65-72.

Wigston DJ, English AW (1992) Fiber-type proportions in mammalian soleus muscle during postnatal development. J Neurobiol 23:61-70.

Williamson TL, Cleveland DW (1999) Slowing of axonal transport is a very early event in the toxicity of ALS-linked SOD1 mutants to motor neurons. Nat Neurosci 2:50-56.

Winterbourn CC, Domigan NM, Broom JK (1995) Decreased thermal stability of red blood cell glu100-->gly superoxide dismutase from a family with amyotrophic lateral sclerosis. FEBS Lett 368:449-451.

Wishart TM, Paterson JM, Short DM, Meredith S, Robertson KA, Sutherland C, Cousin MA, Dutia MB, Gillingwater TH (2007) Differential proteomics analysis of synaptic proteins identifies potential cellular targets and protein mediators of synaptic neuroprotection conferred by the slow Wallerian degeneration (Wlds) gene. Mol Cell Proteomics 6:1318-1330.

Wong PC, Pardo CA, Borchelt DR, Lee MK, Copeland NG, Jenkins NA, Sisodia SS, Cleveland DW, Price DL (1995) An adverse property of a familial ALS-linked SOD1 mutation causes motor neuron disease characterized by vacuolar degeneration of mitochondria. Neuron 14:1105-1116.

Wroe R, Wai-Ling Butler A, Andersen PM, Powell JF, Al-Chalabi A (2008) ALSOD: the Amyotrophic Lateral Sclerosis Online Database. Amyotroph Lateral Scler 9:249-250.

Yahata N, Yuasa S, Araki T (2009) Nicotinamide mononucleotide adenylyltransferase expression in mitochondrial matrix delays Wallerian degeneration. J Neurosci 29:6276-6284.

Yanase S, Onodera A, Tedesco P, Johnson TE, Ishii N (2009) SOD-1 deletions in Caenorhabditis elegans alter the localization of intracellular reactive oxygen species and show molecular compensation. J Gerontol A Biol Sci Med Sci 64:530-539.

Yokota T, Miyagishi M, Hino T, Matsumura R, Tasinato A, Urushitani M, Rao RV, Takahashi R, Bredesen DE, Taira K, Mizusawa H, Andrea T (2004) siRNA-based inhibition specific for mutant SOD1 with single nucleotide alternation in familial ALS, compared with ribozyme and DNA enzyme. Biochem Biophys Res Commun 314:283-291.

Yuen EC, Olney RK (1997) Longitudinal study of fiber density and motor unit number estimate in patients with amyotrophic lateral sclerosis. Neurology 49:573-578.

Zelko IN, Mariani TJ, Folz RJ (2002) Superoxide dismutase multigene family: a comparison of the CuZn-SOD (SOD1), Mn-SOD (SOD2), and EC-SOD (SOD3) gene structures, evolution, and expression. Free Radic Biol Med 33:337-349.

Zhang B, Tu P, Abtahian F, Trojanowski JQ, Lee VM (1997) Neurofilaments and orthograde transport are reduced in ventral root axons of transgenic mice that express human SOD1 with a G93A mutation. The Journal of Cell Biology 139:1307-1315.

Zhang H, Xing L, Rossoll W, Wichterle H, Singer RH, Bassell GJ (2006) Multiprotein complexes of the survival of motor neuron protein SMN with Gemins traffic to neuronal processes and growth cones of motor neurons. J Neurosci 26:8622-8632.

Zherebitskaya E, Akude E, Smith DR, Fernyhough P (2009) Development of selective axonopathy in adult sensory neurons isolated from diabetic rats: role of glucose-induced oxidative stress. Diabetes 58:1356-1364.

Zochodne DW, Verge VM, Cheng C, Sun H, Johnston J (2001) Does diabetes target ganglion neurones? Progressive sensory neurone involvement in long-term experimental diabetes. Brain 124:2319-2334.